ORNL/TM-2022/2724

Delayed Critical and Subcritical Experiments with Polyethylene Moderated Unreflected Thin 15 in. Diameter HEU Metal Plates

John T Mihalczo

February 2023

OAK RIDGE National Laboratory

ORNL IS MANAGED BY UT-BATTELLE LLC FOR THE US DEPARTMENT OF ENERGY

ORNL/TM-2022/2724

Nuclear Energy and Fuel Cycle Division

Delayed Critical and Subcritical Experiments with Polyethylene Moderated Unreflected Thin 15 in. Diameter HEU Metal Plates

John T. Mihalczo

February 2023

Prepared by
OAK RIDGE NATIONAL LABORATORY
Oak Ridge, TN 37831
managed by
UT-BATTELLE LLC
for the
US DEPARTMENT OF ENERGY
under contract DE-AC05-00OR22725

CONTENTS

LIST OF FIGURES

LIST OF TABLES

ABSTRACT

The thin ~15 in. diameter highly enriched uranium (HEU) metal plates were assembled to delayed criticality at the Oak Ridge Critical Experiments Facility (ORCEF) in 1969 with various thicknesses of polyethylene (varying from 1/16 to 2 ⅜ inches) between uranium metal plates. The average ^{235}U enrichment was 93.27 wt. %. These unreflected critical configurations contained 4 ⅔ to 20 ⅚ thin 15 in. diameter HEU metal plates (on loan from Los Alamos National Laboratory [LANL] and shipped to Oak Ridge National Laboratory [ORNL] on June 3, 1969). Depending on the thickness of polyethylene, the enriched uranium masses varying from 28,053 to 135,148 grams. Fractional plate sections consisted of the appropriate number of 60° pie sections. In addition to the measurement at delayed criticality, subcritical measurements were also performed by the inverse kinetic rod drop method. Prompt neutron decay constant measurements were also performed by the Rossi alpha and randomly pulsed neutron method using a time-tagged spontaneous fission californium neutron source; these are briefly reported here. At the time of these measurements in 1969, the thin HEU metal plates were in near-pristine condition with extremely little oxidation, allowing better descriptions of the uranium plates than the use of these plates in a heavily oxidized and deteriorated condition in recent reflected benchmark experiments at the LANL facility at the Nevada Test Site with these same thin highly enriched uranium metal plates.

This report documents the experimental information for the measurements performed so that later researchers can perform the required uncertainty and calculational analyses and documentation to use these data for an International Nuclear Criticality Safety Benchmark Evaluation Program (ICSBEP) or a Nuclear Energy Agency (NEA) benchmark. Data from the experiments described should be acceptable for use as criticality safety benchmark experiments for the ICSBEP and the NEA nuclear criticality safety benchmark program once the uncertainty analysis on the measured neutron multiplication factors is completed. Additional data—such as the dimensional inspection reports, uranium isotopic information, and other relevant particulars—should be retrieved from the Y-12 Plant or LANL and incorporated in the final ICSBEP benchmark. Based on previous ICSBEP benchmarks with this enriched uranium metal at ORCEF, the uncertainties in k_{eff} could be as low as ± 0.0002 for some configurations. Other experiments with smaller-diameter than 15 in. diameter HEU metal plates have been benchmarked in HEU-MET-FAST-001. The prompt neutron time decay measurements could be the basis for an International Reactor Physics Benchmark Program.

Preparation of the present report is part of an effort at ORNL to document more than 15 undocumented critical and subcritical experiments enumerated in ORNL/TM-2019/18 and performed by ORNL at ORCEF and other US Department of Energy critical experiments facilities using more than 500 operational days of critical facility time. This work for this report publication was supported by the Nuclear Criticality, Radiation Transport and Safety NCSP Program at ORNL.

1. INTRODUCTION

This report documents unreflected highly enriched uranium (HEU) metal experiments performed mainly at delayed criticality at the Oak Ridge Critical Experiments Facility (ORCEF) at Oak Ridge National Laboratory (ORNL) between July 14 and Oct 31, 1969, which utilized 60 operational days at ORCEF [1–3]. These ~15 in. diameter, ~0.120 in. thick HEU metal plates were shipped to ORNL by Los Alamos National Laboratory (LANL) on June 3, 1969, as documented by the fissile material transfer document (form AEC-101 given in Appendix A). The masses and ^{235}U enrichments are documented in the May 20, 1960, letter from A. D. Callihan (ORNL) to H. C. Paxton (LANL) also given in Appendix A. These thin HEU metal plates were assembled at ORCEF to delayed criticality with various thicknesses of ~15 in. diameter polyethylene between each highly enriched (average enrichment of 93.27 wt. % ^{235}U) uranium (HEU) metal plates. Based on a letter from A. D. Callihan of ORNL to H. D. Paxton of LANL dated May 20, 1960 (Appendix A), these plates were fabricated at the Y-12 Plant earlier than 1960. The polyethylene part thicknesses were approximately 1/16, 1/8, 1/4, and 1/2 in., and the HEU metal plates were interleaved with the polyethylene layers. Using more than one polyethylene part between uranium metal plates, assemblies with thicknesses of approximately 1.0, 1.5, 2.0, and 2.375 in. thick polyethylene were also assembled to delayed critical. The critical assemblies with 4 ⅓ to 20 and 5/6 thin 15 in. diameter HEU metal plates depending on the polyethylene thickness had masses varying from 28,053 to 135,148 grams. Fractional plate sections were made up of the appropriate number of 60° pie sections. These unreflected uranium metal experiments were assembled with minimal support structure to minimize incidental neutron reflection.

As the polyethylene layer thickness increased, the neutron energy spectrum decreased. Calculations [4] showed that the neutron spectra contained two peaks: one at 2 MeV and another below 1 eV. For 1/16 in. thick polyethylene, the ratio of the magnitude of the peaks was one; and for the thickest polyethylene, the magnitude of the lower energy peak was a factor of 6 higher than the 2 MeV neutron peak. For some subcritical configurations, the subcriticality was measured by the inverse kinetic rod drop technique (IKRD) [5], and they are reported herein. The prompt neutron decay constants were measured by the Rossi-α [6] and randomly pulsed neutron technique [7]—the latter using a time-tagged spontaneous fission californium neutron source—and are briefly summarized in this report. At the time of these measurements in 1969, these thin 15 in. diameter HEU metal plates were in near-pristine condition with extremely little oxidation. This allowed better descriptions of the uranium plates than the use of these plates in a heavily oxidized and deteriorated condition in recent benchmark reflected experiments at the Los Alamos National Laboratory facility at the Nevada Test Site [8]. These deteriorations resulted in the present significantly increased uncertainty in dimensions and masses of the parts in recent experiments. Critical experiments were performed with other thin uranium metal plates starting in 1952 at LANL with smaller diameter uranium metal without ^{236}U before reprocessed reactor fuel was blended in the diffusion process and an International Criticality Safety Benchmark Evaluation Program (ICSBEP) benchmark has been completed [9, 10]

This report documents the experimental information for the measurements performed at ORCEF in 1969 so that researchers can at a later date perform the required uncertainty and calculational analyses and documentation to use these data for an ICSBEP or a Nuclear Energy Agency (NEA) benchmark. The data from the experiments described should be acceptable for use as criticality safety benchmark experiments for the ICSBEP and the NEA nuclear criticality safety benchmark program once the uncertainty analysis is completed. Based on previous ICSBEP benchmarks with enriched uranium metal at ORCEF, the uncertainties in k_{eff} could be very low for some configurations. Other experiments with these thin 15 in. diameter HEU metal plates and polyethylene at the LANL critical facility at the Device Assembly Facility (DAF) at the Nevada Test Site are in process of being benchmarked [8]. The prompt neutron time decay data can be used as the basis of International Reactor Physics Benchmark Program (IRPhE). Co-experimenters in these measurements were J. J. Lynn and R. R. Taylor of ORCEF staff.

Preparation of the present report is part of an effort at ORNL to document more than 15 undocumented critical and subcritical experiments enumerated in ORNL/TM-2019/18 [11] and performed by ORNL at ORCEF and other US DOE critical experiments facilities using more than 500 operational days of critical facility time. This particular documentation was supported by the Nuclear Criticality, Radiation Transport and Safety NCSP Program at ORNL. To date this effort which initiated in 2018 at ORNL has resulted in several reports that are listed in Appendix B.

2. DESCRIPTION OF THE MEASUREMENTS

2.1 OVERVIEW OF EXPERIMENTS

A variety of critical experiments were constructed with unreflected and unmoderated HEU metal during the 1960s and 1970s at ORCEF in support of nuclear criticality safety of the Y-12 Plant [12–19]. HEU metal experiments with 7, 9, 11, 13, and 15 in. diameter HEU metal cylinders were reported and analyzed in HEU-MET-FAST-051 [20]. Other HEU metal experiments at ORCEF already in the NEA benchmark database are HEU-MET-FAST-059, -061, -071, and -100 [21]. Of these hundreds of delayed critical assemblies, the experiments described in this report are the clean critical experiments with HEU (93.27 wt. % ^{235}U) metal mixed with hydrogenous internal moderator. The experiments were performed from July 1969 through Oct 1969. For some polyethylene thicknesses, the experiments were repeated with different HEU metal parts. The experiments were performed to verify the calculational methods for uranium assemblies mixed with polyethylene moderator to produce assemblies with lower energy spectra that can be used to verify calculation with lower energy neutron spectra. The assemblies contained up to 20 ⅚ thin 15 in. diameter enriched uranium metal plates with interleaved polyethylene moderator thicknesses varying from 1/16 to 2 ⅜ inches.

The data from most of these ten critical experiments described should be acceptable for use as criticality safety benchmark experiments in ICSBEP when the uncertainty analysis is performed. Based on previous ICSBEP benchmarks with this enriched uranium metal at ORCEF, it is expected that the uncertainties in k_{eff} could be very low since the procedure for assembly and detailed description of the materials and configurations are the same as previous measurements with HEU metal.

2.2 DESCRIPTION OF THE EXPERIMENTAL CONFIGURATIONS

These experiments were performed in the 35 × 35 × 30 ft. high East cell of ORCEF. The assemblies of uranium metal/moderator were located approximately 11.7 ft from the 5 ft thick concrete west wall, 12.7 ft from the 2 ft thick concrete north wall, and 9.2 ft above the concrete floor. They were performed using the vertical assembly machine of the East cell of the ORCEF. A brief description of the assemblies is given in Table 1 along with the near critical masses and the sum of the heights of the full plates, as well as references to the appropriate logbook page. In assemblies with less than 1.00 in. of polyethylene moderator between these thin 15 in. HEU metal plates, the top full layer on the loading of the diaphragm and the bottom full layer on the lower support section was a full HEU plate. Thus, there was usually one less polyethylene layer than uranium metal, except for one variation of the system with ¼ in. thickness of polyethylene. In addition to the thin 15 in. diameter HEU metal plates there were 60° pie shaped sections for fine adjustment of the neutron multiplication factor. These pie-shaped uranium metal sections had similarly shaped pie sections of various thicknesses of polyethylene. Some uranium metal plates had 1.510 in. diameter axial holes with HEU metal inserts for filling the holes. For two thicknesses of polyethylene, there were multiple critical configurations. In one experiment, a uranium metal HEU metal ring from another experiment was used adjacent to the thin top HEU metal plate.

Table 2.2-1. General description of the measurements.

Experiment number	Polyethylene nominal thickness (in.)	ORCEF Logbook E-24 page and run number	Number of Uranium Plates	Number of full layers of Polyethylene	Mass of Uranium (g)	Sum of Uranium Thickness (in)[a]	System reactivity (cents)
1	1/16	P 38 Run 31	20-5/6	19-5/6	135,148	2.39394	0 with shim 6 in. from surface
2	1/8	P 19 Run 8	17-1/3	16-1/3	112,183	2.03077	+32.4
2a	1/8	P33 Run 37	17	16	112,113	2.0376	0 with shim 6 in. from surface
2b	1/8	P 82 Run 124	16-2/3	16-2/3	108,106	1.91659	-14.85
3	¼	P 47 Run 49	12-2/3	11-2/3	84,034	1.43287	+1
3a	¼	P 24 Run 21	12-2/3	12-2/3	81,845	1.4263	+1
3b	¼	P 82 Run 121	12-1/3	11-1/3	79,760	1.43287	+22.3
4	½	P 51 Run 52	8-1/2	8-1/2	54,865	0.95306	+22
4a	½	P 80 Run 117	7-5/6	6-5/6 less 1/8 of 1/3 of top CH2	50,616	0.83632	+ 7.11
5	1.0	P 75 Run 93	5	4	78,693	0.59598	+15
6	1.25	P 76 Run 101	4-1/2	3-1/2	35,538	0.59598	+10.24
7	1.5	P 77 Run 103	4-1/3	3-1/3	28,053	0.4776	+20.4
8	1.75	P 77 Run 105	4-1/3	3-1/3	28.053	0.4776	-22.01
9	2.0	P 78 Run 108	4-2/3	3-2/3	29,119	0.4776	-23.65
10	2-3/8	P 79 Run 112	6-1/3	5-1/3	41,089	0.71961	+3.60

[a]Sum of thicknesses of full thin 15 in. diameter HEU metal uranium metal plates

The optimum moderator thickness (that with the lower critical mass) is ~ 1.625 in.

2.3 EXPERIMENTAL METODOLOGY

The cylindrical assemblies comprised layers of HEU metal cylinders with alternating layers of polyethylene moderator; uranium and polyethylene dimensions were machined to precise tolerances. The experiments were performed in a deliberate and step-by-step manner, with observed data recorded. The critical assembly was divided into a fixed upper section on a 0.010 in. thick diaphragm and a movable lower section mounted on a low mass tower. These support structures are described in Appendix C. Most of the subcritical configurations were assembled with all materials on the stainless-steel diaphragm.

2.3.1 General Assembly Procedure

The critical assemblies were constructed on a vertical assembly machine that primarily consisted of a hydraulic lift (up to 22 in. vertical motion) to support the lower section (see Figure 2.3-1) and a stationary upper half consisting of four vertical posts spaced 4 ft apart, which held a support for the upper section of critical experiments. Further details of the assembly machine are given in reference 22. Upper support in the photograph was not used in these experiments. The upper section of an experiment was supported by a 30 in. inner diameter, 1.0 in. thick, 4.0 in. wide aluminum clamping ring that held in tension a 0.010 in. thick, stainless-steel (304L) diaphragm. The diaphragm clamping apparatus (two 0.5 in. thick rings) had a total thickness of one inch and was bolted together with thirty-four 0.375 in. diameter 1.5 in. long stainless-steel bolts with appropriate nuts. The clamping ring was supported of the four vertical poles (on 4 ft centers) with a low mass support structure of aluminum. The mating surfaces of the clamping ring were not flat so that when the nuts were tightened the diaphragm was held in tension (see Figure 2.3-2). The lower section was supported on a low-mass aluminum 30 in. high support tower mounted on the vertical lift platform, also shown in Figure 2.3-2. The lower support stand supported the uranium metal–polyethylene assemblies with 0.125 in. thick aluminum edges, oriented vertically and 120° apart. Lateral motion on the lower section was restrained by small aluminum pieces bolted to the 120° vertical members. These are also visible in Figure 2.3-2. The low-mass support stand 0.50 in. thick aluminum base was bolted to the vertical lift as shown in Figure 2.3-2. The upper limit of the lower section was set so that the top of the material on the lower section was raised to the position of the diaphragm with no load. Because of the sag of the diaphragm with loading when the lower section was raised to this position, the vertical lift supported the weight of the upper section. It may also have been in good contact at a slightly lower position of the vertical lift because of the sag of the diaphragm. Calculation may help decide whether these configurations without the full upward position of the lower section can be used for a valid benchmark.

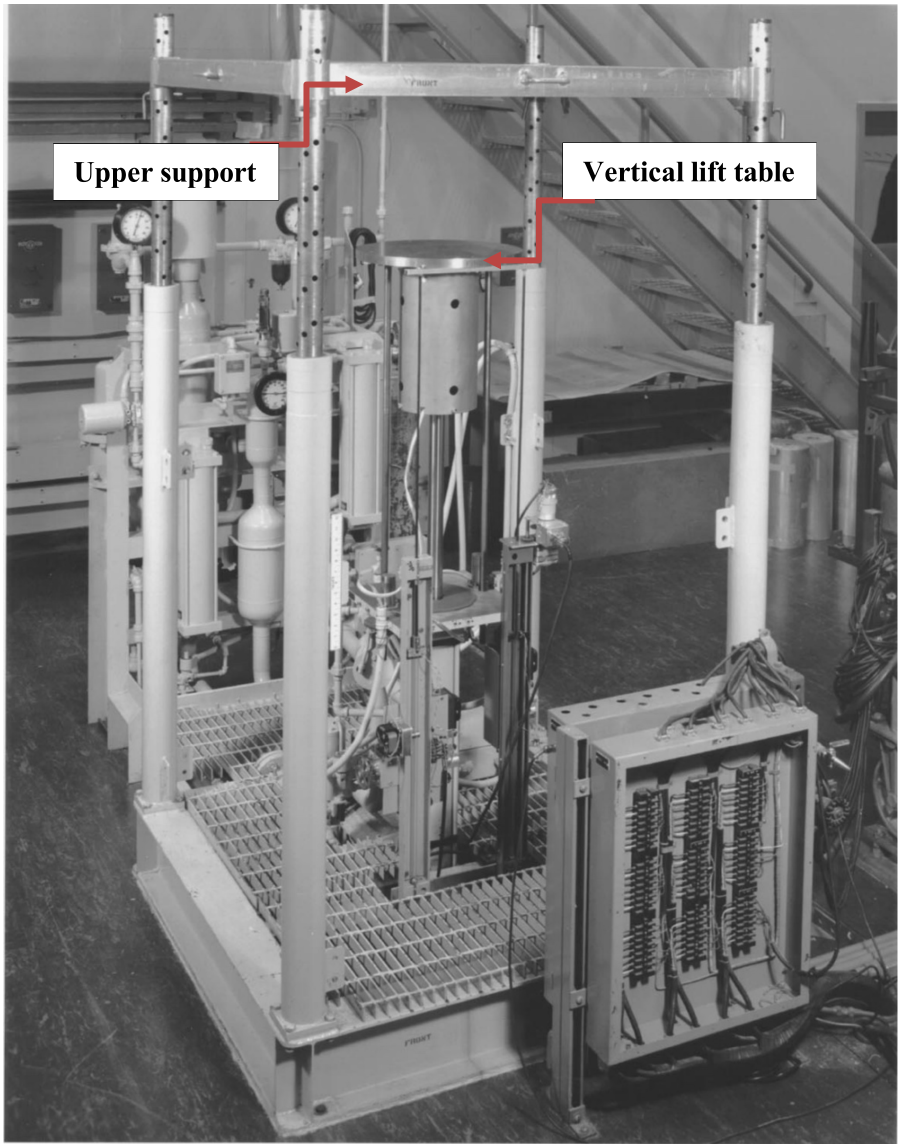

Figure 2.3-1. Photograph of the vertical assembly machine with the movable vertical lift table up. (No lower support structures are in this photograph except for the vertical lift table; upper support structure in the photograph was not used in these experiments).

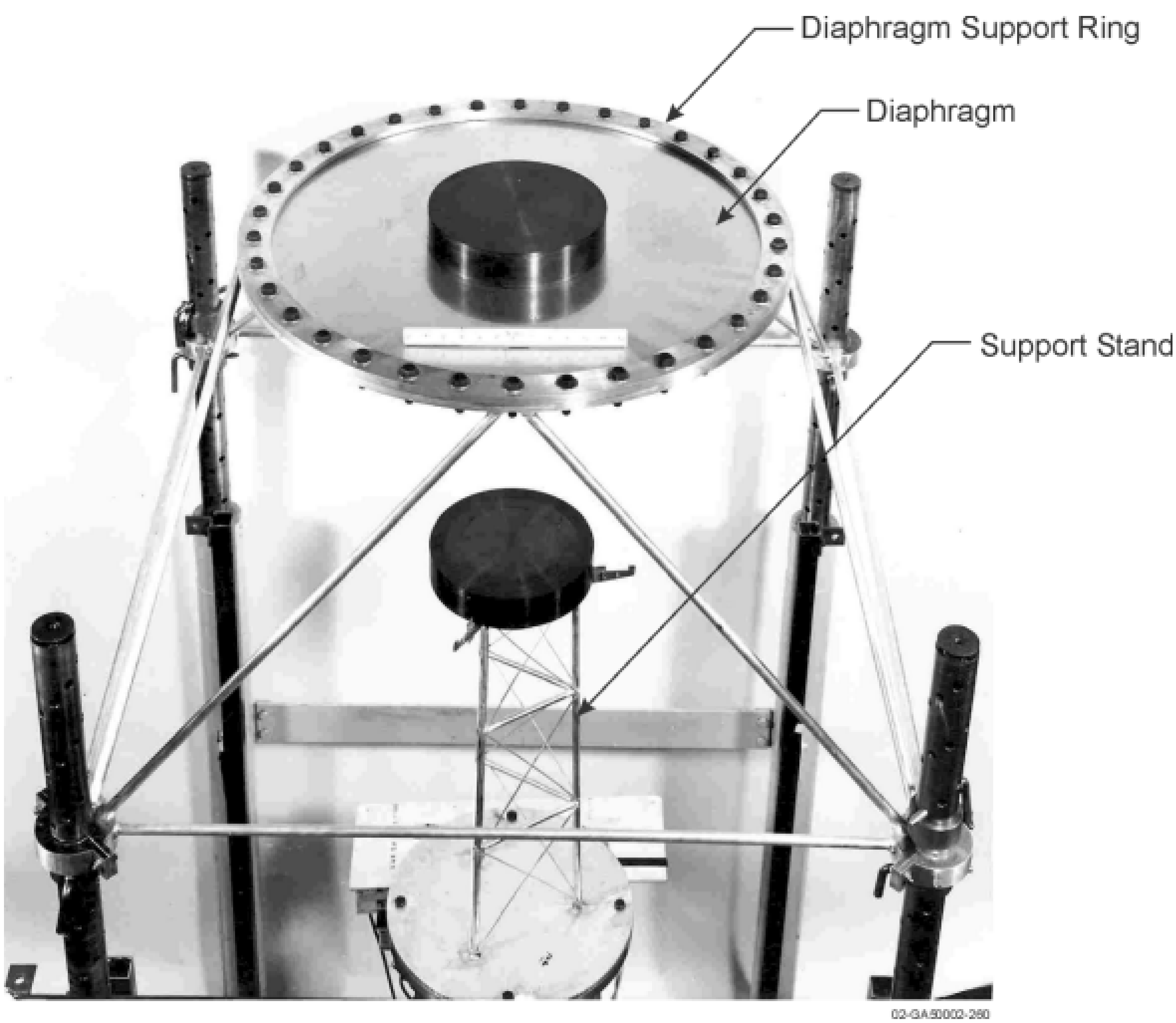

Figure 2.3-2. Photograph of an assembly of another uranium metal experiment on the apparatus with the lower support aluminum tower mounted on the vertical lift table in the down position that was used for these experiments.

Alternating thin 15 in. diameter HEU metal plates and polyethylene were stacked on the diaphragm and on the lower support stand, and the critical configuration was assembled remotely. The bottom part in the lower section for assemblies with polyethylene thicknesses less than 1.0 in. was a uranium metal plate, the upper part of the lower section was polyethylene, and the lower part on the diaphragm and the uppermost part on the diaphragm was uranium metal. In the assembly, the lower section was raised until it lifted the sagging diaphragm to its level position (no sag location determined without material on the diaphragm). Thus, the vertical lift bore most of the weight of the upper section. Each uranium metal plate has a part number scribed on one flat surface. To enhance reproducibility, the parts were always oriented on the assembly machine upper or lower section with the scribed part number on the upper surface and toward the north wall of the facility. In some experiments, the bottom and upper parts of the lower section were polyethylene.

2.3.2 Alignment of Each Half

The upper and lower sections were aligned using the processes described below. Uncertainty in radial alignment of thin top HEU metal section with respect to the bottom uranium metal section was ± 0.005 in.

2.3.2.1 Upper Section

For assembly of the upper section, a uranium metal plate was added to the diaphragm. The uranium metal plate was positioned on the sagging diaphragm and leveled with a high-precision level. This ensured that it was centered. The location of the material was continuously adjusted with a precise high-quality level with the level in one direction and then rotated 90° on the parts. If the HEU metal plate was not exactly centered in the diaphragm, then it would not be precisely level because of the sag in the diaphragm as it was loaded. After this plate was aligned with the plate on the lower support stand, additional material was added to the top section on the same diameter and two precisely machined steel blocks (±0.0001 in.) were used to squeeze the material at the outer radial surface until each section was aligned radially. An edge of the machined blocks was held at the outside radial location, and material was adjusted until minimal light was visible between the machined block and the uranium metal–polyethylene configuration. This process was repeated 90° from the position of the original adjustment and rechecked again at the original position; small adjustments were made if necessary. This process continued until the outside radii of the parts were precisely aligned and the upper section assembly was complete. The alignment of outer radii of the upper or lower section was less than ±0.001 in. Of course, if two positions 90° apart are adjusted, then the positions at 180° and 270° can be off only by the difference in the diameters of the outside parts.

2.3.2.2 Lower section

For the lower section, the same procedure was used except that the parts were leveled by shimming appropriately at selected locations on the underside of the bottom thin 15 in. diameter HEU metal plate with appropriate thicknesses of aluminum foil. The foil was placed between the edges of the support stand and the lowest thin 15-in. diameter HEU metal plate so that the upper surface of the lower plate was level.

2.3.3 Lateral Alignment of the Upper Section with the Lower Section

Two identical fixtures (see Figure 2.3-3) were used for lateral alignment between the upper section and the lower section. They were U-shaped and were machined out of 0.375 in. thick aluminum. The end pieces were carefully machined at the Y-12 shops to be perpendicular to the long direction of the fixture and coplanar with each other. When leveled properly on the diaphragm, the front face of the 4 × 4 × ½ in. end pieces were vertical and in the same plane to within ±0.001 in. This fixture was carefully machined and handled delicately when not in use so as not to damage it. In use, the lower side of the upper leg rested on the top surface of the clamping ring for the diaphragm. The fixture was perpendicular to the outer radial surface of the cylinder. As indicated in previous sections of this report, one thin 15-in. diameter HEU uranium metal plate was located on the diaphragm, and one thin 15-in. diameter HEU metal plate was located on the lower support stand. The fixture was moved inward until it touched the uranium of the top section. The leveling screws were adjusted until the fixture was level. The second fixture was placed 90° apart from the first in a similar manner. Both fixtures were moved back slightly, and the lower section was raised until the plate of the lower section was as high as the lower end piece of the fixture. Then, both fixtures were nearly adjusted properly. The fixtures were moved in until they touched uranium (either on the top or the lower section). When lack of contact was observed at either of the front faces of the fixture, the lower section was lowered to the full-out position, and the position of the uranium on the lower support stand was adjusted. The lower lift table was raised, and the alignment was checked. After the alignment of the two plates, the procedure was repeated with the full loading of the assembly. The process was repeated several times, as necessary. This was a long and tedious procedure that took 12 hours or more; however, it was always performed. This resulted in the top and bottom sections being aligned within ±0.005 in. After alignment, the rest of the materials were placed on the top and lower sections as described in Sections 2.3.2.1 and 2.3.2.2. Whenever the bottom plate in an assembly differed from the previous measurement, these stacking, and alignment procedure were repeated.

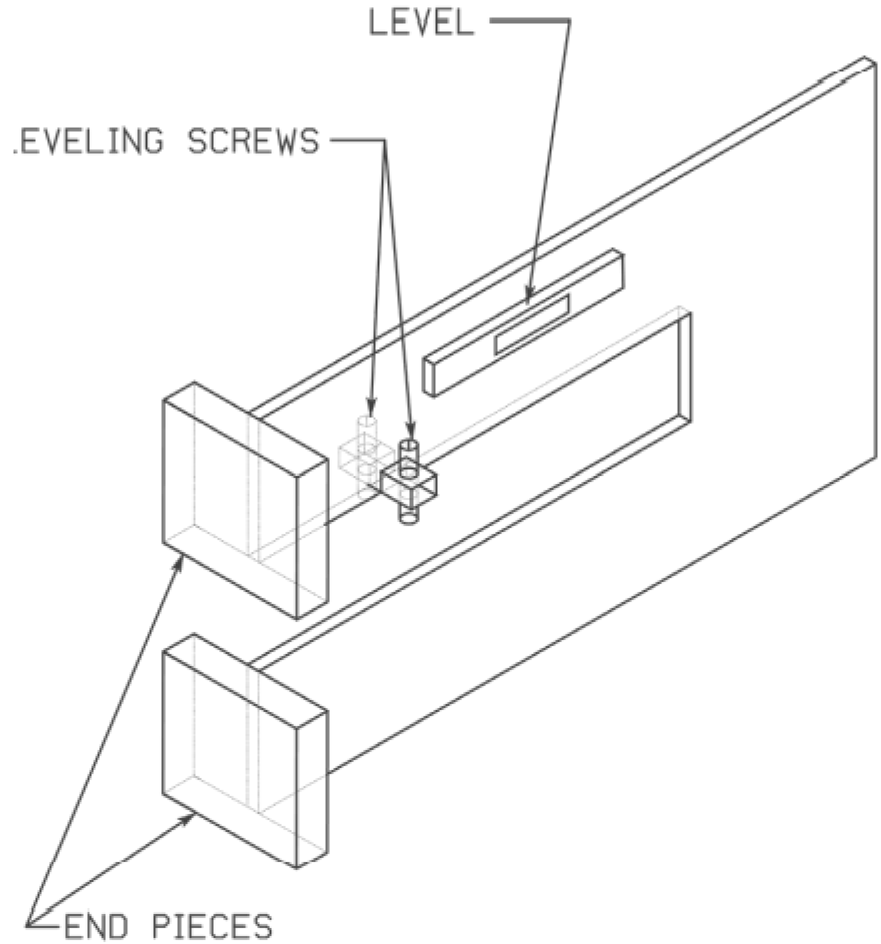

Figure 2.3-3. Sketch of the fixture for lateral alignment of thin 15 in. diameter HEU metal plates.

3. DESCRIPTION OF EXPERIMENTS

These 15 in. diameter cylindrical configurations consisted of alternate layers of uranium metal and polyethylene. For the HEU metal plates with a central hole, HEU metal inserts filled the holes for all critical configurations. For experimental critical assemblies with less than 1.0 in. thick polyethylene, the bottom and top of each assembly was a uranium metal plate. For assemblies with polyethylene greater than or equal to 1.0 in., the top and bottom part of each assembly were sometimes half the thickness of polyethylene between uranium metal plates. This top and bottom polyethylene layer acts as a reflector. Some experiments employed several variations of material—some well-defined and others not so clearly stated in the logbook. There were 60^0 pie shaped sections of uranium metal that were used for finer reactivity adjustment and similar partial sections of polyethylene. Those not clearly stated in the logbook are included in this report. Some ambiguous entries are contained in the logbook, particularly associated with the fractional uranium layers of uranium where the fraction of pie pieces does not agree with the number of pie pieces stated to be on top. If calculations of the k_{eff} of these questionable configurations is not very close to 1.000, then the configurations description are not correct and should be discarded as not of benchmark quality. In some experiments, the identification of the polyethylene layers is not specific, and assumptions were made that must be evaluated in the uncertainty analysis necessary for a benchmark. In other cases, the vertical lift could not be raised to its up position with no load on the diaphragm.

However, the sag of the diaphragm with load might be such that the lower section on the vertical lift was in good contact supporting the upper section.

3.1 GAPS BETWEEN PARTS

For the subcritical configurations for polyethylene thicknesses for which prompt neutron decay constants were measured, the heights of the assembled configurations were measured. The method of measuring the height of the assemblies is described in reference 20, and the measured heights are accurate to ± 0.001 in. These measured heights with the known thicknesses (at the time of the measurements, or 1969) of the uranium and polyethylene parts [2] can be used to determine the average gaps. It is assumed that the gaps for the subcritical configurations up to ½ in. thick polyethylene are the same as those for the critical configurations with the same polyethylene thicknesses and the same number of uranium plates. The gaps for the configurations with 1/16, ⅛, ¼, and ½ in. thick polyethylene are well known since they are based on measurements.

For polyethylene thicknesses greater than ½ in. that used multiple polyethylene layers between uranium metal plates, various assumptions were made for the thickness of the gaps. The gaps between adjacent ½ thick polyethylene layers were assumed to be 0.0043 in., between adjacent 1/4 in. thick polyethylene layers gaps were assumed to be 0.0031 in., between adjacent 1/8 in. thick polyethylene layers gaps were assumed to be 0.0032 in., and between adjacent 1/16 in. thick polyethylene layers gaps were assumed to be 0.0032 in. It was also assumed that these values between the four thicknesses of polyethylene and uranium metal plates were the same. For material adjacent to the diaphragm, it was assumed that the gaps were half these values. For adjacent polyethylene layers of different thicknesses, the average of both gap thicknesses was used. For example, the gap between a 1/16 and ½ in. thick polyethylene layers was 0.00037 in. (0.0043 + 00032)/2 = 0.0037 in.) These gaps are considerably larger than those for other Oralloy parts fabricated at the Y-12 plant at this time. Some stacking densities for 7 in. diameter unreflected and unmoderated uranium metal were as high as 18.75 g/cm^3 [20]. In general, the gaps increase with polyethylene thickness and lower numbers of plates. Since weight of the assembly increases with number of uranium plates because of gravity, increased weight decreases the gaps.

The reactivity effect of gaps between plates should be small. This was demonstrated when these thin 15 in. diameter HEU metal plates were stacked to delayed criticality without any moderator and reflector, and the critical mass was 165.7 kg [1] compared to the critical mass of a 15 in. diameter HEU metal cylinder of 163.7 kg [20] with an average uranium stacking density of 18.68 g/cm^3. This 5.2% change in density only produced a change in critical mass of only 1.22%.

3.2 THIN 15 IN. DIAMETER HEU METAL PLATES WITH ALTERNATING 1/16 IN. THICK POLYETHYLENE LAYERS, EXPERIMENT 1

On July 28, 1969, thin 15 in. diameter HEU metal plates with 1/16 in. thick polyethylene layers between them were assembled to near delayed criticality. This assembly consisted of 20 thin 15 in. diameter HEU metal plates with nineteen polyethylene layers between them. In addition, there were five adjacent 60° pie-shaped uranium and polyethylene layers on the top of the uppermost thin 15-in. HEU metal plate, thus, covering 5/6 of the top. An aluminum 2 × 3 × 1.4 in. thick reflector piece was included for fine adjustment of the reactivity or k_{eff} value. The 2 × 3 plate was vertical with the 3 in. long edge resting on the diaphragm. This was connected to a 12 in. long rod driven by a motor with 12 in. of motion, which could be used to change the distance between the front surface of the aluminum reflector and the assembly. The total reactivity worth of the reflector plate for this assembly was 16.5 cents. For this assembly with a k_{eff} value of 1.0000, this reflector shim was located 0.500 in. from the radial surface of the thin 15-in. diameter HEU metal plates stacked on the diaphragm (Run 31, Page 38 ORCEF logbook E-24). This neutron multiplication factor must be corrected for the reactivity of the aluminum reflector plate, which can be obtained from calculation of the worth as a function of distance from the assembly. The configuration of this delayed critical assembly on the vertical assembly machine is given in Figure 3.2-1 with the part numbers indicated. All uranium part numbers with identification numbers less than U-10933 had axial holes fille with HEU metal inserts. The configuration of the partial top uranium and polyethylene layers is shown in Figure 3.2-2.

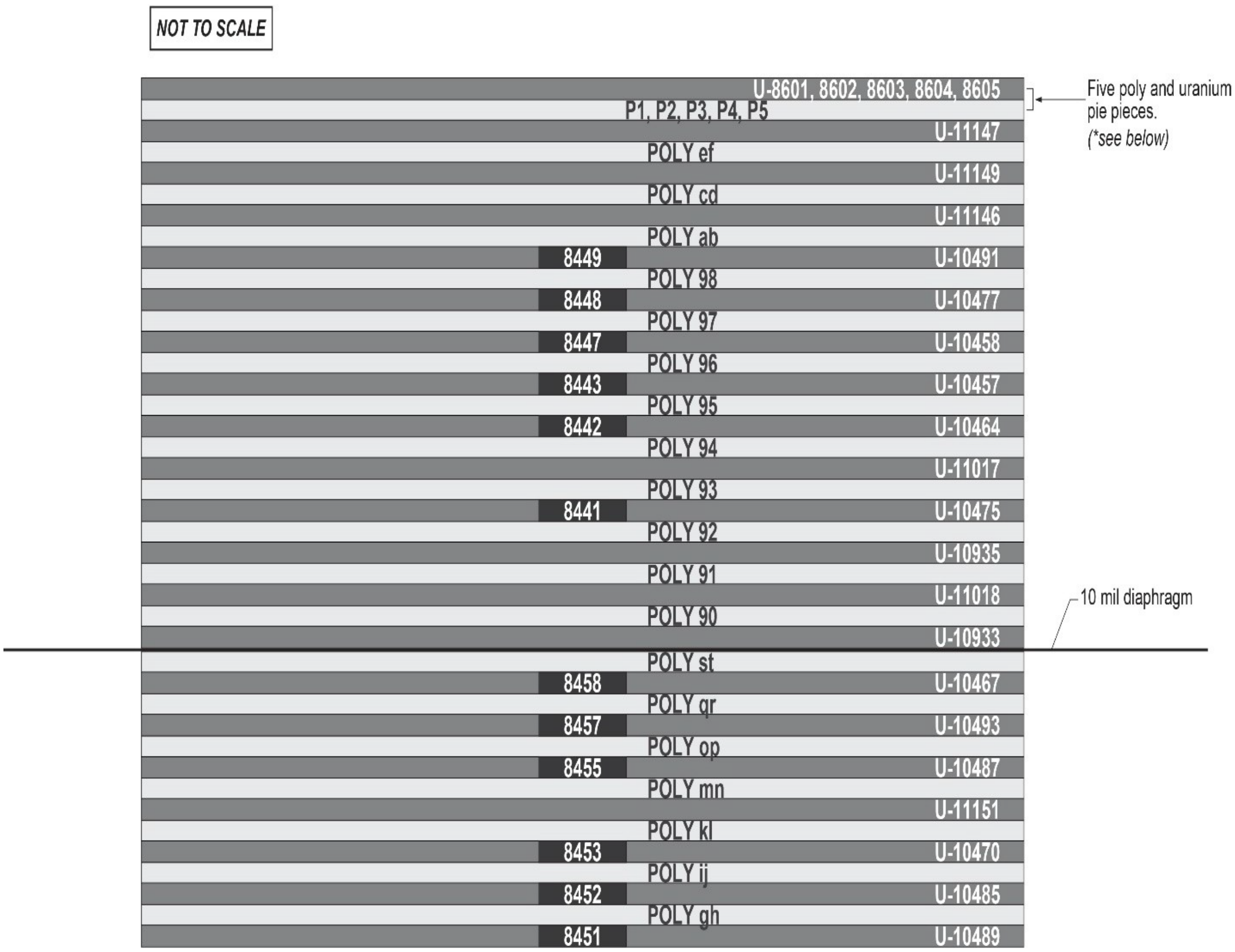

Figure 3.2-1. Configuration of the thin 15 in. diameter HEU metal plate assembly with 1⁄16 in. thick polyethylene between plates, Experiment 1. (Two-dimensional cross section along diameters; based on height measurements for subcritical configurations, the gap between polyethylene and uranium layers for this assembly is 0.0032 in.)

Based on height measurements for subcritical configurations, the gap between all polyethylene and uranium layers for this assembly is 0.0032 in. Adjacent to the diaphragm the gap should be 0.0016 in. between the diaphragm and the parts above and below it. All parts and their locations were specified in the last page of the logbook except the uranium inserts (parts thin 15 in. diameter HEU metal plates with numbers less than U-10933). The identification numbers of the uranium inserts were 8441 to 8458 with number 8444, 8445, 8446, 8450, and 8454 missing) that were in the center of the thin 15 in. diameter HEU metal plates with axial 1.510 in. diameter holes (all not consecutive, as some numbers are missing. The material on the diaphragm was assembled first, and it was assumed that the inserts were used in order from low numbers to high numbers (8441 to 8448), from bottom to top. Then the material on the lower support structure was assembled and the inserts on the bottom used from low number to high numbers from bottom to top (8449 to 8455). For all subsequent configurations given in this report, it was assumed that the uranium inserts were inserted in this manner.

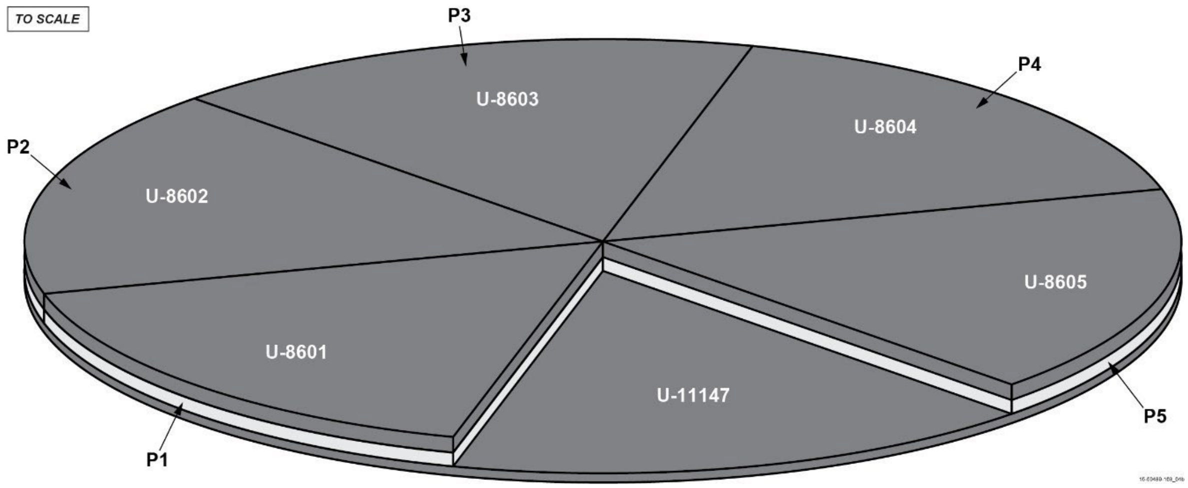

Figure 3.2-2. The configuration of the partial top uranium and ~1/16 in. thick polyethylene parts for Experiment 1. (60^0 polyethylene pie shaped sections are labeled)

The effects of room return should be calculated using Monte Carlo simulations assuming the wall and floor were 2 ft thick, and the concrete was Oak Ridge concrete, which used crushed limestone instead of sand taken together. The 2 ft. thickness for the concrete is adequate for the calculation because neutrons that reach 2 ft into the concrete have little chance of returning to the critical assembly. This calculation should include the air in the room and the aluminum base of the support stand base and the 1 in. thick stainless-steel vertical lift tabletop. The calculations for room return are discussed for a previous unmoderated and unreflected uranium metal cylinder in reference 20. Further details on the construction of the East cell of ORCEF can be found in Reference 21.

3.3 THIN 15 IN.DIAMETER HEU METL PLATES WITH ALTERNATING 1/8 IN. THICK POLYETHYLENE LAYERS, EXPERIMENT 2

On July 15, 1969, thin 15 in. diameter HEU metal plates with ⅛ in. thick polyethylene layers between them were assembled to near delayed criticality (page 19, Run 8 of ORCEF LOGBOOK E-24). This assembly consisted of 17 thin 15 in. diameter HEU metal plates with sixteen polyethylene layers (Page 17 of logbook for plate configuration) between them. In addition, there were two adjacent 60° pie-shaped uranium (8604 and 8605) and polyethylene layers on the top of the uppermost thin 15 in. diameter HEU metal plate, thus covering ⅓ or 33.3% of the top. The configuration of this delayed critical assembly on the vertical assembly machine is given in Figure 3.3-1. The configuration of the partial top uranium and polyethylene layers are shown in Figure 3.3-2. The part numbers are documented in the back inside cover of ORCEF Logbook E-24. The reactivity of this system was plus 32.9 cents, where 100 cents or one dollar is equal to the effective delayed neutron fraction and can be converted to k_{eff} units by multiplying the delayed neutron fraction and the reactivity in dollars and adding it to 1.0000. The effective delayed neutron fraction will have to be obtained from calculations for this configuration. The effective delayed neutron fraction is usually calculated by performing the normal calculation and obtaining the neutron multiplication factor to within a precision of ± 0.00001 and then repeating the calculation of the neutron multiplication factor with the delayed neutron portion of the fission spectrum removed from the neutron emission spectrum after fission. The difference of the neutron multiplication factor is the delayed neutron fraction. The delayed neutrons are more effective than prompt neutrons from fission because their lower energy makes them more likely to induce fission since the fission cross section is higher at lower energy.

Based on height measurements for subcritical configurations, the gap between all polyethylene and uranium layers for this assembly is 0.0032 in.

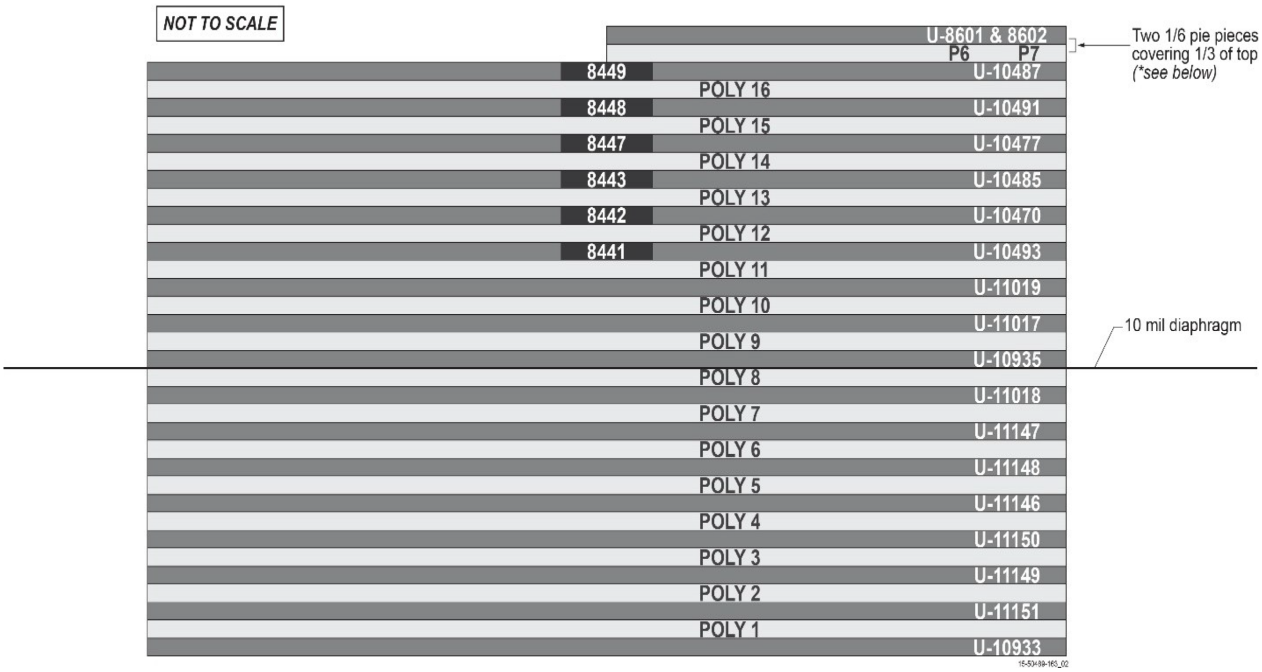

Figure 3.3-1. Configuration of the thin 15-in. diameter HEU metal plate assembly with ⅛ in. thick polyethylene between plates, Experiment 2. (Two-dimensional cross section along diameters; sketch on Page 17 of ORCEF logbook E-24; based on height measurements for subcritical configurations, the gap between polyethylene and uranium layers for this assembly is 0.0032 in.)

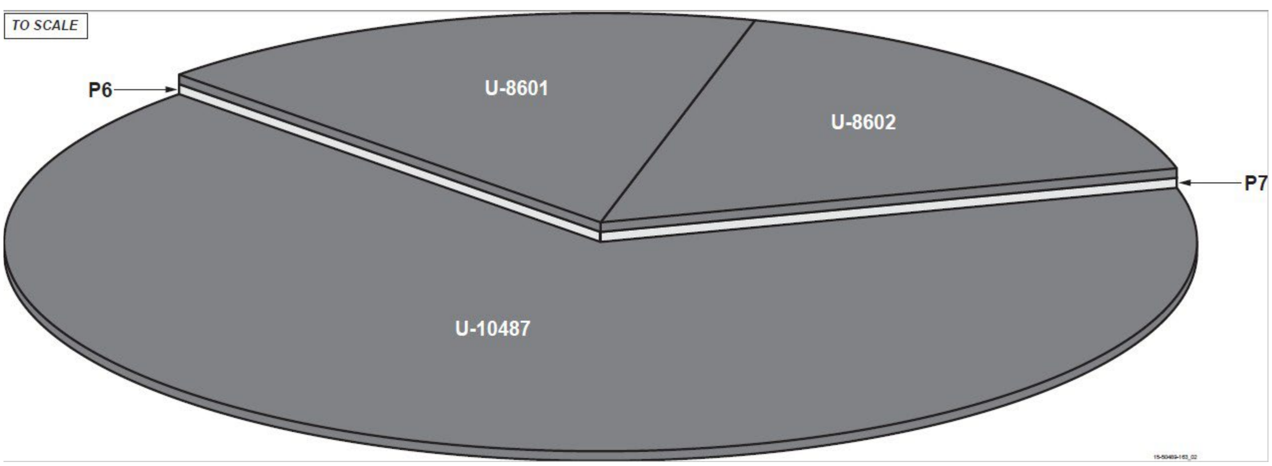

Figure 3.3-2. The configuration of the partial top uranium and ~⅛ in. thick polyethylene parts for Experiment 2.

The effects of room return should be calculated using Monte Carlo simulations assuming the wall and floor were 2 ft thick, and the concrete was Oak Ridge concrete, which used crushed limestone instead of sand taken together. The 2 ft thickness for the concrete is adequate for the calculation because neutrons that reach 2 ft into the concrete have little chance of returning to the critical assembly.

3.4 THIN 15-IN. DIAMETER HEU METAL PLATES WITH ALTERNATING 1/8 IN. THICK POLYETHYLENE LAYERS, EXPERIMENT 2A

On July 24, 1969, thin 15 in. diameter HEU metal plates with ⅛ in. thick polyethylene layers between them were assembled to delayed criticality with a configuration for Rossi alpha measurements. This assembly on page 33, Run 37 of ORCEF logbook E-24 consisted of 17 HEU metal plates with sixteen polyethylene layers between them. In addition, there were two small 1.5 in. diameter cylindrical uranium discs near the center on the top uranium plate. Also, there was a uranium ring (15 in. OD-13 in. ID from a previous uranium metal experiment) on the top HEU metal plate. This was part number 2758 with a mass of 1685 g. In addition, the two detectors for the Rossi alpha measurements were in 0.25 in. thick lead cups on the diaphragm adjacent to the radial surface of the assembly. One detector was a 0.5 in. thick, 2 in. diameter NE-102 plastic scintillator, and the other was of the same type but 0.25 in. thick. The detectors were located 120° apart. The configuration of this delayed critical assembly on the vertical assembly machine is given in Figure 3.4-1 without the detectors. The configuration of the partial top uranium and polyethylene layers is shown in Figure 3.4-2. The system was at delayed criticality and thus the neutron multiplication factor k_{eff} = 1.0000 with the two detectors present.

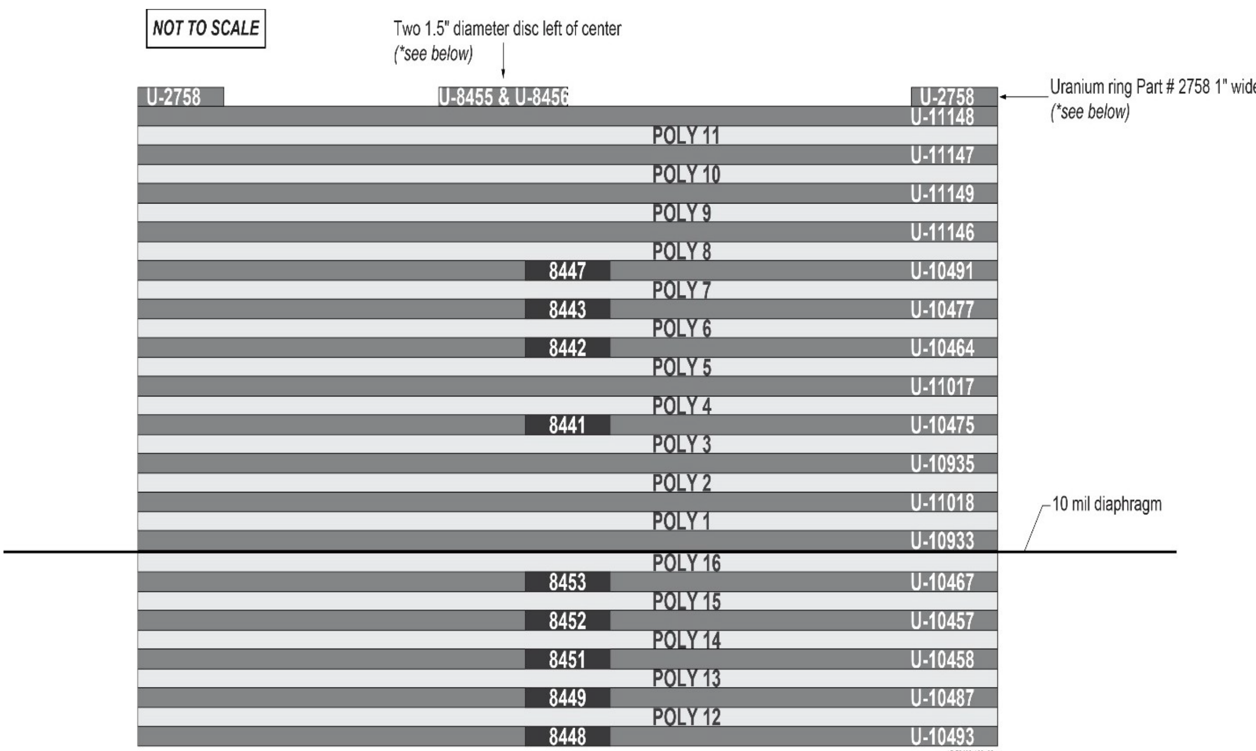

Figure 3.4-1. Configuration of the thin 15-in. diameter HEU metal plate assembly with ⅛ in. thick polyethylene between plates, Experiment 2a. (Two-dimensional cross section along diameters; based on height measurements for subcritical configurations, the gap between polyethylene and uranium layers for this assembly is 0.0032 in.; above and below and adjacent to the diaphragm the gap should be 0.0016 in.)

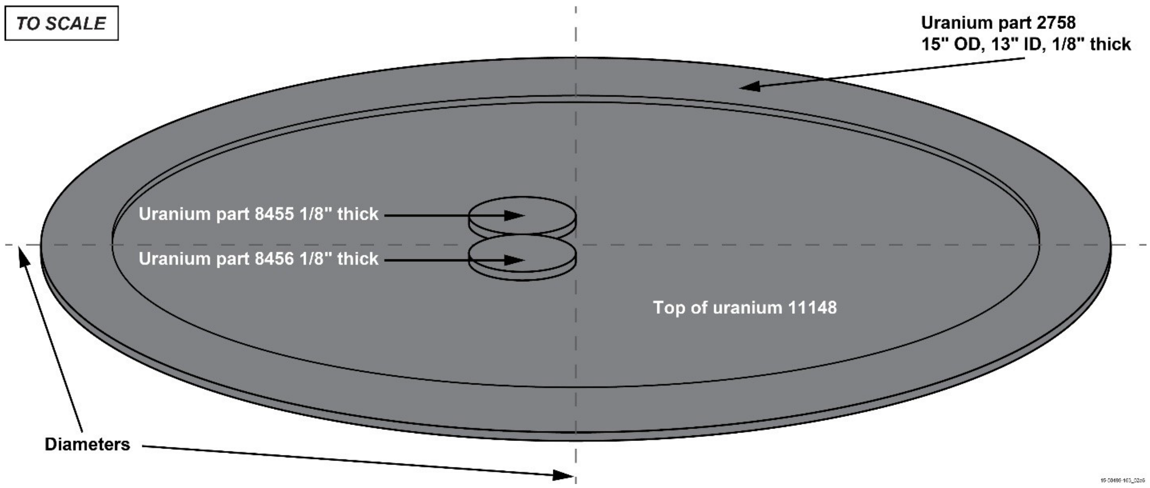

Figure 3.4-2. The configuration of the partial top uranium and ~⅛ in. thick polyethylene parts for Experiment 2a.

The effects of room return need not be calculated for this assembly, but the value from Experiment 2 should be used.

3.5 THIN 15 IN. DIAMETER HEU METAL PLATES WITH ALTERNATING 1/8 IN. THICK POLYETHYLENE LAYERS, EXPERIMENT 2B.

This configuration was assembled on October 16, 1969 (Page 82, Run 124, ORCEF logbook E-24) and had a thin layer of polyethylene on the bottom. It was originally assembled with 17 HEU metal plates and 16 polyethylene layers with Poly 95 and Poly 97 as thin bottom and top reflectors but was super delayed critical, with the lower section not in the full up position, and the reactivity was not measured. One HEU metal plate was removed, and the configuration of the uranium metal and polyethylene is shown in Figure 3.5-1. The configuration of the top is shown in Figure 3.5-2. The reactivity of the assembly was −14.85 cents. To convert this to k_{eff} units, the value of the effective delayed neutron fraction for Experiment 2 can be used. It is not clear from the logbook as to the configuration on top. This ambiguity may be resolved via calculation by assuming other configurations on top like POLY 16 on top of uranium part 11147 with the pie sections shown in Figure 3.5-2 with Poly pie section P1 to P4 under the uranium metal and POLY 97 as a top reflector. Whichever of these two configurations calculates closest to −14.85 cents reactivity could be the proper configuration. If neither, this assembly may not be of benchmark quality.

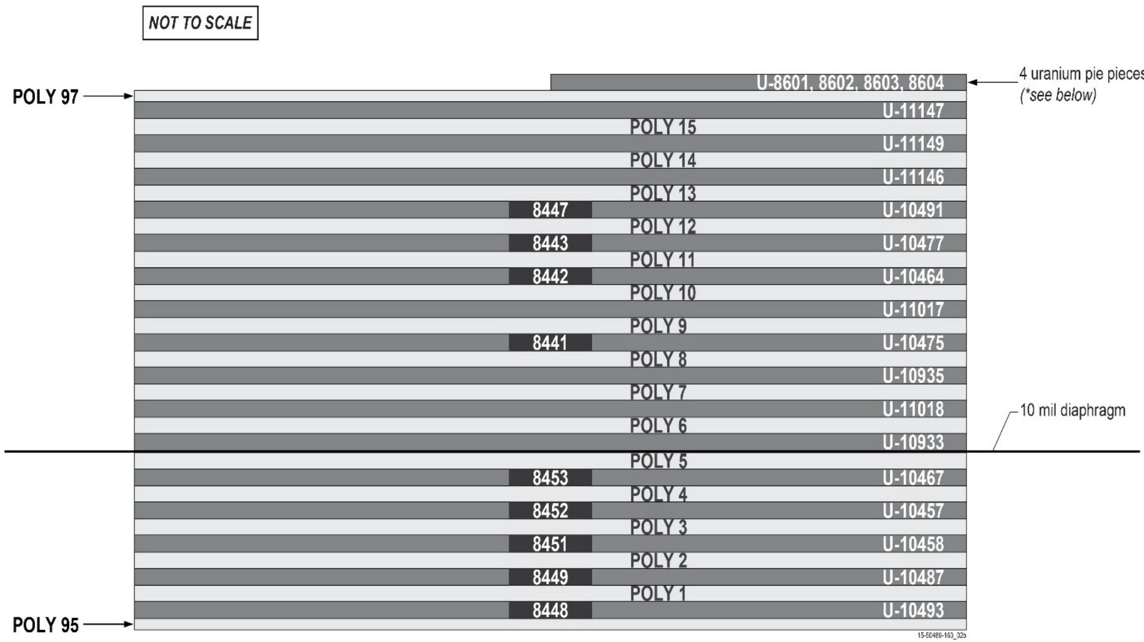

Figure 3.5-1. Configuration of the thin 15 in. diameter HEU metal plate assembly with ⅛ in. thick polyethylene between plates, Experiment 2b. (Two-dimensional cross section along diameters; based on height measurements for subcritical configurations, the gap between polyethylene and uranium layers for this assembly is 0.0032 in.; above and below and adjacent to the diaphragm should be 0.0016 in.)

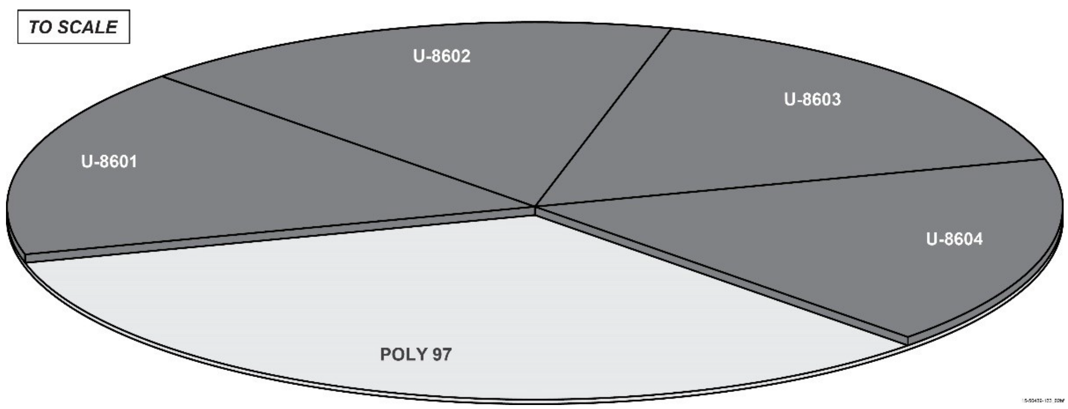

Figure 3.5-2. The configuration of the partial top uranium and ~⅛ in. thick polyethylene parts for Experiment 2b.

The effects of room return need not be calculated for this configuration, but the value from Experiment 2 should be used.

3.6 THIN 15 IN. DIAMETER HEU METAL PLATES WITH ALTERNATING 1/4 IN. THICK POLYETHYLENE LAYERS, EXPERIMENT 3

On Aug 6, 1969, an assembly of 12 ⅚ thin 15 in. diameter HEU metal plates with eleven alternating ¼ in. thick polyethylene layers was assembled. The assembly included five adjacent pie sections of uranium parts on top with appropriate polyethylene underneath them. The assembly also included two NE-102 plastic scintillators in 0.25 in. thick lead cups on the diaphragm with the front of the lead adjacent to the assembly. The plastic scintillators were 120° apart and were 0.50 and 0.25 in. thick. This configuration is described in ORCEF logbook E-24 page 47, Run 49. The configuration of this delayed critical assembly on the vertical assembly machine is given in Figure 3.6-1, and the configuration of the pie shaped parts on top is given in Figure 3.6-2. The reactivity of this assembly was +1 cent, slightly above delayed criticality. The reactivity with the two detectors for the Rossi-α measurements is located and described in Section 3.4. To convert this reactivity to k_{eff} units, the delayed neutron fraction must be calculated and used.

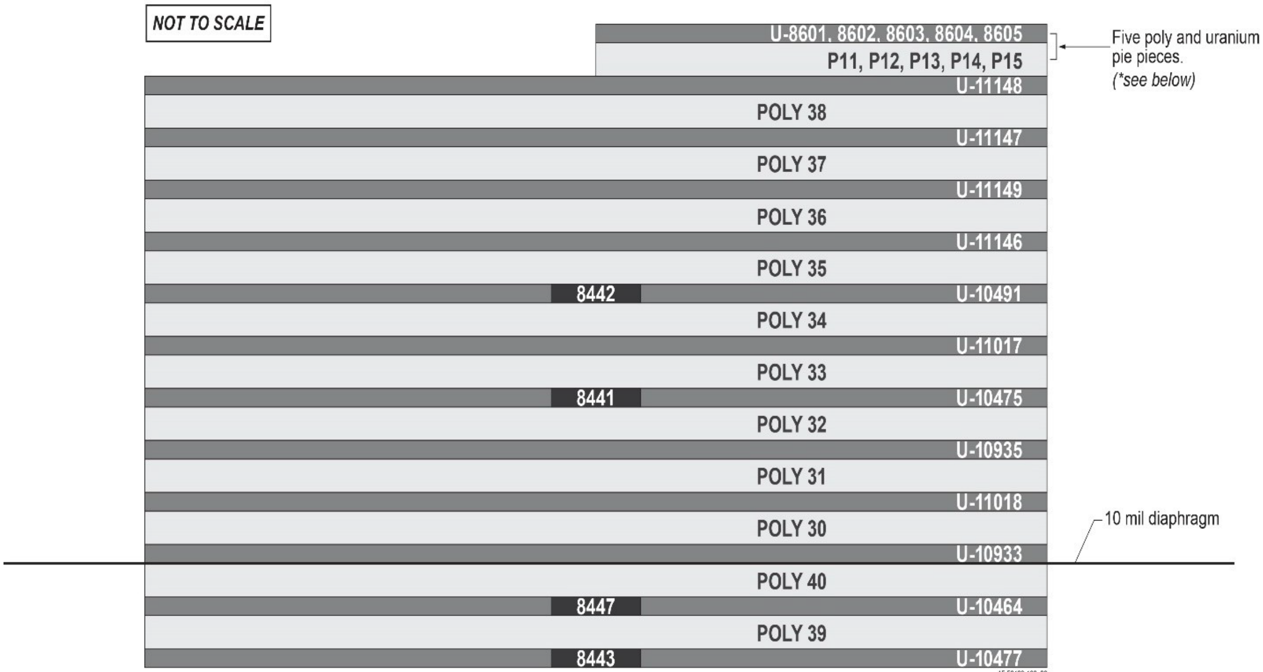

Figure 3.6-1. Configuration of the thin 15 in. diameter HEU metal plate assembly with ¼ in. thick polyethylene between plates, Experiment 3. (Two-dimensional cross section along diameters; based on height measurements for subcritical configurations, the gap between polyethylene and uranium layers for this assembly is 0.0031 in.; above and below and adjacent to the diaphragm should be 0.0015 in.)

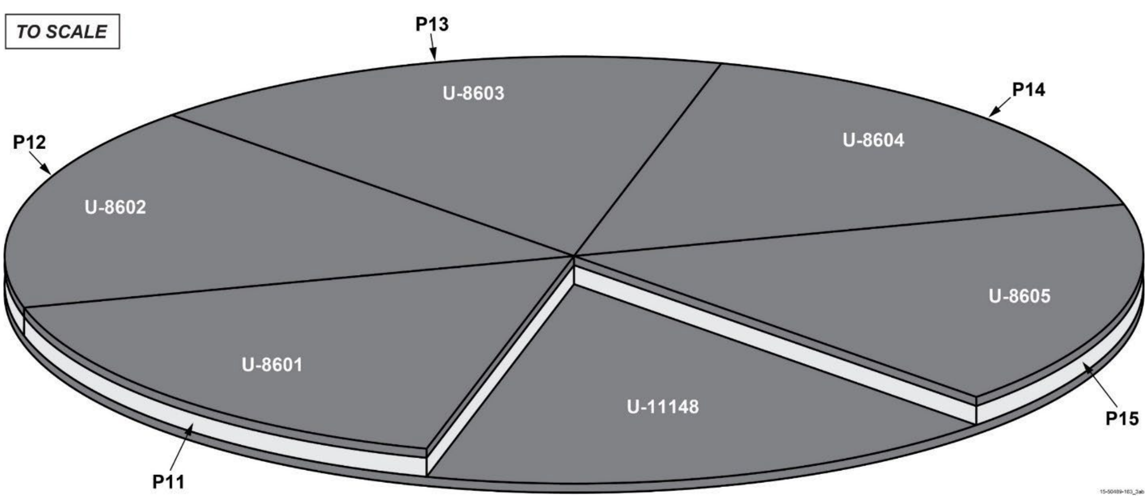

Figure 3.6-2. The configuration of the partial top uranium and ~¼ in. thick polyethylene parts for Experiment 3.

The effects of room return should be calculated using Monte Carlo simulations assuming the wall and floor were 2 ft thick, and the concrete was Oak Ridge concrete, which used crushed limestone instead of sand in the aggregate. The 2 ft thickness for the concrete is adequate for the calculation because neutrons that reach 2 ft into the concrete have little chance of returning to the critical assembly.

3.7. THIN 15 IN. DIAMETER HEU METAL PLATES WITH ALTERNATING 1/4 IN. THICK POLYETHYLENE LAYERS, EXPERIMENT 3A

On July 16, 1969, thin 15 in. diameter HEU metal plates with ¼ in. thick polyethylene layers between them were assembled to near delayed criticality (Page 24, Run 20 ORCEF Logbook E-24). This assembly consisted of 12 thin 15 in. diameter HEU metal plates and twelve polyethylene layers with four uranium pie sections on top. In addition to the pie sections, there were three 1.5 in. diameter cylindrical discs along a radius on top of POLY 41. The configuration of this delayed critical assembly on the vertical assembly machine is given in Figure 3.7-1, and the configuration of the top is given in Figure 3.7-2. The reactivity of the assembly was +61 cents. The effective delayed neutron fraction from Experiment 3 can be used to convert this to a k_{eff} value.

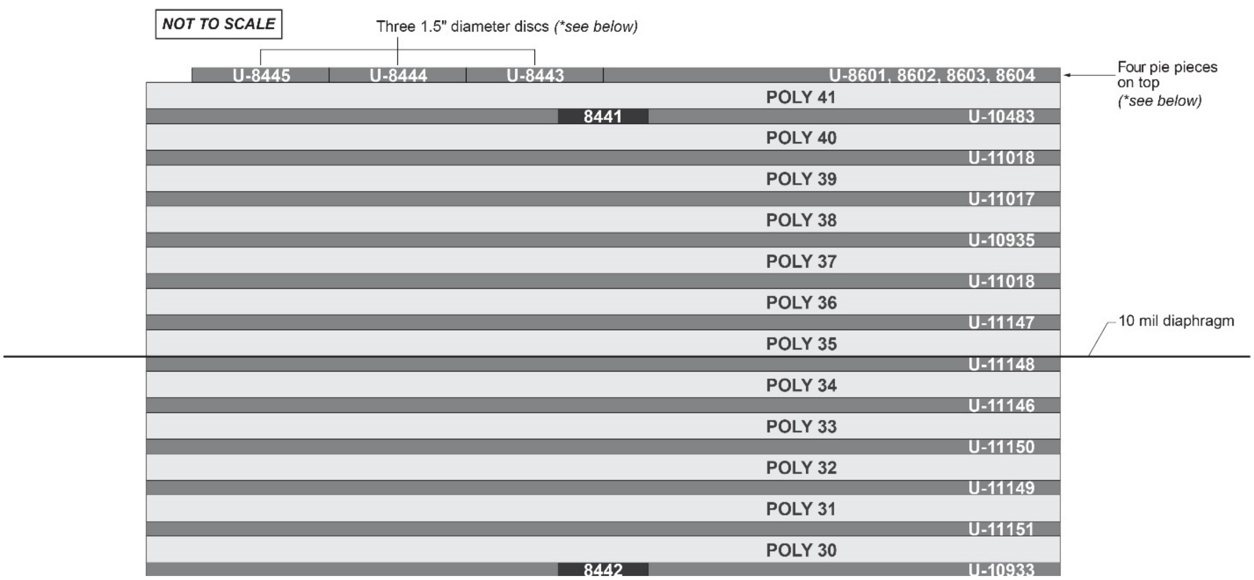

Figure 3.7-1. Configuration of the thin 15 in. diameter HEU metal plates with 1/4 in. thick polyethylene between uranium plates, Experiment 3a. (Two-dimensional cross section along diameters; based on height measurements for subcritical configurations, the gap between polyethylene and uranium layers for this assembly is 0.0031 in.; above and below and adjacent to the diaphragm the gap should be 0.0015 in.).

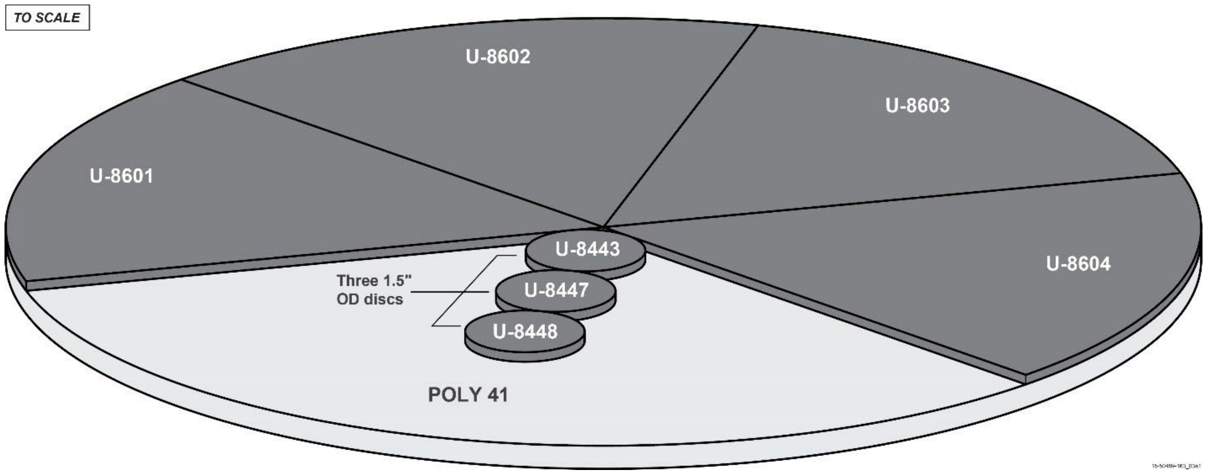

Figure 0-2. The configuration of the partial top uranium and ~¼ in. thick polyethylene parts for Experiment 3a.

The effects of room return need not be calculated, but the value from Experiment 3 should be used.

3.8. THIN 15 IN. DIAMETER HEU METAL PLATES WITH ALTERNATING ¼ IN. THICK POLYETHYLENE LAYERS, EXPERIMENT 3B

On Oct 16, 1969, 12-1/3 thin 15 in. diameter HEU metal plates were assembled (ORCEF logbook E-24, page number 82, Run 121) with ¼ -in. thick polyethylene moderator. This assembly differed from the previous in that it was assembled with the top and bottom full layer consisting of 1/8 in thick polyethylene. The configuration is given in Figure 3.8-1 and the partial top layer in Figure 3.8-2. The pie sections were only uranium on top of the top layer of polyethylene. The reactivity of the assembly was + 22.3 cents and the uranium mass was 79,760 g. The reactivity effect of adding the NE213 scintillator with its lead front cap was an increase in the reactivity of 4.82 cents. The addition of one uranium pie section on top increased the reactivity 99.2 cents to +22.3 cents from the previous run with a reactivity of -76.9 cents.

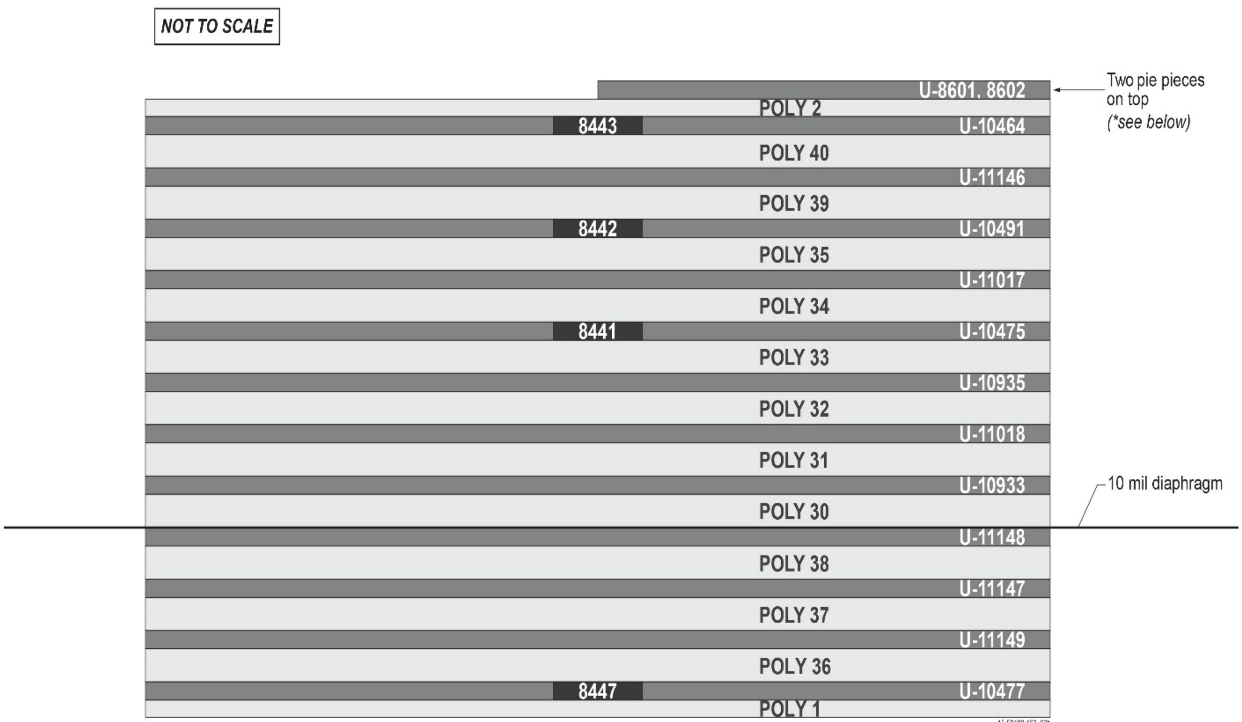

Figure 3.8-1. Configuration of the thin 15 in. diameter HEU metal plate assembly with ¼ in. thick polyethylene between plates, Experiment 3b. (Two-dimensional cross section along diameters; based on height measurements for subcritical configurations, the gap between polyethylene and uranium layers for this assembly is 0.0031 in.; above and below and adjacent to the diaphragm be 0.0015 in.)

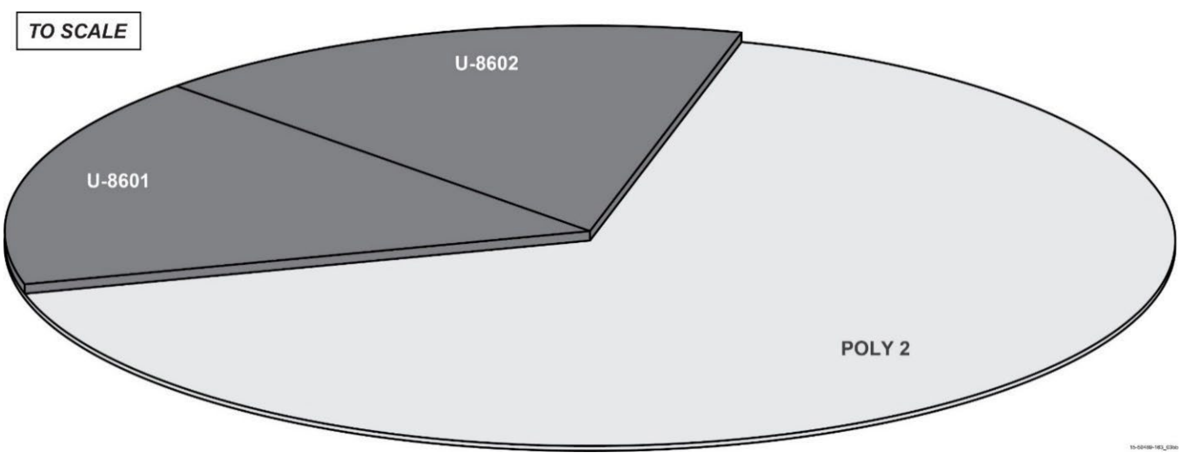

Figure 3.8-2. The configuration of the partial top uranium and ~¼ in. thick polyethylene parts for Experiment 3b.

The effects of room return need not be calculated, but the value from Experiment 3 should be used.

3.9. THIN 15 IN. DIAMETER HEU METAL PLATES WITH ALTERNATING ½ IN. THICK POLYETHYLENE LAYERS, EXPERIMENT 4

On August 9, 1969 (page 51, Run 52, ORCEF logbook E-24), thin 15 in. diameter HEU metal plates with ½ in. thick polyethylene layers between them were assembled to near delayed criticality. This assembly consisted of 8 thin 15 in. diameter HEU metal plates with seven polyethylene layers between them. In addition, there were three equally spaced 60° pie-shaped uranium and polyethylene layers on the top of the uppermost HEU plate, thus covering ½ or 50% of the top. The reactivity of the assembly was +22 cents. The configuration of this delayed critical assembly on the vertical assembly machine is given in Figure 3.9-1, and the configuration of the material on the top layer is shown in Figure 3.9-2.

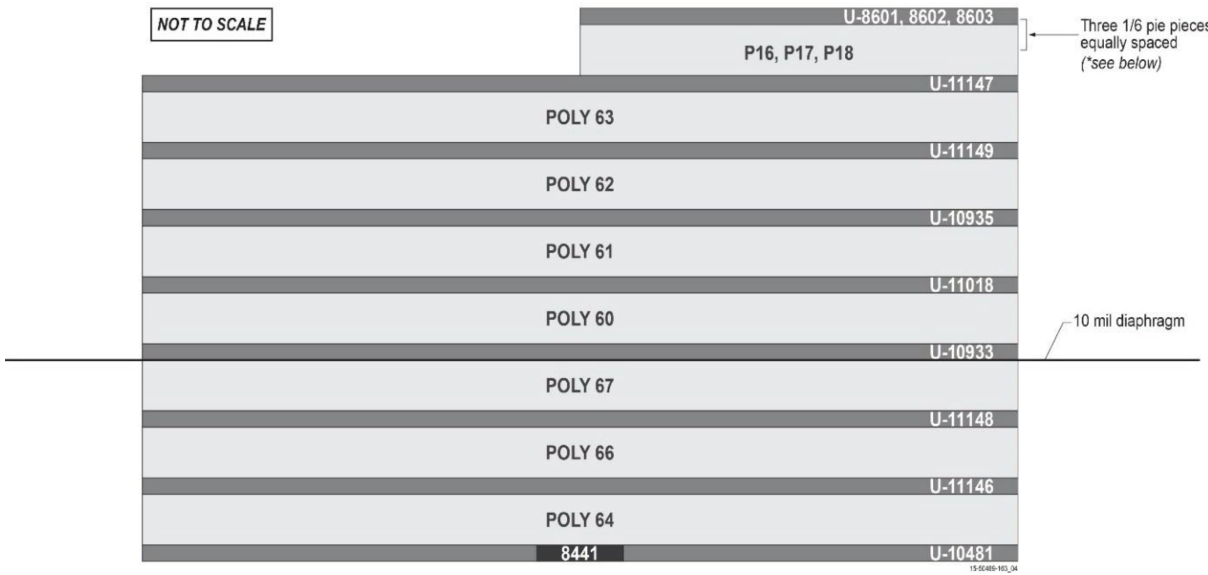

Figure 3.9-1. Configuration of the thin 15 in. diameter HEU metal plate assembly with ½ in. thick polyethylene between plates, Experiment 4. (Two-dimensional cross section along diameters; based on height measurements for subcritical configurations, the gap between polyethylene and uranium layers for this assembly is 0.0043 in.; above and below and adjacent to the diaphragm should be 0.0022 in.).

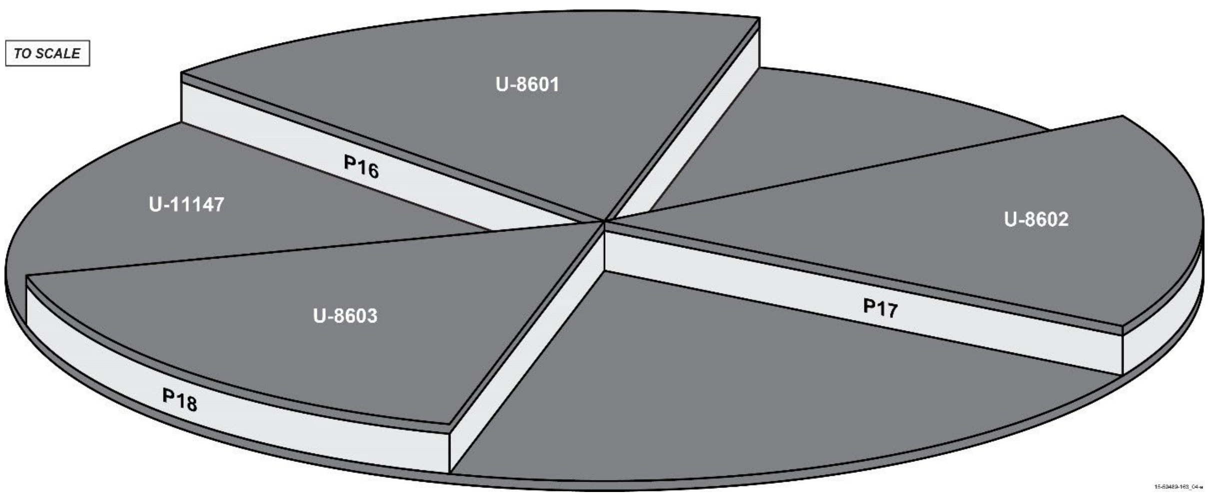

Figure 3.9-2. The configuration of the partial top uranium and ~½ in. thick polyethylene parts for Experiment 4. (Pie sections are 60° apart).

The effects of room return should be calculated using Monte Carlo simulations assuming the wall and floor were 2 ft. thick, and the concrete was Oak Ridge concrete, which used crushed limestone instead of sand in the aggregate. The 2 ft. thickness for the concrete is adequate for the calculation because neutrons that reach 2 ft into the concrete have little chance of returning to the critical assembly.

3.10. THIN 15 IN. DIAMETER HEU METAL PLATES WITH ALTERNATING ½ IN. THICK POLYETHYLENE LAYERS, EXPERIMENT 4A

On October 15, 1969, seven HEU metal plates with ½ in. thick polyethylene layers between them were assembled to near delayed criticality with ¼ in. thick polyethylene above the top uranium plate on the diaphragm and below the lower uranium plate on the lower support stand. This assembly on page 80, run 115 in ORCEF logbook E-24 consisted of 7 thin 15 in. diameter HEU metal plates with six ½ in. polyethylene layers between them. In addition, there were five equally spaced 60° pie-shaped uranium pieces on the top of the uppermost HEU plate, thus covering five-sixths of the top. The stacking order of the parts is given on page 80 of the logbook, run 114. The additional layers of polyethylene reflector on top and bottom reduced the amount of uranium compared to Experiment 4. The vertical lift table with the lower support stand was 0.100 in. from the up position and the reactivity was +29.6 cents above delayed critical. With the sag of the diaphragm, it is assumed that the lower section was in good contact with and supporting the upper section. This assumption can be verified by calculation of the neutron multiplication factor. If calculated k_{eff} agrees with the measured reactivity converted to kef units using the delayed neutron fraction then the contact was good. The configuration of this delayed critical assembly on the vertical assembly machine is given in Figure 3.10-1 and consists of seven uranium plates with ½ in. thick polyethylene between them and a ¼ in. thick layer of polyethylene reflector above the top and bottom uranium plates, and it was assumed that the uranium pie sections were on top of the ¼ in. thick polyethylene layer on the top. The configuration of the partial top layer is given in Figure 3.10-2.

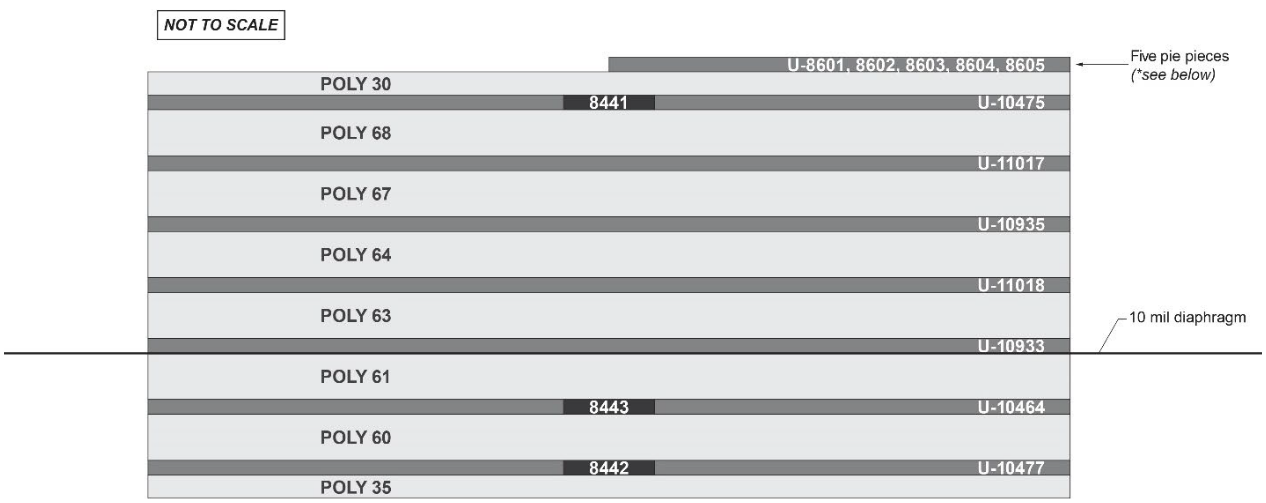

Figure 3.10-1. Configuration of the thin 15 in. diameter HEU metal plate assembly with ½ in. thick polyethylene between plates, Experiment 4a. (Two-dimensional cross section along diameters; based on height measurements for subcritical configurations, the gap between polyethylene and uranium layers for this assembly is 0.0043 in.; the gap between polyethylene and uranium layers for this assembly is 0.0043 in. based on measurements; above and below and adjacent to the diaphragm should be 0.0022 in.)

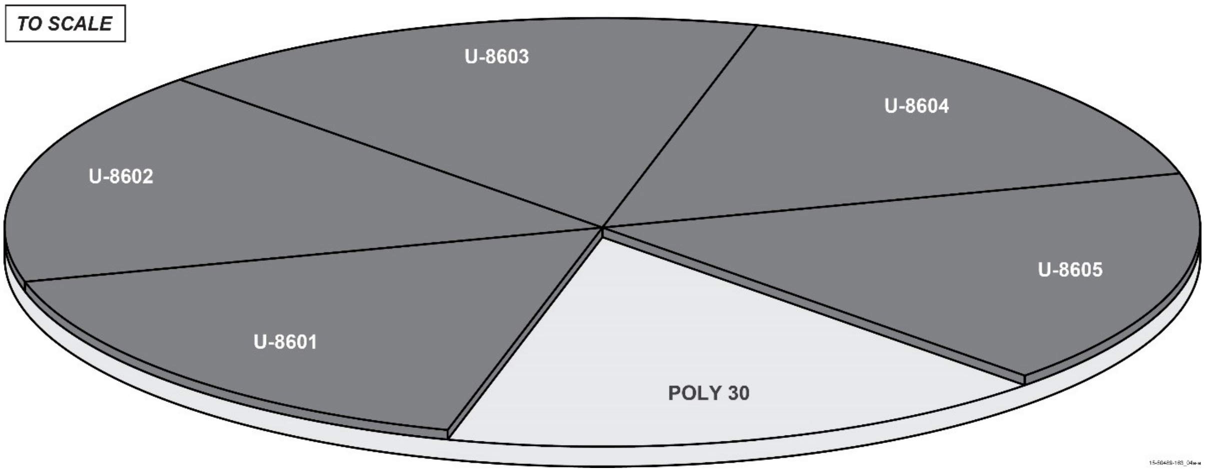

Figure 3.10-2. The configuration of the partial top uranium and ~½ in. thick polyethylene parts for Experiment 4a.

Another configuration for experiment 4a is that the ¼ in. thick layer was removed, and the polyethylene pie sections P16 to P20 were adjacent and on top of the last full uranium plate with uranium metal pie sections (uranium parts 8601 to 8605) on top of the polyethylene pie sections.

The actual configuration of the experiment may be determined by calculation of the various configurations and that closest to the measured reactivity may be the appropriate configuration. If none are close, then this Experiment would not be an appropriate benchmark.

The effects of room return need not be calculated, but the value from Experiment 4 should be used.

3.11. THIN 15 IN. DIAMETER HEU METAL PLATES WITH ALTERNATING 1 IN. THICK POLYETHYLENE LAYERS, EXPERIMENT 5

For experiments 5 to 10 and their variations, the identification of the polyethylene parts is not given in the logbook. The polyethylene parts on the diaphragm were assumed for a given thickness in the experiments. It was assumed that the part number identification number increased from the lowest to the highest on the diaphragm and then sequentially from the lowest polyethylene part on bottom of the lower section to the highest on the top of the lower section as described in the last page of the logbook

On Oct 13, 1969, thin 15 in. diameter HEU metal plates with 1.0 in. thick polyethylene layers between them were assembled to near delayed criticality. This assembly consisted of 5 thin 15 in. diameter HEU metal plates with polyethylene layers between them. In addition, there was a ½ in. thick polyethylene reflector layer on bottom and the top reflector was ⅜ in. of polyethylene. The configuration of this delayed critical assembly on the vertical assembly machine is given in Figure 3.11-1. The reactivity of this assembly was recorded on Page 75 of ORCEF logbook E-24, run 91 and was +15.0 cents. The mass of this configuration was 78,693 g.

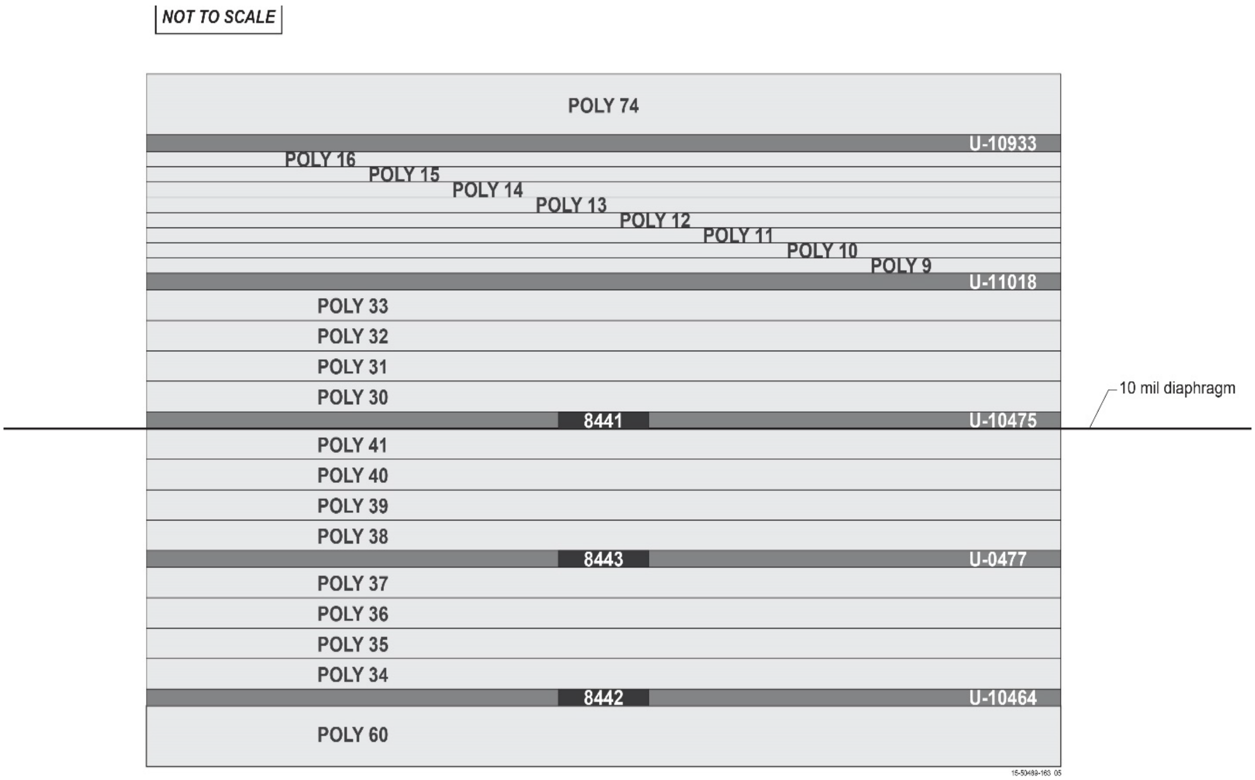

Figure 3-11-1. Configuration of the thin 15 in. diameter HEU metal plate assembly 1 in. thick polyethylene between plates, Experiment 5. (Two-dimensional cross section along diameters.)

The polyethylene as bottom reflector was not specified by part number but only by the nominal thickness of half an inch, and it was assumed that it was part number POLY 60. The uncertainty in this assumption will have to be evaluated in the final benchmark analysis. The gap between parts was not measured for assemblies with polyethylene thickness more than one half inch. It was assumed that the gap between Poly 60 and 74 and the adjacent uranium layers was 0.0043 in. It was assumed the gaps associated with Poly 9 to Poly 16 were 0.0032 in., and the gaps associated with Poly 30 to Poly 41 were 0.0031 in. Above and below and adjacent to the diaphragm the gaps should be 0.0015 in.

There was a variation of the top reflector that reduced the reactivity. The ORCEF logbook E-24 states that removing another 1/32 in. thick top reflector (Run 95, page 76) reduced the reactivity to −3.67 cents. This configuration had a top reflector thickness of 11/32 in. The reactivity change in reducing the top reflector by 1/32 in. was −30.5 cents.

The effects of room return should be calculated using Monte Carlo simulations assuming the wall and floor were 2 ft thick, and the concrete was Oak Ridge concrete, which used crushed limestone instead of sand in the aggregate. The 2 ft thickness for the concrete is adequate for the calculation because neutrons that reach 2 feet into the concrete have little chance of returning to the critical assembly.

3.12. THIN 15 IN. DIAMETER HEU METAL PLATES WITH ALTERNATING 1.25 IN. THICK POLYETHYLENE LAYERS, EXPERIMENT 6

On Oct 13, 1969, thin 15 in. diameter HEU metal plates with 1.25 in. thick polyethylene layers between them were assembled to near delayed criticality. This assembly consisted of four thin 15 in. diameter HEU metal plates with polyethylene layers between them. In addition, there were three adjacent 60° pie-shaped uranium and polyethylene layers on the top of the uppermost thin 15 in. diameter HEU metal plate, thus covering half of the top. The reactivity of the near delayed critical configuration was +10.24 cents. The configuration of this delayed critical assembly on the vertical assembly machine is given in Figure 3.12-1, and the configuration of the top of the assembly is given in Figure 3.12-2. The identification of the polyethylene moderator parts was not defined in the logbook. It was assumed that the lowest polyethylene part above the diaphragm was the lowest of a given thickness and increases towards the upper polyethylene layer. The part numbers continued to increase from the bottom to top of the section below the diaphragm. The lowest part numbers for the ⅛, ¼, and ½ were 1, 30, and 60, respectively.

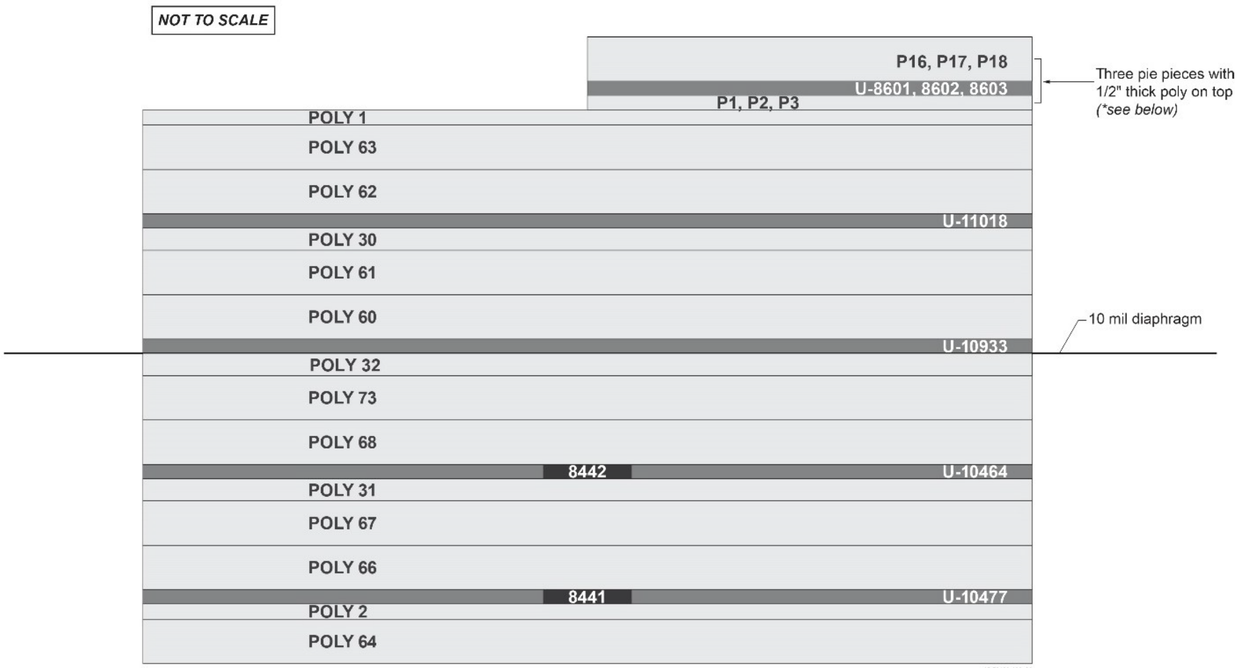

Figure 3-12-1. Configuration of the thin 15 in. diameter HEU metal plate assembly with 1.25 in. thick polyethylene between plates, Experiment 6. (Two-dimensional cross section along diameters).

The gap between parts was not measured for this assembly and was assumed to be 0.0043 in. between ½ in thick polyethylene layers; between ¼ and ½ in. thick polyethylene layers, the gap was assumed to be 0.0031 in.; between the ¼ in. thick polyethylene and the uranium plates, it was assumed to be 0.0031 in.; above and below and adjacent to the diaphragm the gap should be 0.0015 in.

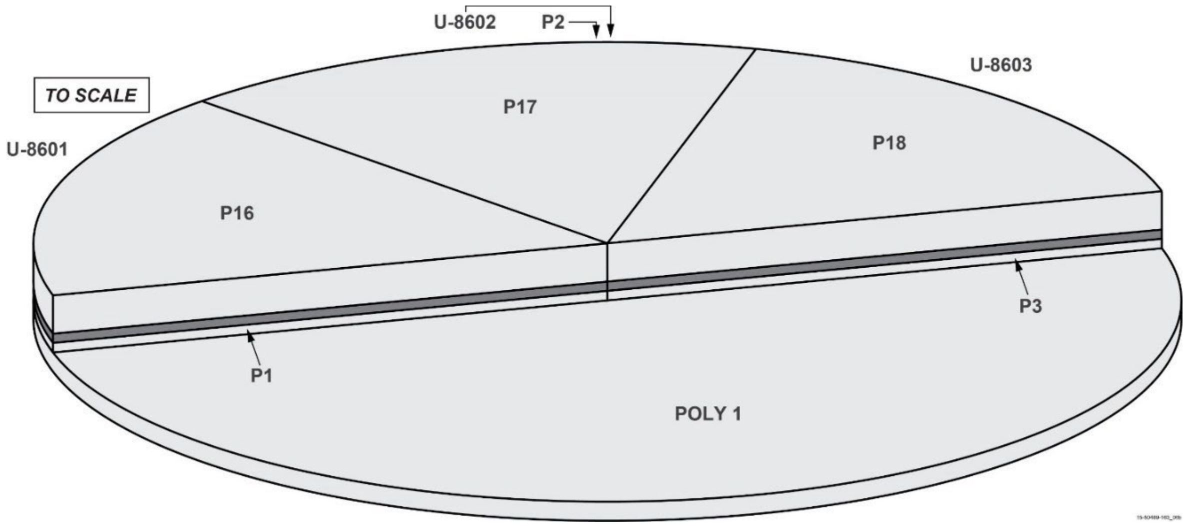

Figure 3-11-2. The configuration of the partial top uranium and ~1.25 in. thick polyethylene parts for Experiment 6.

The effects of room return should be calculated using Monte Carlo simulations assuming the wall and floor were 2 ft thick, and the concrete was Oak Ridge concrete, which used crushed limestone instead of sand in the aggregate. The 2 ft thickness for the concrete is adequate for the calculation because neutrons that reach 2 ft into the concrete have little chance of returning to the critical assembly.

3.13. THIN 15 IN. DIAMETER HEU METAL PLATES WITH ALTERNATING 1.5 IN. THICK POLYETHYLENE LAYERS, EXPERIMENT 7

On Oct 14, 1969, thin 15 in. diameter HEU metal plates with 1.5 in. thick polyethylene layers between them were assembled to near delayed criticality (page 77, run 103, ORCEF logbook E-24). This assembly consisted of 4 thin 15 in. diameter HEU metal plates with polyethylene layers between them. In addition, there were two adjacent 60° pie-shaped uranium and polyethylene layers on the top of the uppermost HEU plate, thus covering ⅓ or 33% of the top. The configuration of this delayed critical assembly on the vertical assembly machine is given in Figure 3.13-1 after removal of ⅛ in. thick polyethylene from under the two uranium pie pieces. The configuration of the top of the assembly is given in figure 3.13-2. The reactivity of the assembly was +20.4 cents before removal and +9.72 cents after.

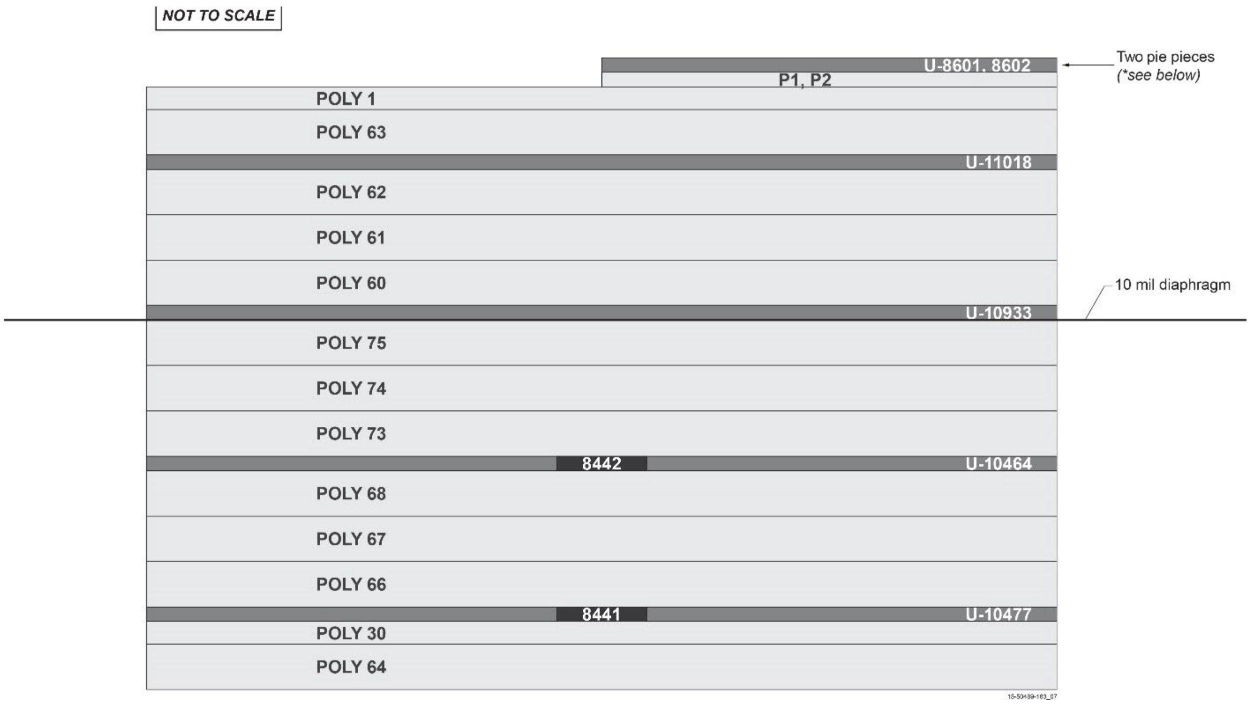

Figure 3-13-1. Configuration of the thin 15 in. diameter HEU metal plate assembly 1.5 in. thick polyethylene between plates, Experiment 7. (Two-dimensional cross section along diameters; the gap between parts was not measured for this assembly was assumed to be 0.0043 in. between ½ in. thick polyethylene layers and ½ in. thick polyethylene and uranium metal layers. Above and below and adjacent to the diaphragm the gap should be 0.0022 in.)

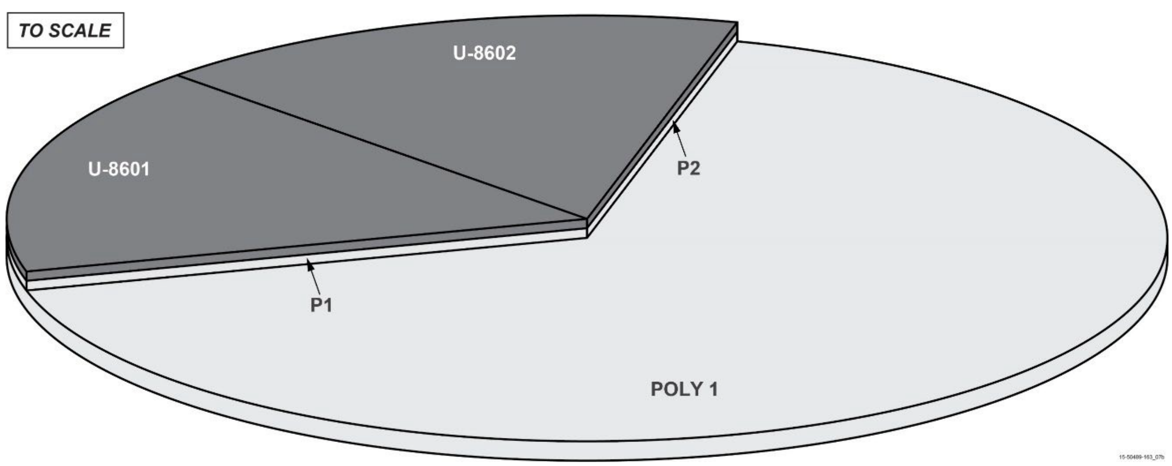

Figure 3.13-2. The configuration of the partial top uranium and ~1.5 in. thick polyethylene parts for Experiment 7.

The effects of room return should be calculated using Monte Carlo simulations assuming the wall and floor were 2 ft thick, and the concrete was Oak Ridge concrete, which used crushed limestone instead of sand in the aggregate. The 2 ft thickness for the concrete is adequate for the calculation because neutrons that reach 2 ft into the concrete have little chance of returning to the critical assembly.

3.14. THIN 15 IN. DIAMETER HEU METAL PLATES WITH ALTERNATING 1.75 IN. THICK POLYETHYLENE LAYERS- EXPERIMENT 8

On Oct 14, 1969, thin 15 in. diameter HEU metal plates with 1.75 in. thick polyethylene layers between them were assembled to near delayed criticality (ORCEF logbook E-24, page 77, Run 106). This assembly consisted of 4 thin 15 in. diameter HEU metal plates with three polyethylene layers between them. In addition, there were two adjacent 60° pie-shaped uranium and polyethylene layers on the top of the uppermost HEU plate, thus covering ⅓ or 33.3% of the top. The configuration of this near delayed critical assembly on the vertical assembly machine is given in Figure 3.13-1, and the configuration of the top is given in Figure 3.13-2. The reactivity of the system was −22 cents.

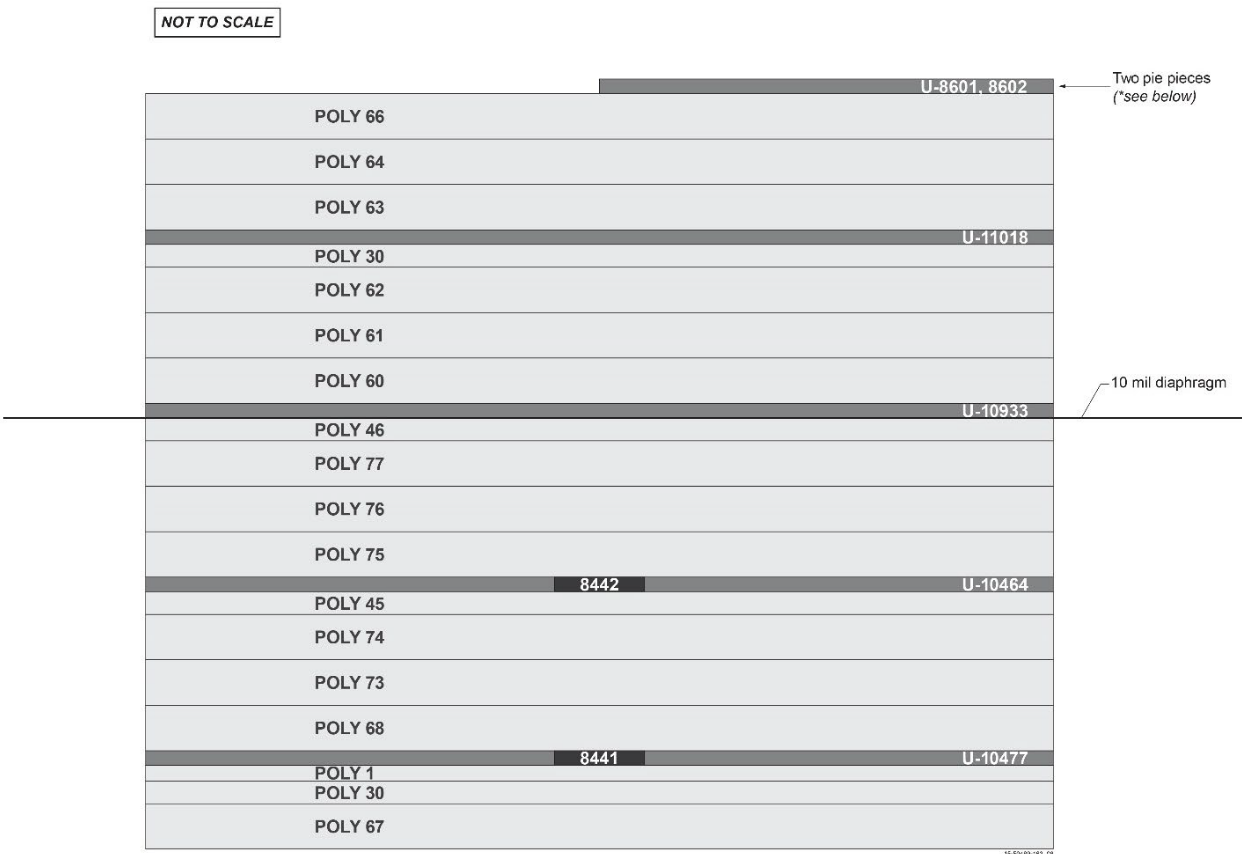

Figure 3.14-1. Configuration of the thin 15 in. diameter HEU metal plate assembly with 1.75 in. thick polyethylene between plates, Experiment 8. (Two-dimensional cross section along diameters; the gap between parts was not measured for this assembly. The gap between ½ in. thick polyethylene layers and ½ in. thick polyethylene and uranium metal layers was assumed to be 0.0043 in. Above and below and adjacent to the diaphragm the gap should be 0.0016 in. The gap between the ½ and ¼ in. thick polyethylene layers is assumed to be 0.0037 in.)

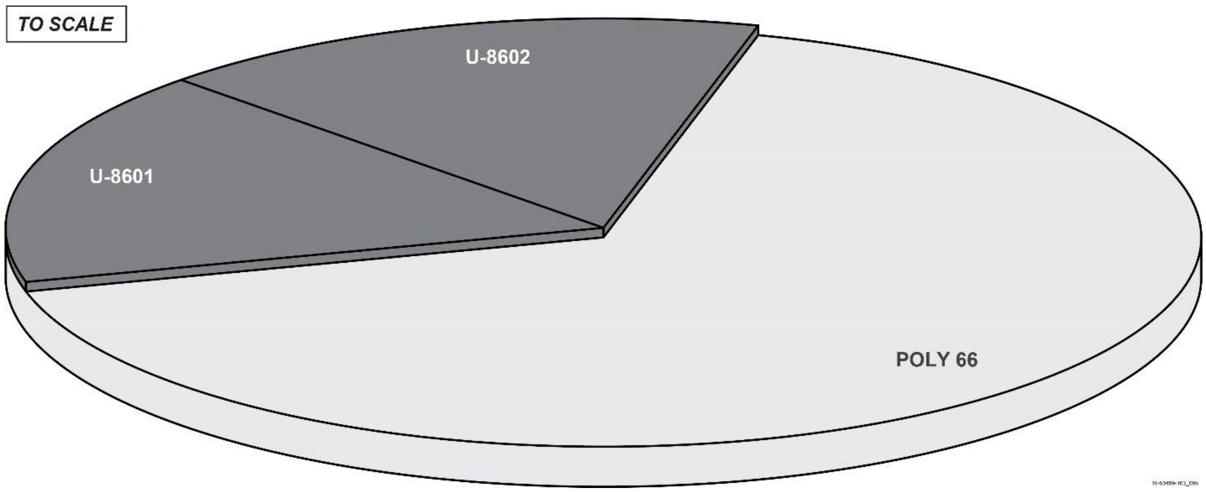

Figure 3.14-2. The configuration of the partial top uranium and ~1.75 in. thick polyethylene parts for Experiment 8.

The effects of room return should be calculated using Monte Carlo simulations assuming the wall and floor were 2 ft thick, and the concrete was Oak Ridge concrete, which used crushed limestone instead of sand in the aggregate. The 2 ft thickness for the concrete is adequate for the calculation because neutrons that reach 2 ft into the concrete have small chance of returning to the critical assembly.

3.15. THIN 15 IN. DIAMETER HEU METAL PLATES WITH ALTERNATING 2.0 IN. THICK POLYETHYLENE LAYERS, EXPERIMENT 9

On Oct 14, 1969, thin 15 in. diameter HEU metal plates with 2.0 in. thick polyethylene layers between them were assembled to near delayed criticality. This assembly consisted of 4 thin 15 in. diameter HEU metal plates with three polyethylene layers between them. In addition, there were four adjacent 60° pie-shaped uranium and polyethylene layers on the top of the uppermost thin 15 in. diameter HEU metal plate, thus covering ⅔ or 67% of the top. The reactivity of the assembly was −23.85 cents. The configuration of this delayed critical assembly on the vertical assembly machine is given in Figure 3.15-1, and the configuration of the top is given in Figure 3.15-2.

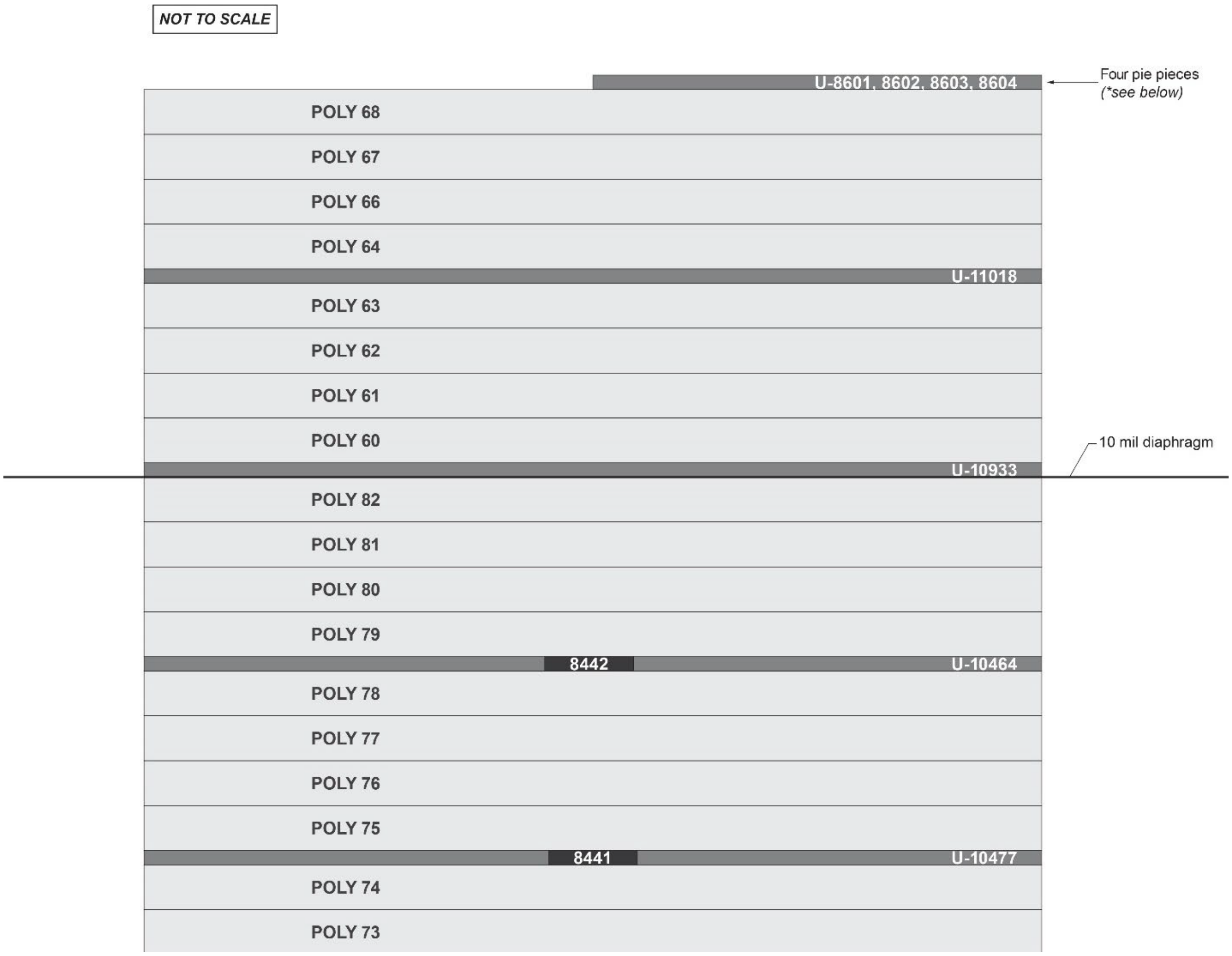

Figure 3.15-1. Configuration of the thin 15 in. diameter HEU metal plate assembly with 2.0 in. thick polyethylene between plates, Experiment 9. (Two-dimensional cross section along diameter; the gap between parts was not measured for this assembly and was assumed to be 0.0043 in. Above and below and adjacent to the diaphragm the gap should be 0.0022 in.)

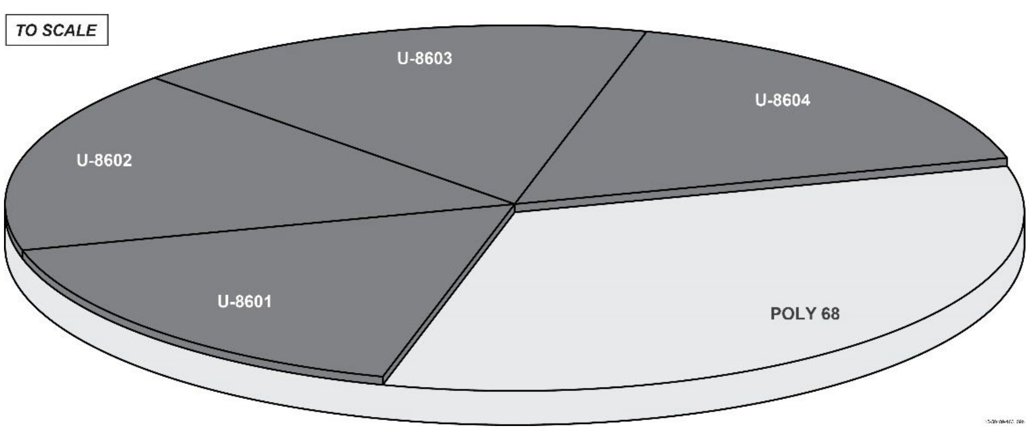

Figure 3.15-2. The configuration of the partial top uranium and 2.0 in. thick polyethylene parts for Experiment 9.

The effects of room return should be calculated using Monte Carlo simulations assuming the wall and floor were 2 ft thick, and the concrete was Oak Ridge concrete, which used crushed limestone instead of sand in the aggregate. The 2 ft thickness for the concrete is adequate for the calculation because neutrons that reach 2 ft into the concrete have little chance of returning to the critical assembly.

3.16. THIN 15 IN. DIAMETER HEU METAL PLATES WITH ALTERNATING 2.375 IN. THICK POLYETHYLENE LAYERS, EXPERIMENT 10

On Oct 15, 1969 (Page 79, Run 112, ORCEF logbook E-24), thin 15 in. diameter HEU metal plates with 2.375 in. thick polyethylene layers between them were assembled to near delayed criticality. This assembly consisted of 6 thin 15 in. diameter HEU metal plates with five polyethylene layers between them. In addition, there were two adjacent 60° pie-shaped uranium and polyethylene layers on the top of the uppermost HEU plate, thus covering ⅓ of the top. The reactivity of the assembly was +3.6 cents. The configuration of this delayed critical assembly on the vertical assembly machine is given in Figure 3.16-1. There is some ambiguity about the pie section on top, as the logbook states that there were two pie pieces on top but also says the number of uranium layers was 6 1/2 which would mean three pie pieces. This ambiguity may be resolved by calculations. The assumed configuration of the top is given in Figure 3.16-2.

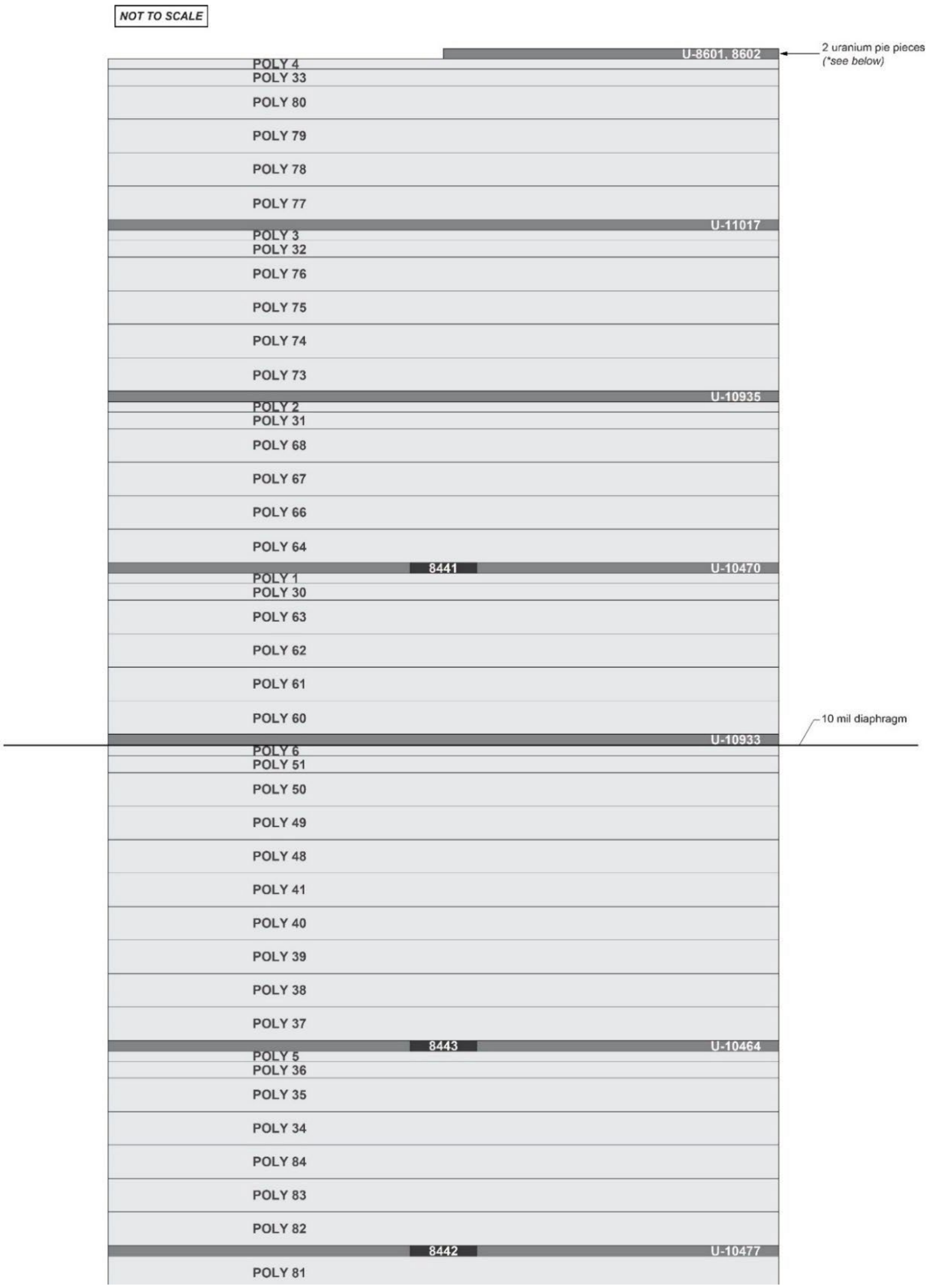

Figure 3.16-1. Configuration of the thin 15 in. diameter HEU metal plate assembly with 2.375 in. thick polyethylene between plates, Experiment 10. (Two-dimensional cross section along diameter; the gap between all ½ in. thick polyethylene layers and uranium metal layers was not measured for this assembly and was assumed to be 0.0043 in. The gap between ⅛ and ¼ in. thick polyethylene layers and between ¼ in. polyethylene layers and metal layers was assumed to be 0.00032 in. The gap between Poly 4 and the pie-shaped pieces on top is also 0.0032 in. and below and adjacent to the diaphragm the gap should be 0.0016 in. The gap between the bottom polyethylene layer and the lowest uranium metal plate was assumed to be 0.0043 in.)

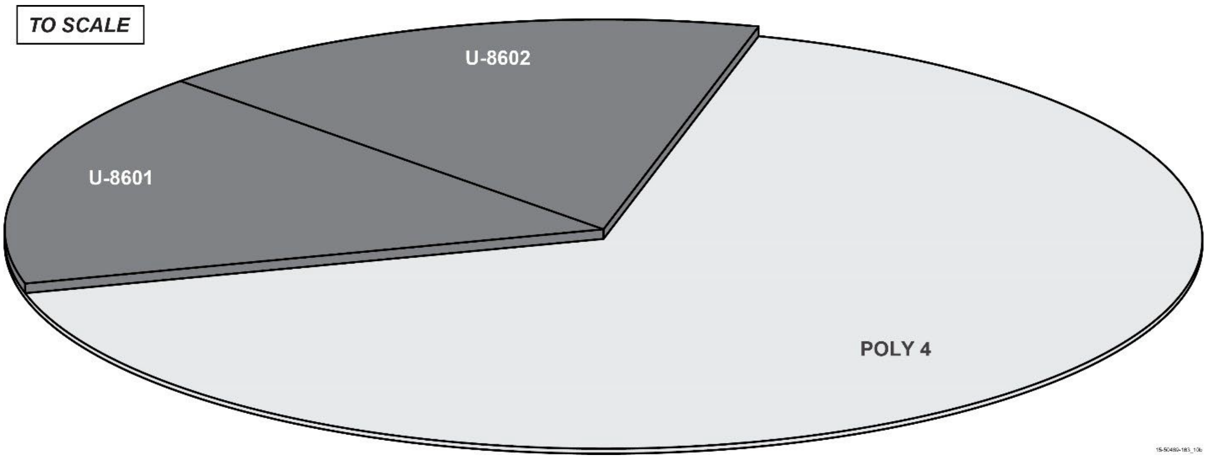

Figure 3.16-2. The configuration of the partial top uranium and ~2.375 in. thick polyethylene parts for Experiment 10.

The effects of room return should be calculated using Monte Carlo simulations assuming the wall and floor were 2 ft thick, and the concrete was Oak Ridge concrete, which used crushed limestone instead of sand in the aggregate. The 2 ft thickness for the concrete is adequate for the calculation because neutrons that reach 2 ft into the concrete have little chance of returning to the critical assembly.

3.17. SUMMARY OF THE NEAR DELAYED CRITICAL CONFIGURATIONS

A wide variety of configurations with polyethylene layers have been assembled. Some of the configurations are well defined in the logbook and others are not. Those that are well defined can serve as the basis of future ICSBEP benchmarks. Calculations may help decide whether those that are not well defined will be adequate benchmarks. Calculation for slightly varying configurations could be used to decide which configuration was assembled. The ambiguities of the configurations are identified in the previous descriptions of the measurements. The reactivity in dollars can be converted to k_{eff} values using calculated effective delayed neutron fractions where 100 cents equals the delayed neutron fraction. A calculation of the delayed neutron fraction will be required for each assembly configuration with different polyethylene thicknesses. For the subcritical measurements made by the inverse kinetics rod drop (IKRD) method described below, k_{eff} values can be obtained in the same way. These subcritical configurations can also be used for the basis of future ICSBEP benchmarks.

4. SUPPLEMENTAL MEASUREMENTS

4.1. INVERSE KINETIC ROD DROP MEASUREMENTS OF SUBCRITICALITY

The IKRD technique (described in reference [3]) was used to measure the subcritical reactivity in dollars using an analog computer designed, built, and provided to ORNL by Caesar Sastre of Brookhaven National Laboratory [22]. In this method, the system is brought to delayed criticality and until delayed neutron equilibrium. In these measurements near delayed criticality, an external Cf source was not present. The other way to perform such a measurement for a subcritical configuration is to assemble the system to the subcritical state with a neutron source present; then, with the source present, remove part of the system and measure the final reactivity of the remaining system with the source present. The system was brought to the assembled condition, and then the lower part on the vertical lift was removed and the time dependence of the counts in a detector is measured. A configuration of an assembly is shown in the photograph of Figure 4.1-1. The system to be measured was located on the diaphragm. On the lower section was additional material to achieve the assembled condition. The lower section on the support stand was raised till contact with the diaphragm until the diaphragm was level. The lower section in Figure 4.1-1 contained only one thin 15 in. diameter HEU metal uranium plate with one polyethylene layer above it. Unlike the assembly shown in Figure 4.1-1, the subcritical assemblies had full uranium plates and full layers of polyethylene. The bottom of the detector for these measurements (ORCEF logbook E-24 Page 6) was located 42 inches above the diaphragm. Below the detector was a section of 8 × 8 × 2 in. thick lead to reduce any gamma response. The detector was a 2 in. diameter, 18 in. long BF_3 counter wrapped with 0.037 in. thick cadmium except for the bottom and top. The axis of the counter was vertical and coincided with the extension of the axis of the assemblies. The analog computer gave the subcritical reactivity in dollar units where one dollar (100 cents) was equivalent to the effective delayed neutron fraction. To obtain the subcriticality in k_{eff} units the effective delayed neutron fraction must be calculated for each configuration of each assembly with different polyethylene thicknesses. These measurements were not performed for the polyethylene thicknesses greater than 0.5 in. The results of these measurement are given in Table 4.1-1 and 4.1-2.

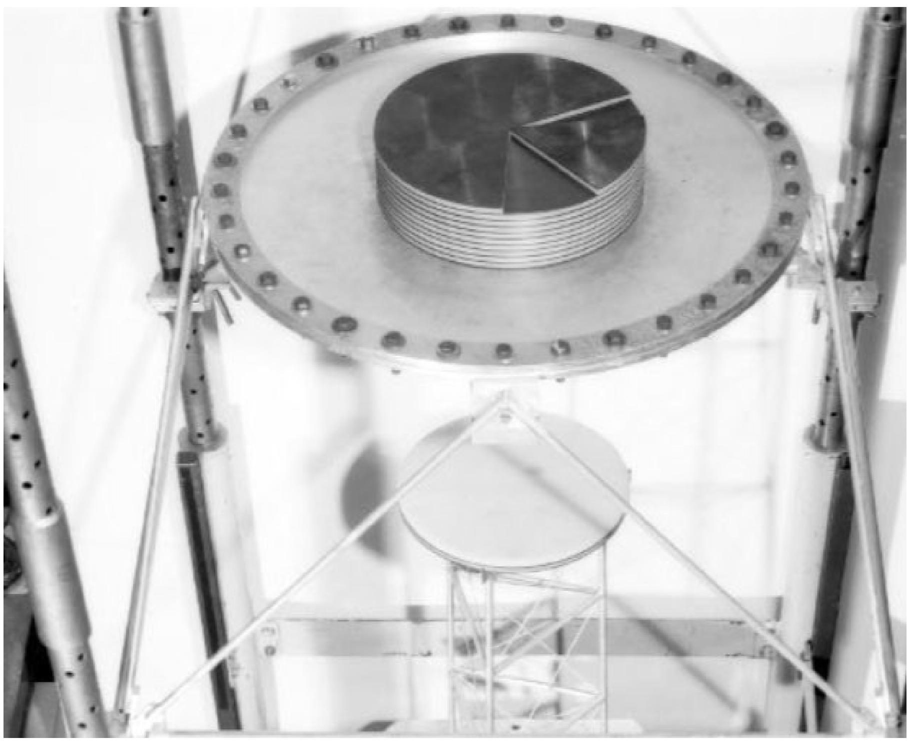

Figure 4.1-1. Typical configuration of assemblies for IKRD measurements. (For subcritical configurations, a source was present, and all assemblies had a full uranium plate on top and bottom. The lower section on the vertical lift was up just prior to the IKRD measurement. The delayed neutrons were allowed to come to equilibrium before the lower section was removed quickly and the analog computer which was recording the count rate determined the reactivity of the material on the diaphragm)

The results given in Table 4.1-1 are for configurations for which the HEU metal plates were accurately defined in the logbook. The results in Table 4.1-2 are for configurations that are not given in the logbook. The specified configurations of Table 4.1-1 could result in more accurate benchmarks. For the measurement in Table 4.1-2, it is assumed that the order of the uranium metal parts was the same as some of entries of Table 4.1-1.

For benchmarking calculations, the subcritical neutron multiplication factor (k_{eff}) can be obtained using the equivalency between the calculated effective delayed neutron fraction and the reactivity. The reactivity in dollars is converted to k_{eff} units using the fact that one dollar equals the value of the delayed neutron fraction. Calculation would have to be performed for each configuration. After this conversion these subcritical measurements could be subcritical benchmarks.

Table 4.1-1. Subcritical reactivity in dollars for the subcritical assemblies from the IKRD measurement for the subcritical configurations that are defined in the logbook.

Nominal Poly thickness (in.)	Page & run	Number of HEU plates	Order of U parts bottom to top[a]	Poly layers	Order of poly parts bottom to top	Reactivity [b] (dollars)
1/8	p30 30 & 31	12	10933, 11018, 10935, 10475 (8441), 11017, 10464(8442), 10477(8443), 10491(8447), 11146, 11148.	11	1 to 11	−21.00, −21.97, −22.63, −21.48, −22.22
1/8	p43 33	14 U as on July 25	10933, 11018, 10935, 10475 (8441),11017, 10464(8442), 10457(8443), 10458(8447), 10477(8448), 10491(8449), 11146, 11149, 11147, 11148	13	3 to 15	−12.74
1/8	p43 34	15	Added to top 10467(8451) on top	14	Added poly 16 on top	−8.57
1/16	p44 35	17	10933, 11018, 10935, 10475 (8441), 11017, 10464(8442), 10457(8443),10458(8447), 10477(8448), 10491(8449), 11146, 11149, 11147, 11148, 10467(8451), 10493(8452), 10487(8453)	16	Poly 90 to 98, Poly op, qr, st, mn, kl, ij, gh	−14.23
1/16	p44 36	18	Added 11151	17	Added ef to top	−10.42
1/16	p44 37	15	Removed from top11151, 10487(8453), 10493(8452)	14	Removed ef, gh, ij from top	−20.71
1/16	p44 38	13	10933, 11018, 10935, 10475(8441), 11017, 10464(8442), 10457(8443), 10458(8447), 10477(8448), 10491(8449), 11146, 11149, 11147,	12	Poly 90 to 98, op, qr, st	−25.46
1/16	p44 39	11	Removed from top 1147 and 1149	10	Poly 90 to 98, op	−28.84
1/4	p45 40	6	10933, 11018, 10935, 11149, 11147, 11148	5	Poly 30 to 34	−16.46
1/4	p45 41	7	Added to top 11146	6	Added Poly 35 to top	−26.61
1/4	p45 42	8	Added to top 10475(8441)	7	Added Poly 36 to top	−23.17
1/4	p45 43	9	Added to top 11151	8	Added Poly 37 to top	−19.52
1/4	p46 44	10	Added to top11017	9	Added Poly 38 to top	−14.44

1/4	p46 45	11	Added to top 10464(8442)	10	Added Poly 39 to top	−9.36

Table 4.1-1. Subcritical reactivity in dollars for the subcritical assemblies from the IKRD measurement for the subcritical configurations that are defined in the logbook (continued).

Nominal Poly thickness (in.)	Page & run	Number of HEU plates	Order of U parts bottom to top[a]	Poly layers	Order of poly parts bottom to top	Reactivity [b] (dollars)
1⁄2	p46 46	5	10933, 11018, 10935, 11149, 11147	4	Poly 60 to 63	−24.77
1⁄2	p46 47	6	Added to top 11148	5	Added Poly 64 to top	−19.05
1⁄2	p46 48	7	Added to top 11146	6	Added Poly 66 to top	−11.29
1⁄2	p67 64	7	10933, 11018, 10475(8441), 10491(8442), 10464(8443), 10477(8447), 10458(8448)	6	Poly 61 to 63, Poly 69, Poly 70, Poly 71	−12.22, −12.13, −11.99, −12.13
1⁄2	p67 65	5	Removed 10477(8447) and 10458(8448)	4	Removed Poly 70 and 71 from top	−26.43,−25.89

[a] The bottom U plate was adjacent to the diaphragm and all plates with axial holes (with numbers less than 10933) had the holes filled with uranium inserts in order from 8441 upward to the top. Numbers in parenthesis are the part numbers of the inserts.
[b]Values given in the logbook with more significant figures than accurate.

Table 4.1-2. Subcritical reactivity in dollars for the subcritical assemblies from the IKRD measurement for which the configurations are not defined in the logbook.

Nominal Poly thickness (in.)	Page	Run	Number of HEU plates	Order of U parts bottom to top[a]	Number of Poly layers	Order of poly parts bottom to top [b]	Reactivity [c] (dollars)
1⁄4	68	66	10	10933, 11018, 10935, 10475(8441),11017, 10464(8442), 10457 (8443), 10458(8447), 10477(8448), 10491 (8449)	9	Poly 30 to Poly 38	−15.82, −15.71
1⁄4	68	67	8	10933, 11018, 10935, 10475(8441),11017, 10464(8442), 10457(8443), 10458(8447),	7	Poly 30 to 36	−23.50, −24.6, −24.2
1⁄4	68	68	6	10933, 11018, 10935, 10475(8441),11017, 10464(8442),	5	Poly 30 to 34	−28.0
1⁄8	68	69	15	10933, 11018, 10935, 10475(8441),11017, 10464(8442), 10457 (8443), 10458(8447), 10477(8448), 10491 (8449), 11146, 11149, 11147, 11148, 10467(8451)	14	Poly 1 to 14	−9.98,

Table 4.1-2. Subcritical reactivity in dollars for the subcritical assemblies from the IKRD measurement for which the configurations are not defined in the logbook (continued).

Nominal Poly thickness (in.)	Page	Run	Number of HEU plates	Order of U parts bottom to top[a]	Poly layers	Order of poly parts bottom to top [b]	Reactivity [c] (dollars)
1/8	69	70	15	10933, 11018, 10935, 10475(8441),11017, 10464(8442), 10457 (8443), 10458(8447), 10477(8448), 10491 (8449), 11146, 11149, 11147, 11148, 10467(8451)	14	Poly 1 to 14	−9.97, −9.97, −9.97
1/8	69	71	14	Removed from top 10464(8451)	13	Poly 1 to 13	−14.10, −14.42, −13.9. −14.23
1/8	69	72	12	Removed from top11148 &11147	11	Poly 1 to 11	−22.5, −22.6, −22.6, −22.6, −23.5
1/8	69	73	10	Removed from top 11149 & 11146	9	Poly 1 to 9	−26.7, −28.5, −25.8
1/16	70	74	12	10933, 11018, 10935, 10475(8441),11017, 10464(8442), 10457 (8443), 10458(8447), 10477(8448), 10491(8449), 11146, 11149	11	Poly 90 to 98, ab. cd, ef. gh	−27.85, −28.93, −28.14
1/16	70	75	14	10933, 11018, 10935, 10475(8441),11017, 10464(8442), 10457 (8443), 10458(8447), 10477(8448), 10491(8449), 11146, 11149, 11147, 11148	13	Poly 90 to 98, ab, cd, ef, gh, ij, kl	−23.50, −23.92, −24.1
1/16	70	76	14	10933, 11018, 10935, 10475(8441),11017, 10464(8442), 10457 (8443), 10458(8447), 10477(8448), 10491(8449), 11146, 11149, 11147, 11148	13	Poly 90 to 98, ab, cd, ef, gh, ij, kl	−23.31, −23.0, −24.0
1/16	70	77	15	Added on top 10467 (8451),	14	Poly 90 to 98, ab, cd, ef, gh, ij, kl. mn	−21.73
1/16	71	78	15	10933, 11018, 10935, 10475(8441),11017, 10464(8442), 10457 (8443), 10458(8447), 10477(8448), 10491 (8449), 11146, 11149, 11147, 11148, 10467 (8451)	14	Poly 90 to 98, ab, cd, ef, gh, ij, kl. mn	−23.00, −22.37, −21.48

Table 4.1-2. Subcritical reactivity in dollars for the subcritical assemblies from the IKRD measurement for which the configurations are not defined in the logbook (continued).

Nominal Poly thickness (in.)	Page	Run	Number of HEU plates	Order of U parts bottom to top[a]	Poly layers	Order of poly parts bottom to top [b]	Reactivity [c] (dollars)
1/16	71	79	16	Added on top 10493 (8452)	15	Poly 90 to 98, ab, cd, ef, gh, ij, kl. mn, op	−18.40, −19.41
1/16	71	80	18	Added on top 10489 (8453) & 10483 (8455)	17	Added qr & st	−11.90, −11.58

[a] The bottom U plate was adjacent to the diaphragm and all plates with axial holes (with numbers less than 10933) had the holes filled with uranium inserts in order from 8441 upward to the top. Insert numbers in each plate are given in parentheses.

4.2. PROMPT NEUTRON DECAY MEASUREMENTS

The prompt neutron decay constant was measured at delayed criticality and at subcritical configurations with a reduced numbers of thin 15 in. diameter HEU metal plates. The data from these measurements by the Rossi-alpha and randomly pulsed neutron measurements are available from the Records Services Management Services Department of ORNL using the following link: https://recordsmgmt.ornl.gov/ERS/Detail/Records/Record_View.cfm?RecordID=50543. They can also be accessed from OSTI (https://www.osti.gov/servlets/purl/1617461) and from the ICSBEP at Idaho National Laboratory. A data transfer program like GLOBUS can be used to transfer the data. The best way to search for the data is the date of the measurement in the title of the file and then the run number. Difficulty in accessing the data can be resolved by contacting the Records Management Services Division of ORNL.

4.2.1 Californium ionization sources

Four sources were available for these measurements. A sketch of these singly contained aluminum chambers is shown in Appendix D in Figure D.1. The sources were designated A, B, C, and D and had fission rates of 8,170, 125,000, 33,700, and 700 fissions per second, respectively on July 1, 1969. The diameter of the Cf deposits was 1.00 cm, except for Chamber B, which was 2.54 cm. The outside diameter of the chambers was 2.39 cm except for Chamber B which had a diameter of 3.17 cm. Further details of the Cf chamber are in reference 2. The pulses were amplified with a gain of 3,500 and a rise time less than 1 ns by an amplifier designed, built, and provided by N. W. Hill of ORNL. The discrimination of the alpha pulses from the fission pulses was over 99% effective, as can be seen from the oscilloscope trace of the amplified electronic pulses associated with fission and alpha pulses given in Figure D.2 of Appendix D.

4.2.2 Detectors

The detectors were of two types: plastic (Nuclear Enterprise NE-102) and liquid (NE-213) scintillators. The density of the plastic and liquid was 1.032 and 0.874 g/cm^3, respectively and the H/C ratios were 1.103 and 1.213. The latter was capable of discriminating gamma rays from neutrons. Because of the high gamma ray emission from the thin 15 in. diameter HEU metal plates (factor of 2 to 44 above that for unirradiated uranium metal at Y-12) from previous use by LANL at high fission rates, the gamma discrimination capability of the liquid scintillator electronics (over a factor of 1,000 reduction in gamma ray response) was essential for the measurement for subcritical configurations. The relative sensitivity of the detector to gamma ray emission from all 26 thin 15 in. diameter HEU metal plates was measured and compared to standard Y-12 Plant Oralloy at ORCEF is given in Appendix E. Lead shields ¼ in. thick for the NE-102 scintillator covered the front face adjacent to the assembly and 1 in. back on the sides from the front of the plastic scintillator—and 2 in. back for the liquid scintillator. These additional lead shields reduced the sensitivity to gamma-ray pileup an additional 60%. Further details of the detection systems are given in reference 2. The detector threshold for the plastic scintillators was adjusted using a ^{137}Cs source that emits 0.666 MeV gamma rays. The photomultiplier voltage was adjusted so that the output pulses from the ^{137}Cs source were 150 mV, and the discriminator threshold was set so that the discrimination levels for neutrons were 1 MeV and 2 MeV for the half and quarter inch thick detectors, respectively. The pair of plastic scintillators for measurement at delayed critical were usually located with the flat surface of the lead adjacent to the radial surface of the fissile assembly and 120° apart.

The diameter of the NE 102 plastic scintillators was 2.0 in. with thicknesses of 0.5 and 0.25 in., and the dimensions of the NE 213 liquid were 4.60 cm diameter and 4.65 cm thick. The glass enclosure for the liquid had an outside diameter and thickness of 5.08 cm. For measurements, the front face of the liquid scintillation detector was also adjacent to the radial surface of the assembly. The efficiency of the liquid scintillation detector was measured by a time-of-flight measurement in air with the time tagged Cf source and detector separated about 100 cm apart. The time-of-flight results for the liquid scintillator are given in Figure 4.2-1 with and without gamma discrimination. The gamma rays arrive at the detector first, followed by the neutron distribution. The detector response has been delayed with respect to the Cf source pulses so that the full gamma peak can be shown to accurately determine the time of fission. The time of emission of the prompt gamma is 3.3 nanoseconds (flight time of gammas to travel 100 cm) before the gamma ray peak.

From these data, the detection efficiency of the liquid scintillator for neutrons hitting the front face of the scintillator can be determined and is shown in Figure 4.2-2. The neutron efficiency with gamma discrimination was about 25% for a neutron energy of ~2.2 MeV. The neutron response has been reduced slightly by gamma discrimination. This efficiency as a function of neutron energy is given in Figure 4.2-2 and is dependent on the energy spectrum of neutrons from Cf fission. This should be re-calculated from the data of Figure 4.2-1 with the present day accepted neutron distribution from Cf fission. For the subcritical measurements by both the Rossi-α and randomly pulsed neutron method with time-tagged neutron source, the liquid scintillator with gamma discrimination was used. For measurement at delayed criticality, the two plastic scintillators were used, and the time distribution of counts in the 0.25 in. thick plastic scintillator was measured with respect to the previous event in the 0.5 in. thick plastic scintillator.

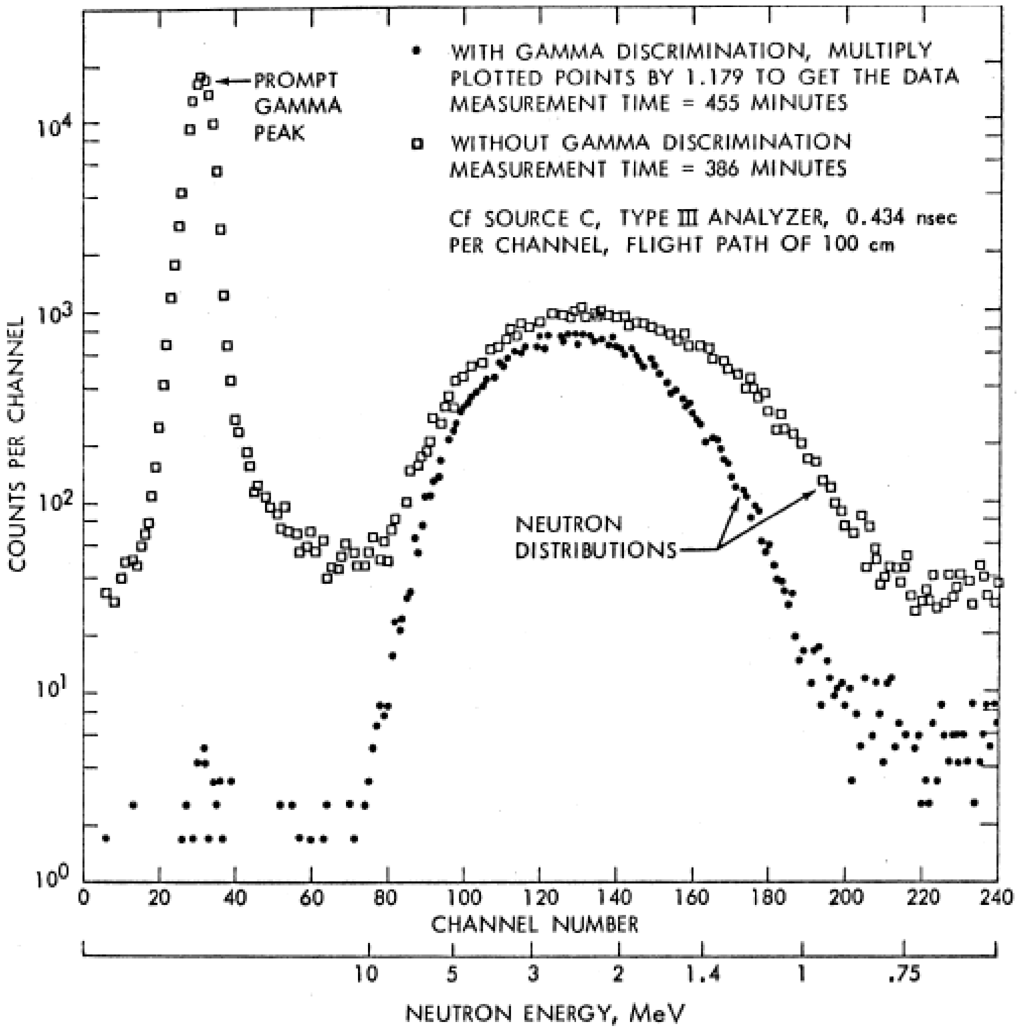

Figure 4.2-1. Time of flight distribution after Cf fission for the liquid scintillator with and without gamma discrimination. (A Type 3-time analyzer accepts one trigger and stores only the next count from the detector and then takes a few microseconds to be ready to accept the next trigger.)

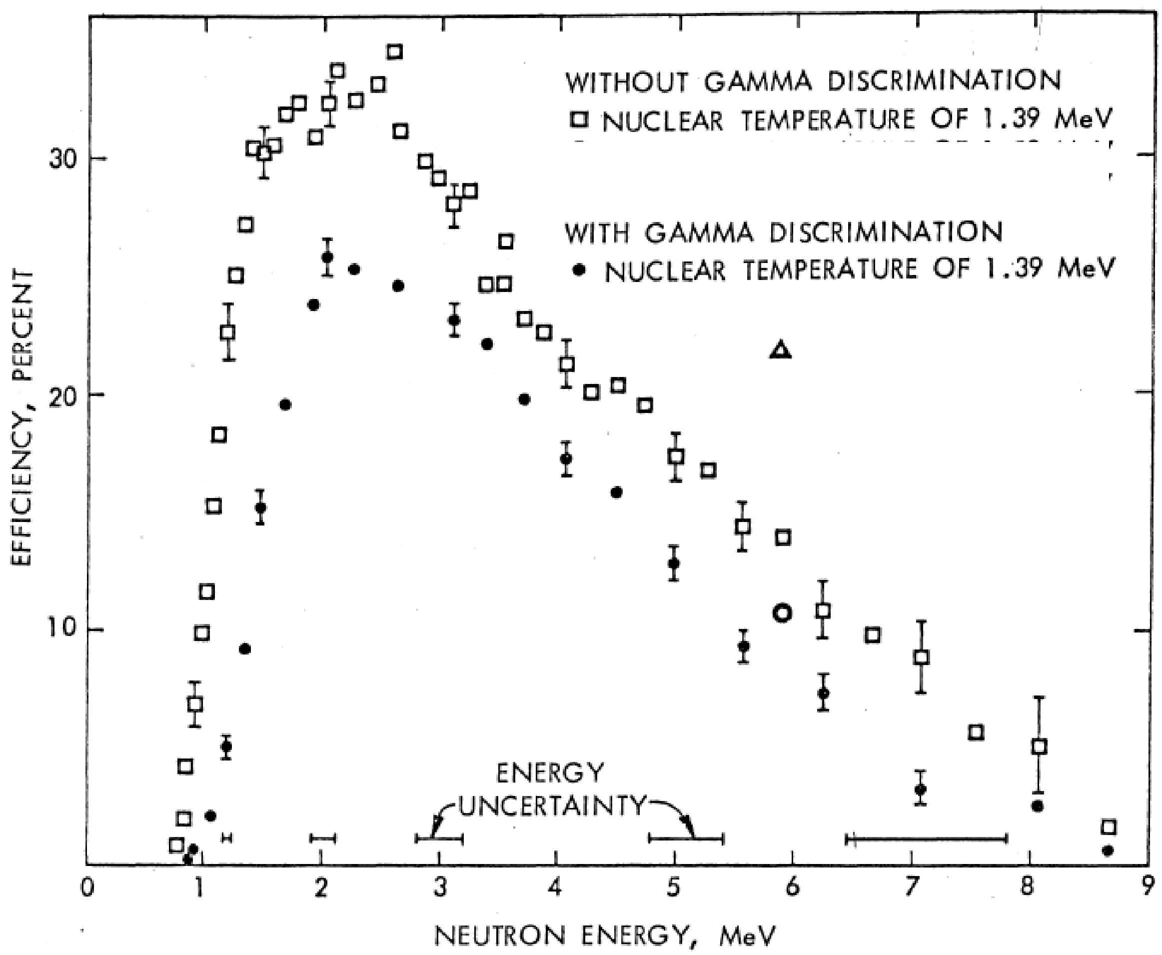

Figure 4.2-2. The detection efficiency of the liquid scintillator as a function of neutron energy. (The present nuclear temperature of neutron emission spectrum is a couple of percent different from that used in 1969.)

4.3. TIME ANALYSIS EQUIPMENT

Three types of time analyzers [23] were used: (1) a 19-channel shift register from LANL with two inputs; (2) a 32-channel time analyzer, which was a stack of 32 scalers (that could be gated on for 10 ns time intervals and up) triggered by one detector and the time distribution of counts in a second detector with no limitation on detector counts per channel; and (3) a Technical Measurement Corporation (TMC) multichannel time analyzer triggered by one detector and the time distribution of counts in another detector measures with respect to each trigger. Further details are discussed in reference 2. Not all measurements used all three types of time analyzers.

4.4. MEASUREMENTS AT DELAYED CRITICALITY

For the measurements at delayed criticality, the arrangement of the uranium metal parts was adjusted to achieve a configuration that was exactly delayed critical. At delayed criticality, only Rossi-alpha [4] measurements were performed with the plastic scintillator detectors adjacent to the radial surface of the assembly. A photograph in Figure 4.4-1 shows the location of the source and detectors for a subcritical configuration on the diaphragm with the detectors located as for the delayed critical configurations. However, for the measurements at delayed critical, the neutron source was not present. The fission rate was adjusted to a level at which the fission chains did not overlap significantly so as not to increase the random background. The data from these Rossi-alpha measurements can be fitted by least squares techniques to determine the prompt neutron decay constant. The data were least squares fitted to the functional form of a constant plus a constant time exponential ($e^{-\alpha t}$). The values given in the table are average values of several measurements, with each individual measurement weighted with the uncertainty of each measurement. The results of these measurements at delayed criticality are given in Table 4.4-1, and the results are plotted in Figure 4.4-2. At delayed criticality, the prompt neutron decay constant equals the effective delayed neutron fraction divided by the prompt neutron lifetime. The prompt neutron lifetime was obtained from the prompt neutron decay constant using a delayed neutron fraction of 0.00667. For the final benchmark, the delayed neutron fraction needs to be calculated for critical configurations with the moderator thicknesses of 1/16, 1/8, 1/4 & 1/2 in. and used to obtain the correct prompt neutron lifetime. These calculated delayed neuron fractions will be larger than the assumed 0.00667, resulting in larger prompt neutron lifetimes.

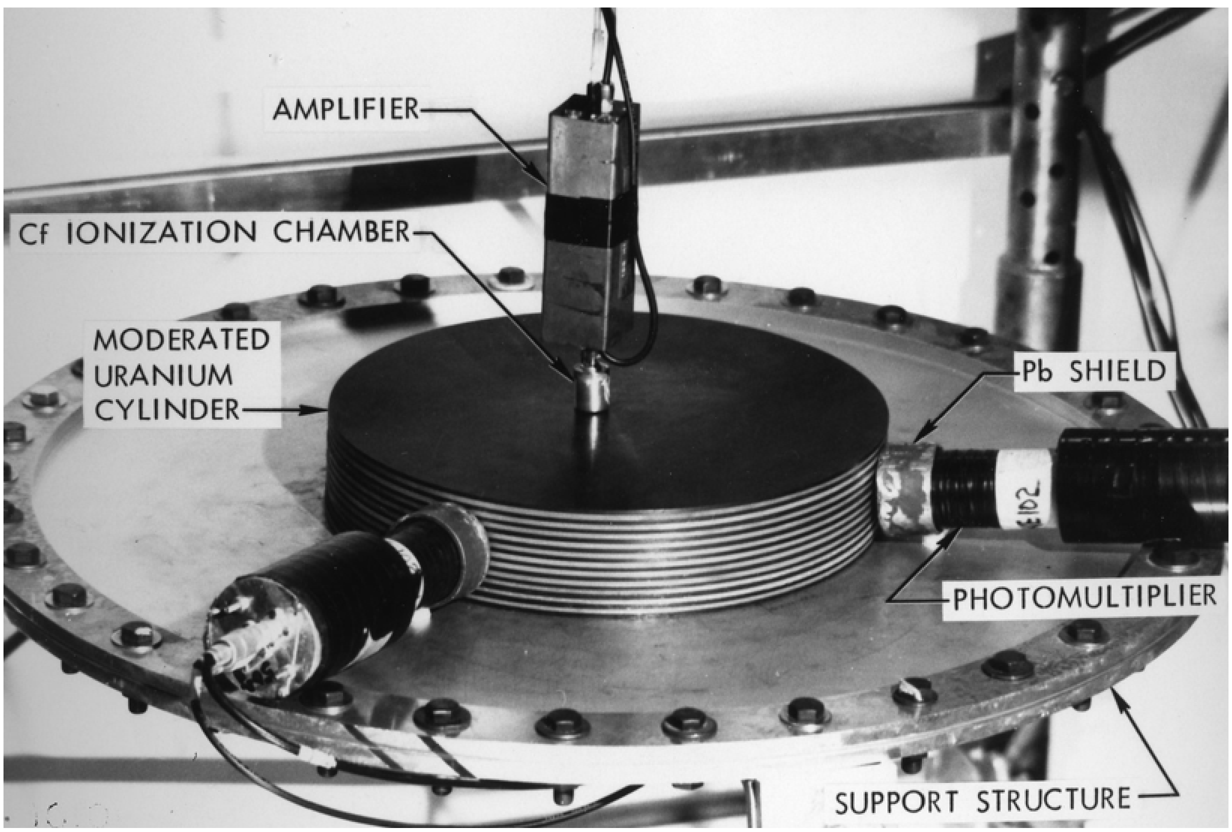

Figure 4.4-1. Configuration of Cf source and detectors for the prompt neutron decay constant measurements for the subcritical thin 15 in. diameter HEU metal plate configuration with ¼ in. thick polyethylene and twelve uranium metal plates.

Table 4.4-1. Dimensions of and prompt neutron decay parameter of delayed critical polyethylene moderated thin 15 in. diameter HEU metal plates.

Number of plates [a]	Nominal Polyethylene thickness (in.)	Number of pie sections	Angular void between pie sections	Prompt neutron decay constant [b] ($nsec^{-1}$)	Prompt neutron lifetime [c] (nsec)	Measured Assembly height[a] (cm)
20 Expt. 1	1/16	5	0, 0, 0, 0, 60	177.7 ± 0.9	38	9.326
17 Expt. 2A	1/8	0 [d]	Not applicable	54.7 ± 0.03	122	10.611
12 Expt. 3	¼	5	20, 0, 20, 0, 20[e]	14.4 ± 0.1	163	10.649
8 Expt. 4	½	3	7.6, 7.6, 164.8 [f]	3.16 ± 0.03	2110	11.495

[a]These values do not include the pie sectors on top. Assembly height does not include the diaphragm, but only full plates and polyethylene layers.
[b]These values are the weighted average of several measurements where the weights were the inverse of the uncertainty in each individual measurement.
[c]These values were obtained from the prompt neutron decay constant assuming a value of 0.00667. For the final benchmark analysis, the effective delayed neutron fraction should be calculated for each configuration and the lifetimes changed appropriately.
[d]For this assembly, a 1 in. wide, 15 in. outside diameter, 1/8 in. thick uranium metal ring from another measurement (Uranium Part 2758) was on top of the assembly along with two 1.488 in. diameter HEU metal discs near the center on top of the upper thin 15 in. diameter HEU metal plate.
[e]Re-arranged pie sections from Experiment 3 to achieve delayed criticality exactly with the detector present.
[f]One HEU metal pie section adjacent to the 164.8² sector of void contained 1/8 in. thick polyethylene underneath it. Pie sections re-arranged from Experiment 4 to achieve delayed criticality exactly with the detector present.

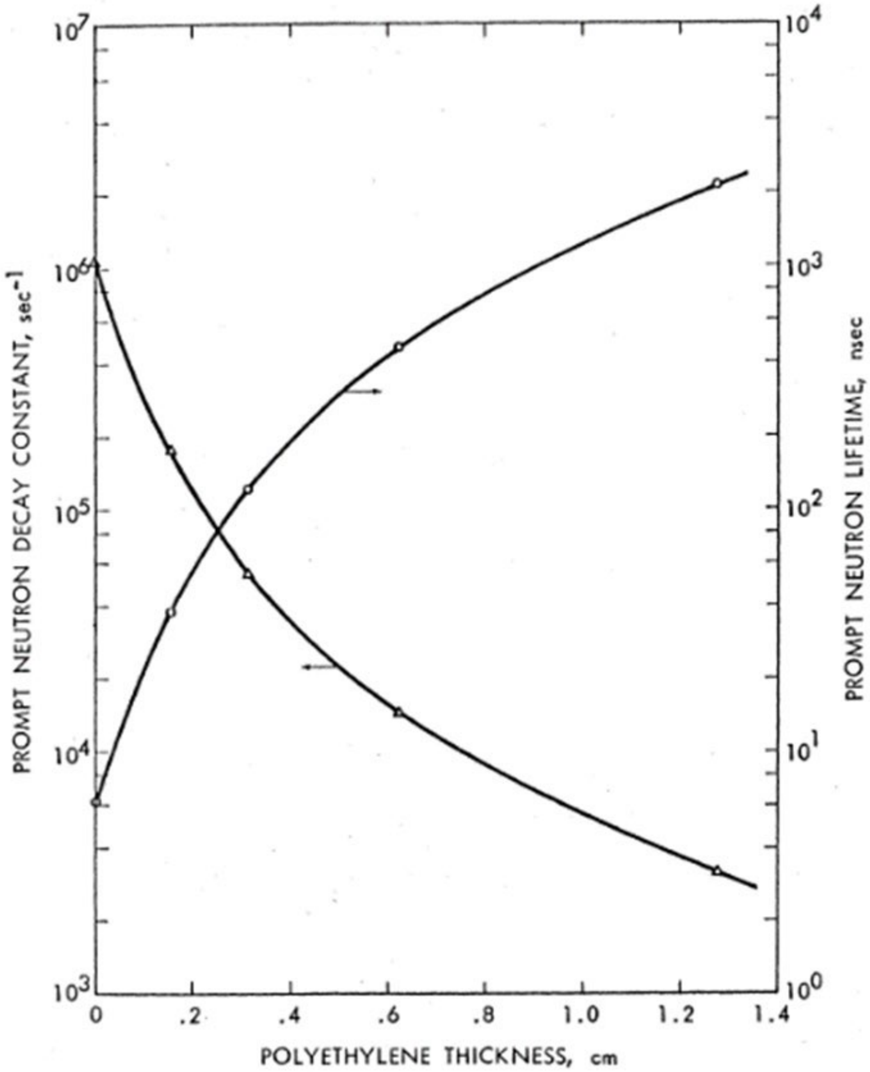

Figure 4.4-2. The prompt neutron decay constant and prompt neutron lifetime for delayed critical assemblies of uranium and polyethylene as a function of moderated thickness.

The prompt neutron decay constant decreases almost three decades from an unmoderated 15 in. diameter HEU uranium metal cylinder with decay constant of 1.07×10^6 sec^{-1} [24] to 3160 sec^{-1} for an HEU uranium metal cylinder with ½ in. thick polyethylene moderator. Both Sn and Monte Carlo transport methods can be used to calculate these decay constants.

4.5. MEASUREMENT FOR SUBCRITICAL CONFIGURATIONS

For the subcritical measurements, the Cf source was present, and the top and bottom uranium layer of the assemblies were complete thin 15 in. diameter HEU metal plates. The prompt neutron decay constant was measured by both the Rossi-α, and the randomly pulsed neutron method using time-tagged Cf neutron sources for a variety of thin 15 in. diameter HEU metal plates and moderator thicknesses. For most of these measurements, the source was in a re-entrant axial (1.510 in. diameter) hole in the top half of the assembly but near the vertical center of the full assembly. Usually for assemblies with an even number of plates, the source was adjacent to the central polyethylene layer; and for those with an odd number of uranium metal plates, the source was adjacent to the central uranium plate. The measurement closest to critical the configurations were like those for Experiments 1, 2A, and 3, with the uranium and polyethylene pie sections removed from the top and for experiment 2A, the ring and small cylindrical discs. For these three subcritical configurations, the Cf source was located in contact with the top uranium plate. Some examples of the uranium/polyethylene subcritical configurations along with the prompt neutron decay data are presented, and the configurations of the other subcritical assemblies are given in Appendix D. All three types of multichannel time analyzers [23] were used for most measurements.

Randomly pulsed neutron measurements were performed with the liquid scintillator with and without pulse shape discrimination to reduce the sensitivity to gamma rays using Cf source C. The data from these measurements were fitted by least squares analysis to a functional form: A + B exp($-\alpha_1$t) + C exp($-\alpha_2$t). The data without gamma discrimination were not fitted because of the large value of A (factor of 100 higher that with gamma discrimination). The time analyzer for the measurements was that described as type 3 from reference 22. As a result of the fitting the two values of the decay constants, α_1 and α_2 are determined.

4.5.1 Fourteen thin 15 in. diameter HEU metal plates with 1/16 in thick polyethylene

The configuration of 14 thin 15 in. diameter HEU metal uranium metal plates with 1/16 in. thick polyethylene is given in Figure 4.5-1. The liquid scintillation detector's lead shield was centered vertically with the front face of the lead shield 1.27 cm from the radial surface of the assembly.

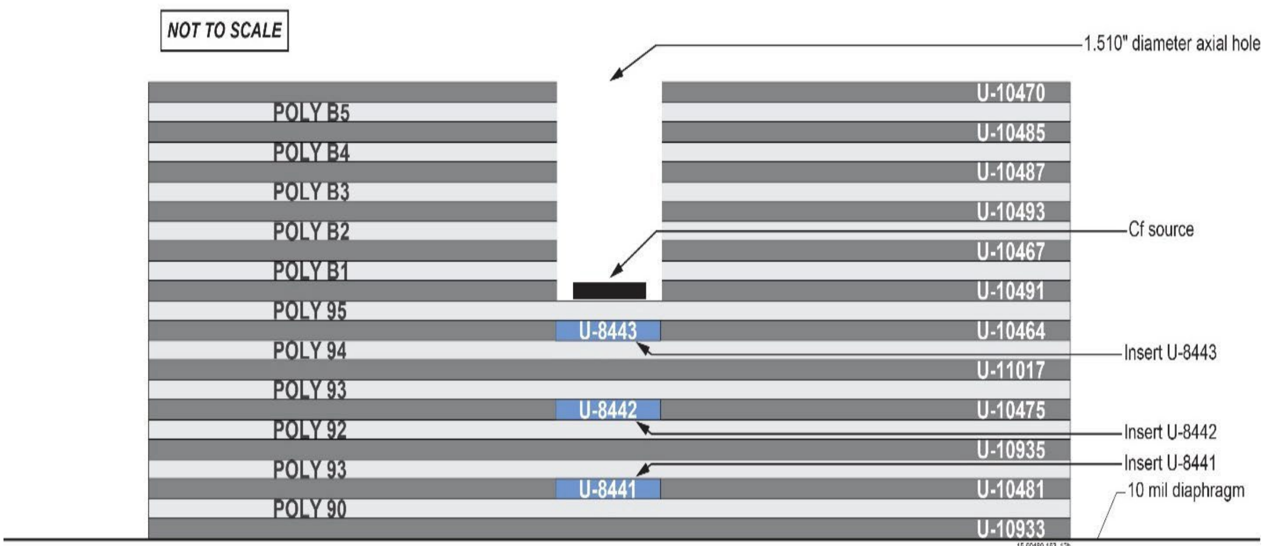

Figure 4.5-1. Subcritical configuration of 14 thin 15 in. diameter HEU metal plate assembly 1/16 in. thick polyethylene between plates. (Two-dimensional cross section along diameters; based on height measurements for subcritical configurations, the gap between polyethylene and uranium layers for this assembly is 0.0032 in.)

The data from a randomly pulsed neutron measurement using a detector with pulse shape discrimination with Cf source C as located in Figure 4.5-1 are given in Figure 4.5-2. The time analyzer used for this measurement accepts only one detection after the Cf source trigger and then resets itself to wait for the next trigger from the Cf source. The data were least squares fitted to the function: A + B [exp($-\alpha_1$t)] + C [exp($-\alpha_2$t)], and the results are shown in Figure 4.5-2 where the two components of the decay are separated. The values of α_1 and α_2 were 7.36 ± 0.39 and 1.86 ± 0.07 μsec^{-1}. The values of A, B and C in units of counts per californium fission were: $5.15 \pm 0.02 \times 10^{-7}$, $5.78 \pm 0.06 \times 10^{-5}$, and $3.43 \pm 0.06 \times 10^{-6}$, respectively. This type of fitting was used for the other subcritical configurations, and the results for some of the measurements are summarized in Table 4.5-1. Because the Type 3 analyzer cannot accept every pulse from the Cf ionization chamber as a trigger, the amplitude of the exponential terms should be increased 0.5 and 3.2% to obtain the true amplitudes of the fast and slow components of the decay, respectively. The configuration of the parts for the subcritical assemblies is given in tabular form in Appendix E and as sketches.

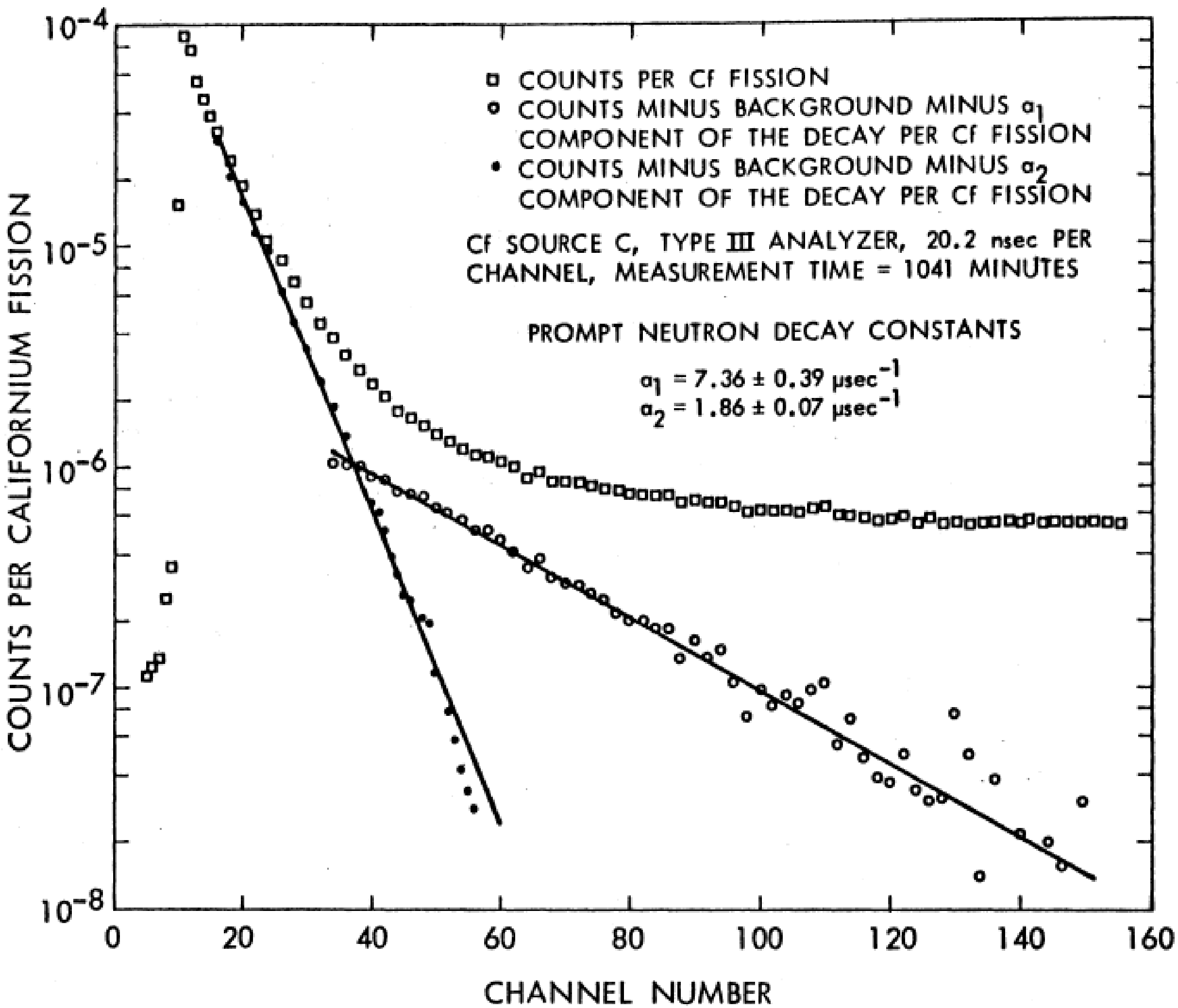

Figure 4.5-2. The prompt neutron decay in a randomly pulsed neutron measurement with gamma discrimination for an assembly of 14 thin 15 in. diameter HEU metal plates with 1/16 in. thick polyethylene using Cf source C.

4.5.2 Ten thin 15 in. diameter HEU metal plates with 1/8 in. thick Polyethylene

The subcritical configuration of an assembly with 10 thin 15 in. diameter HEU metal plates with 1/8 in. thick polyethylene is given in Figure 4.5-3 and the prompt neutron time decay measured with and without gamma discrimination is given in Figure 4.5-4.

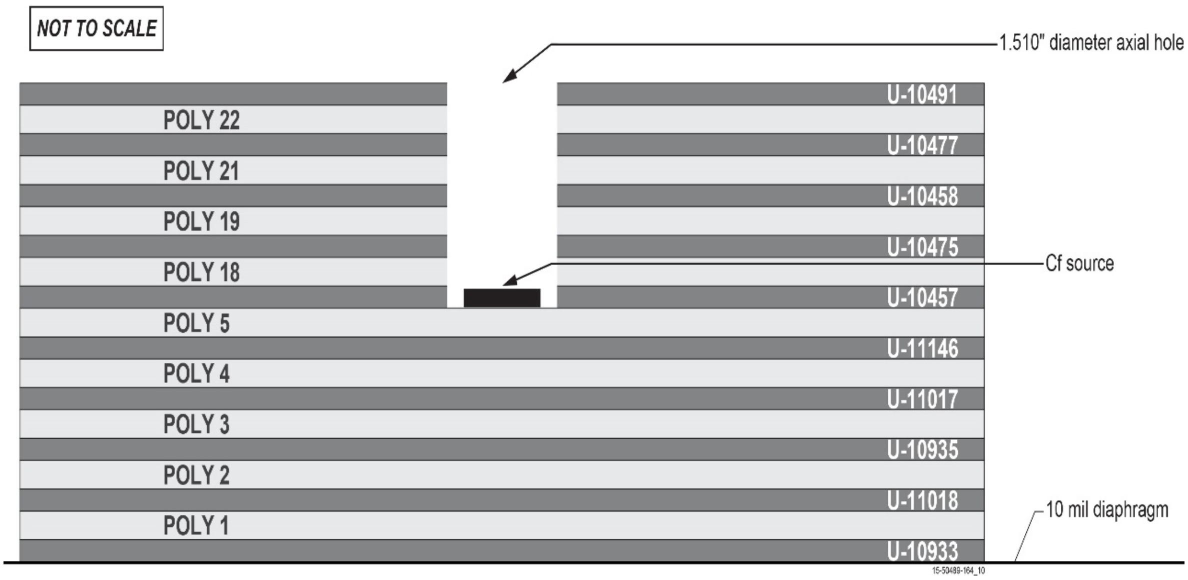

Figure 4.5-3. Ten thin 15 in. diameter HEU metal plates with 1/4 in. thick Polyethylene between plates.
(Two-dimensional cross section along diameters; the measured gap between uranium and polyethylene layers was 0.00337 in.)

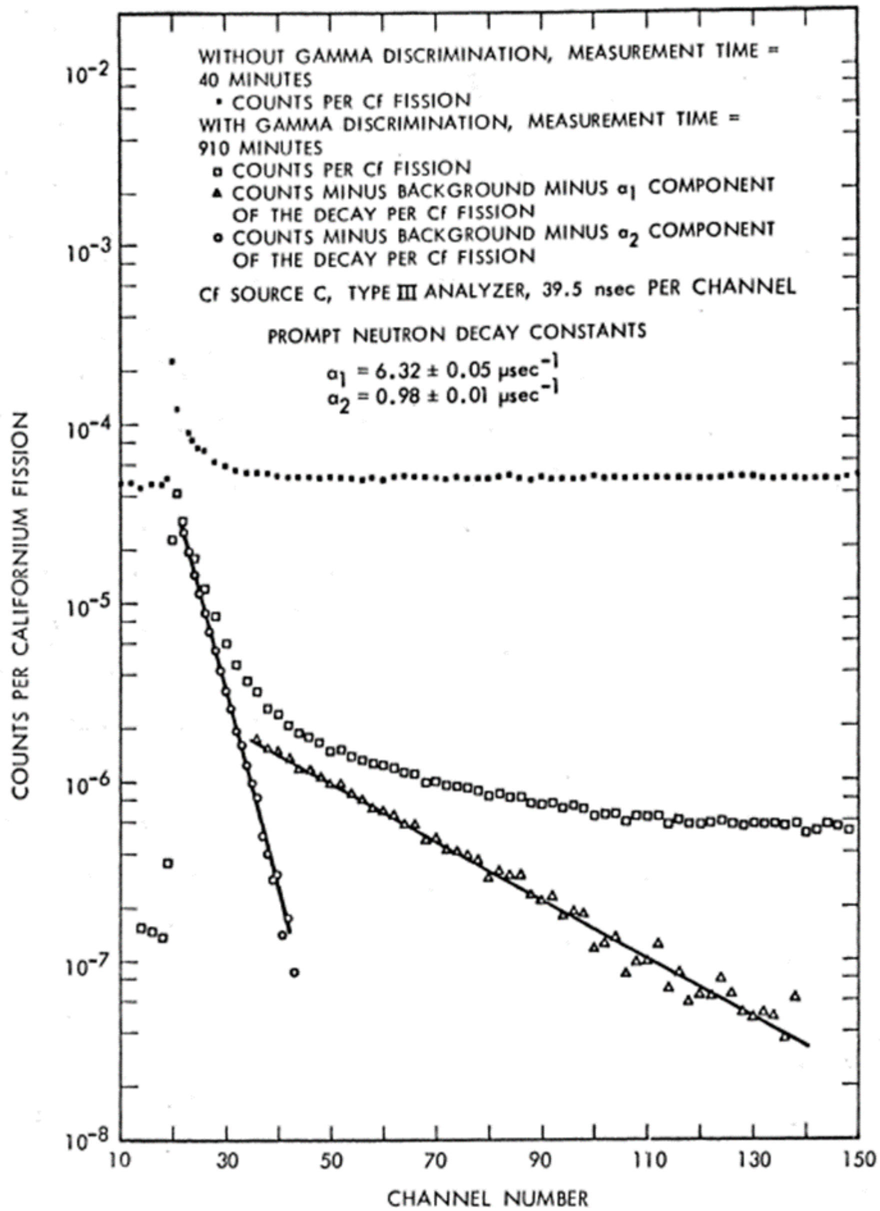

Figure 4.5-4. The prompt neutron decay in randomly pulsed neutron measurements with and without gamma discrimination for an assembly of 10 uranium discs with 0.125 cm thick polyethylene.

4.5.3. Ten thin 15 in. diameter HEU metal plates with 1/4 in. thick Polyethylene

The subcritical configuration of an assembly with 10 thin 15 in. diameter HEU metal plates with 1/4 in. thick polyethylene is given in Figure 4.5-5 and the prompt neutron time decay measured with gamma discrimination is given in Figure 4.5-6.

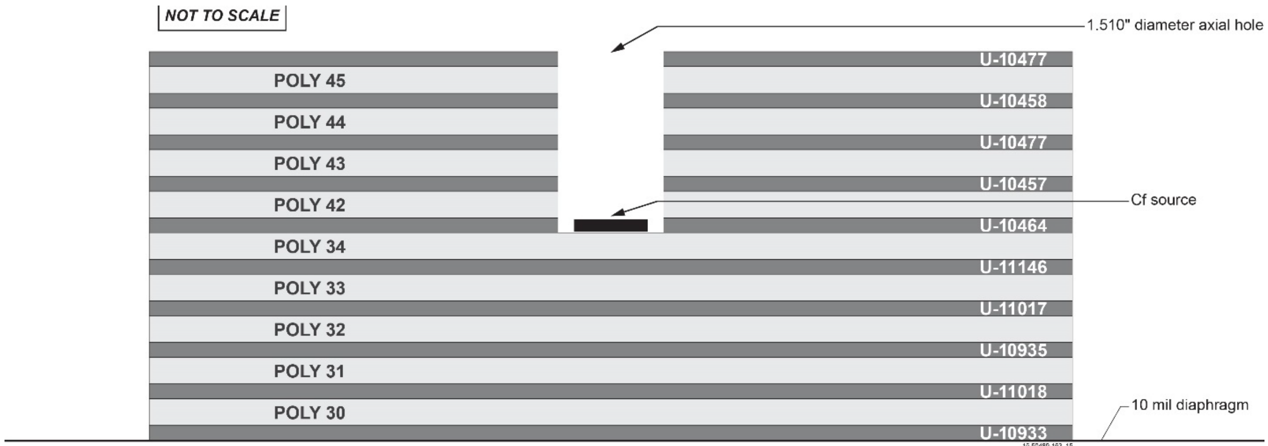

Figure 4.5-5. Subcritical configuration of 10 thin 15 in. diameter HEU metal plate assembly ¼ in. thick polyethylene between plates. (Two-dimensional cross section along diameters; the measured gap between uranium and polyethylene layers was 0.00333 in.)

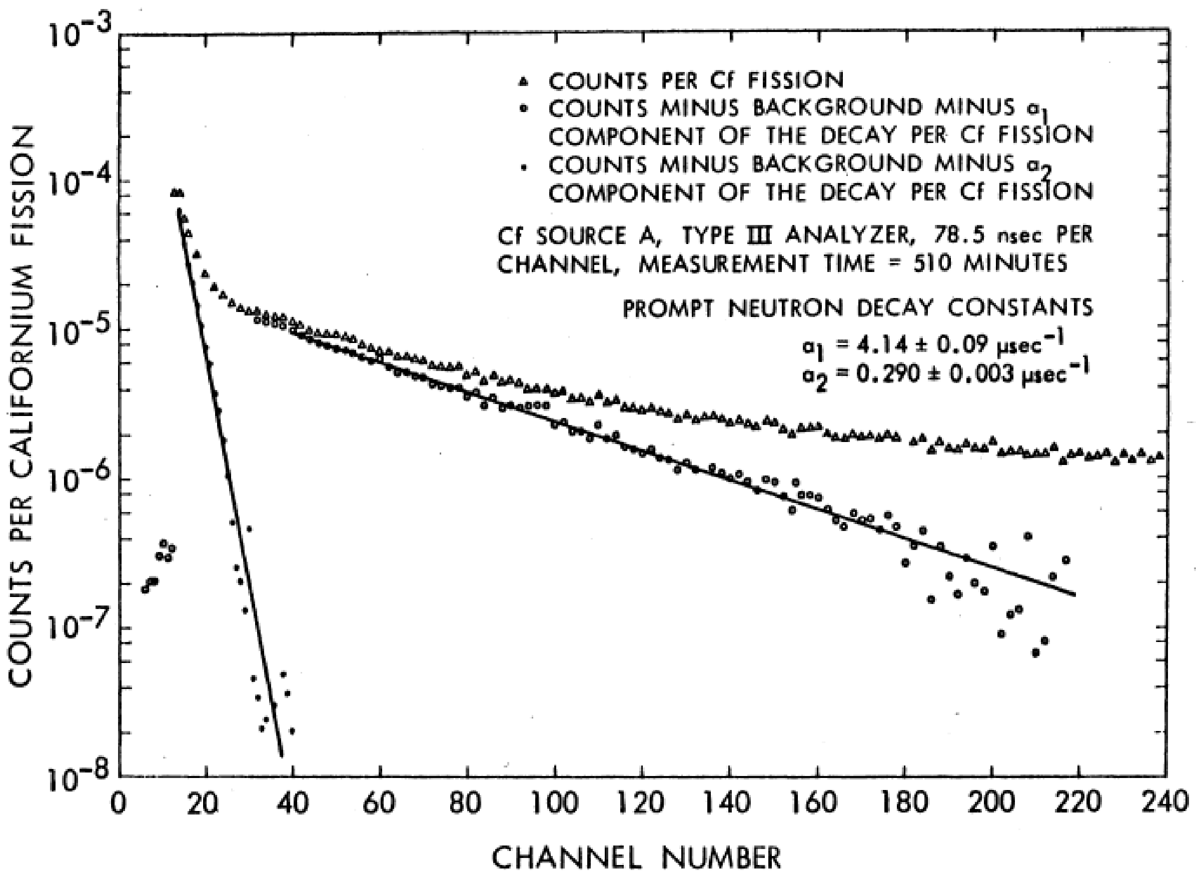

Figure 4.5-6. The prompt neutron decay in randomly pulsed neutron measurements with gamma discrimination for an assembly of 10 uranium discs with 1/4 in. thick polyethylene.

4.5.4 Four thin 15 in. diameter HEU metal plates with ½ in. thick Polyethylene

The configuration of the 4 thin 15 in. diameter HEU metal plates is given in Figure 4.5-7. The liquid scintillator and Cf source C was centrally located vertically with the front face of the lead shield adjacent to the radial surface. A time analyzer accepted one trigger from the Cf source electronics and measured the time distribution of the next count from the liquid scintillator electronics; then, after a short delay, it waited for the next trigger from the Cf source and repeated the process. The prompt neutron decay as a function of time is shown in Figure 4.5-8. The data were fitted by least squares techniques to determine the decay constants.

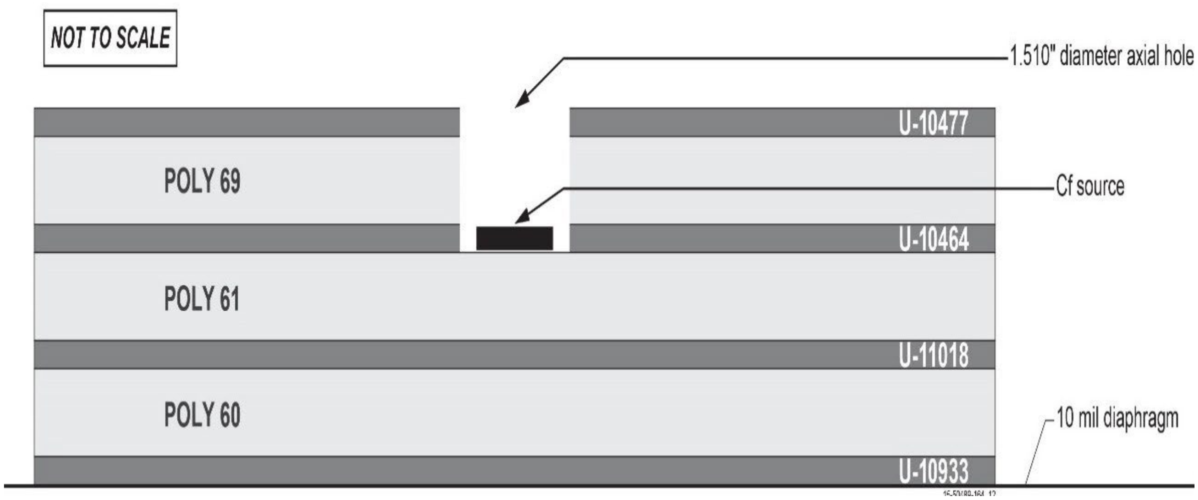

Figure 4.5-7. Subcritical configuration of 4 thin 15 in. diameter HEU metal plate assembly ½ in. thick polyethylene between plates for prompt neutron decay measurements. (Two-dimensional cross section along diameters; the measured gap between uranium and polyethylene layers was 0.00815 in.)

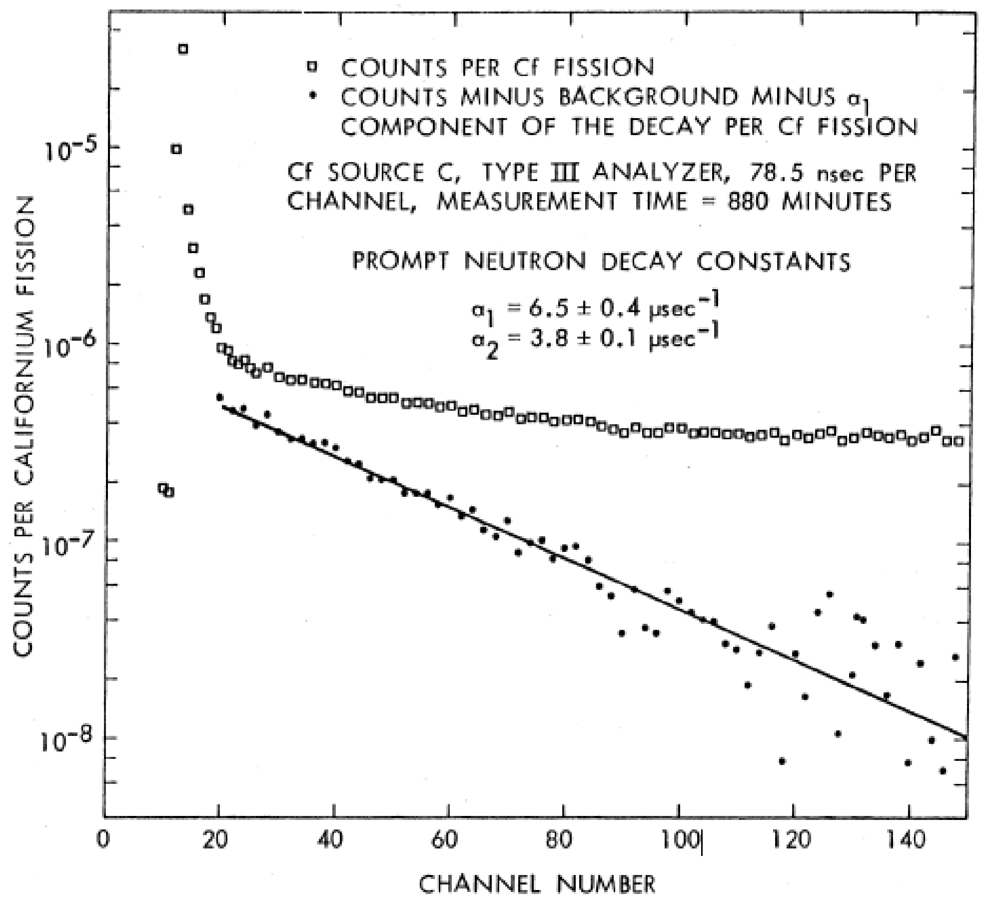

Figure 4.5-8. The prompt neutron decay in randomly pulsed neutron measurements with gamma discrimination for an assembly of 4 uranium discs with ½ in. thick polyethylene.

4.5.5. Summary of prompt neutron decay constants

The largest prompt neutron decay constants (α_1) for all the measurements are given in Table 4.5-1. Additional configurations of these assemblies are given in Appendix D, and additional analysis of the prompt neutron decay data is given in reference 2. As the number of plates decreases, time decay increases; as the polyethylene thickness increases, time decay decreases.

Table 4.5-1. Dimensions and prompt neutron decay constants for moderated subcritical uranium metal cylinders for various numbers of thin 15 in. diameter HEU metal plates and moderator thicknesses.

Polyethylene thickness (in.) & ORCEF logbook page number	Number of uranium plates	Total Uranium Thickness (cm)	Total Polyethylene Thickness (cm)	Measured Assembly height (cm)[c]	Prompt Neutron Decay[a] (nsec^{-1})	Gaps (in.)
1/16 (55)	20[b]	6.083	2.932	9.326	745 ± 4	0.00323
1/16 (58)	19	5.786	2.803	8.883	1063 ± 7	0.00322
1/16 (58)	18	5.486	2.653	8.458	1234 ± 21	0.00369
1/16 (59)	14	4.262	2.027	6.543	1860 ±40	0.00385
1/16 (63)	10	3.041	1.401	4.610	7368 ± 250	0.00366

Table 4.5-1. Dimensions and prompt neutron decay constants for moderated subcritical uranium metal cylinders for various numbers of thin 15 in. diameter HEU metal plates and moderator thicknesses (continued).

Polyethylene thickness (in.) & ORCEF logbook page number	Number of uranium plates	Total Uranium Thickness (cm)	Total Polyethylene Thickness (cm)	Measured Assembly height (cm)[c]	Prompt Neutron	Gaps (in.)
1/8 (40)	16[b]	4.868	4.901	10.012	298 ± 4	0.00319
1/8 (58)	15	4.568	4.532	9.363	529 ± 3	0.00370
1/8 (59)	12	3.658	3.566	7.422	829 ± 10	0.00354
1/8 (60)	10	3.048	2.924	6.126	991 ±10	0.00337
1/4	12[b]	3.658	6.873	10.707	102 ± 4	0.00315
1/4 (59)	10	3.043	5.625	8.818	296 ±8	0.00333
1/4 (60)	8	2.432	4.381	6.956	476 ±10	0.00402
1/4 (60)	6	1.823	3.126	5.074	634 ± 15	0.00440
1/2 (64)	8	2.439	8.929	11.52	14.8 ± 0.1	0.00425
1/2 (67)	7	2.138	7.653	9.970	38.5 ± 0.2	0.00587
1/2 (64)	4	1.214	3.831	5.169	381 ± 10	0,00815

[a] These values are the fundamental mode decay constants and are a weighted average if more than one measurement was performed. The weights were the reciprocal of the standard deviation of the decay constant obtained from the least squares analysis.
[b]These assemblies did not contain axial holes and the source was in contact with the center of the upper uranium metal plate. These assemblies are Experiments 1, 2a, and 3 without extraneous pie sections and other material on top of the upper plate.
[c]Assembly heights were measured within 0.001 in. or 0.0025 cm.

The data from these measurements are available from the Records Management Services Department of ORNL, from OSTI, and from the ICSBEP project at INL. These prompt neutron decay data can be calculated by transport theory methods (both Sn and Monte Carlo) and thus can be used as the basis for IRPhE benchmarks. The prompt neutron time constants of the decay depend significantly on the neutron energy distribution in the subcritical configuration and the subcriticality.

The data from these two detector Rossi-alpha and randomly pulsed neutron measurements can be fitted by least squares techniques to determine the prompt neutron decay constant. The values given are average values of several measurements with each individual measurement weighted with the uncertainty of each measurement. At delayed criticality, the prompt neutron decay constant equals the effective delayed neutron fraction divided by the prompt neutron lifetime. To obtain better estimates of the prompt neutron lifetime from the prompt neutron decay constant for the final benchmark, an effective delayed neutron fraction should be used that is calculated for each assembly with different polyethylene thicknesses.

Measurements of the prompt neutron decay was measured for many subcritical configurations of the thin 15 in. diameter HEU metal plates. In these measurements, only complete thin 15 in. diameter HEU metal plates were used, and there was usually always one more uranium plate than polyethylene layer. Each of these subcritical configurations has a uranium plate on the top and bottom, and all the material was on the diaphragm. For the polyethylene thickness of 1/16 in., measurements were performed for 10, 12, 14, 16, 18, and 19 uranium metal plates. The data from the prompt neutron decay constant measurements in digital form is available from the Records management Services Department of ORNL, OSTI, and the

ICSBEP at INL. The link at ORNL to access these data is as follows: https://recordsmgmt.ornl.gov/ERS/Detail/Records/Record_View.cfm RecordID=50543. The link at OSTI is https://www.osti.gov/servlets/purl/1617461, in an archive called CADES. A software data transfer program like GLOBUS can download the prompt neutron decay data. The first line of each data file contains the date of the measurement and a brief description of the measurement configuration that can be traced to the ORCEF logbook. The unclassified ORNL Logbook H00174 at ORNL describes these measurement configurations. The descriptions of the measurements performed and their location are given in this logbook. Two types of measurements were performed: Rossi-α [4] and randomly pulsed neutron measurements [5]. The configurations of the systems for which decay constants were measured are given in Appendix E.

5. DESCRIPTION OF MATERIALS

5.1. DESCRIPTION OF THE URANIUM METAL PARTS

The 14.998 in. outside diameter HEU metal plates were borrowed from LANL in 1969 for these measurements. These plates were originally fabricated in the late 1950s at the Y-12 Plant. As was the custom with Oralloy parts at the ORCEF, the thin 15 in. diameter HEU metal plates were coated in the measurements with a very thin (<0.00005 in.) layer of fluorocarbon oil to reduce oxidation. The oil was applied and then wiped to remove most of the oil, leaving only a thin layer of fluorocarbon oil.

5.1.1. Masses and dimensions

The part numbers, mass, and ^{235}U enrichment of the plates are given in Table 5.1-1. Some of the plates had a 1.510 in. diameter central (axial) hole in which HEU metal cylinders with diameters of less than 1.500 in. could be inserted to fill the holes. There were also six partial (60° sections) plates for finer adjustment of reactivity. When the HEU metal plates were in ORCEF in 1969, they were free of oxidation and were of equal quality to those of other Oralloy supplied to ORCEF by the Y-12 Plant at this time. After these measurements at ORCEF these plates were shipped back to LANL, and the central holes were enlarged for use in the BIGTEN critical assembly at LANL. Data from these measurements at ORCEF do not include dimensional inspection reports. Dimensions, masses, and uranium isotopics (other than ^{235}U) may be retrievable from Y-12 plant records on dimensional analysis, isotopic analysis, chemical analysis, and from Nuclear Material Control and Accountability records. For the final benchmark analyses, an attempt to retrieve these records from the Y-12 Plant and LANL archives should be made, and they should be included in the final benchmark. The thicknesses in the table were calculated assuming the uranium metal density of 18.740 g/cm^3 from reference 2, the masses from the Callihan to Paxton letter (Appendix A), the outside diameter of 14.998 in. [2], and inner diameter of the central holes of 1.510 in. (several plates measured by the author with an inside micrometer gave the same result and were entered on page 16 of the logbook). The average thickness obtained was 0.1196 in. This value is consistent with an average thickness given in reference 2 of 0.303 cm or 0.1193 in. As a result of this consistency, these calculated values for each plate should be used for benchmark models unless dimensional inspection reports can be retrieved from the Y-12 plant or LANL. Average recently measured thicknesses given in the table are from reference 24, which presents the results of LANL thickness measurements after some oxidation and deformation of the plates. The thicknesses given from recent LANL give uranium densities much lower than the standard Oralloy density at the Y-12 plant at this time. The average uranium metal density of the thin 15 in. diameter HEU metal plates in 1969 at ORCEF was 18.740 g/cm^3. The present condition with heavy oxidation and damage to the plates precludes determining the thickness of the plates in 1969 at ORCEF. Because of this, the weights determined in 2005, when the material was shipped to the Device Assembly Facility (DAF) at the Nevada Test Site, and 2019 measurements at the DAF are not appropriate for the measurements in 1969 at ORCEF. The only information that may be appropriate from the LANL characterizations are the impurity contents for the plates. The masses given are from a letter dated May 20, 1960, from A.D. Callihan of ORNL to H. C. Paxton of LANL; these should be used for the masses of the plates in 1969. The author of this ORNL technical memorandum was personally involved in weighing these plates at ORCEF in 1969; in most cases, they agree with those in the letter. Some average thicknesses from LANL are listed in the table. The Oralloy density calculated with the LANL dimensions and masses are not consistent and are not realistic for Y-12 Plant Oralloy at this time for which the density was 18.750 g/cm^3. This report assumes the density was 18.740 g/cm^3 [2] and calculates the thickness based on this assumption. The present condition of a plate shown in Figures 5.1-1 and 5.1-2 precludes obtaining any useful information from reinspection for the condition of the plates in 1969 at ORCEF. The deformation of uranium plate 11150 is shown in Figure 5.1-1, and the material (metal chips and uranium oxide) in the plastic bag shown in Figure 5.1-2 was originally part of plate 11150. The increased thicknesses and reduced densities of the uranium metal (from the LANL dimensions) are the result of deterioration, which is obvious from the two figures. The LANL measurement combined with the ORNL dimensions might be used to quantify the oxidation or the deteriorated 15 in. diameter plates that are not deformed.

The thin 15 in. diameter HEU metal plates were in near-pristine condition in 1969, consistent with other Oralloy in use for the experiments at ORCEF at that time. There was very little oxidation, only enough to discolor the uranium metal from its brassy color after machining. It was sufficiently free of removable oxidation such that the personnel handling the uranium metal wore street clothes with lab coats and leather gloves for handling the uranium metal and no shoe covers. Thus, there were minimal contamination concerns during the measurements at ORCEF. The gamma emission from plate 11150 and 11019 were at least a factor of 40 higher than the Y-12 Oralloy, indicating that they had been in a high fission rate experiment in the past. These two plates (11150 1n 11019) were not used in all but one ORCEF measurement to minimize radiation exposure of the personnel and equipment.

Table 5.1-1. Mass and ^{235}U enrichment of the 14.998 in. diameter cylindrical thin 15 in. diameter HEU metal plates.

Part number	Uranium (a) mass (g)	^{235}U enrichment(a) (wt %)	Thickness (b) (in.)	Diameter (in.)
10932{22}(c) H(d)	6498 (6498)	93.15 (93.143) (e)	0.12093 <0.125>	14.998 (f)
10491 {12}H	6415 (6415)	93.37	0.12125 <0.123>	14.998
11150{4}	6445 (6446)	93.17	0.11888 <0.1218>	14.998
11149 {3}	6410 (6411)	93.24	0.11820 <0.122>	14.998
11017 {21}	6518 (6514)	93.31	0.12014 <0.1208>	14.998
10477 {11} H	6505 (6504)	93.35	0.12106 <0.1235>	14.998
11146 {5}	6426 (6423)	93.20	0.11844 not meas	14.998
11019 {23}	6477 (6477)	93.18	0.11978 <0.1237>	14.998
10493 {8} H	6427 (6423)	93.25 (93.261) (d)	0.11961 < 0.1228>	14.998
10489 {28} H	6473 (6472)	93.39	0.12047< 0.1232>	14.998
11148 {6}	6441 (6442)	93.44	0.11817 not meas	14.998
10457 {26) H	6587 (6586)	93.18	0.12258<0.1255>	14.998
10935 {20}	6471 (7471)	93.38	0.12020 not meas	14.998
10464 {30}H	6376 (6375)	93.24	0.11866 <0.1295>	14.998
10485 {10}H	6448 (6448)	93.41	0.12000 Not meas	14.998
10470 {9}H	6409 (6409)	93.16	0.11928 <0.1220>	14.998
10933 {1}	6486 (6486)	93.16	0.11955 Not meas	14.998
11018 {19}	6420 (6420)	93.19 (93.208) (d)	0.11833 <0.1192>	14.998
10475 {14}H	6361 (6361)	93.40	0.11838<0.1285>	14.998
10483 {25}H	6339 (6339)	93.24	0.11797 Not meas	14.998

Table 5.1-1. Mass and ^{235}U enrichment of the 14.998 in. diameter cylindrical thin 15 in. diameter HEU metal plates (continued).

Part number	Uranium (a) mass (g)	^{235}U enrichment(a) (wt %)	Thickness (b) (in.)	Diameter (in.)
10467 {27}H	6455 (6453)	93.41	0.12013 <0.1246>	14.998
10487 {13}H	6396 (6344)	93.26	0.11908< 0.1203>	14.998
10458 {15}H	6477 (6477)	93.40 (93.507)(d)	0.12054 Not meas	14.998
11147 {7}	6537 (6536)	93.17	0.12049 < 0.1196>	14.998
11151 {2}	6380 (6380)	93.19	0.11760	14.998
10481 {18}H	6431 (6428)	93.23	0.1197 <0.1206>	14.998
8601	1072	93.13	0.11855 <0.1212>	r = 7.4875
8602	1076	93.13	0.1190 <0.1207>	r = 7.487
8603	1066	93.13	0.11789 <0.1203>	r = 7.4836
8604	1074	93.13	0.11977 <0.1212>	r = 7.488
8605	1073	93.13	0.11977 <0.1198>	r = 7.483
8606	1086	93.13	0.1202 <0.1218>	r = 7.488
8441	60 (62)	93.40	0.1132	1.484 (g)
8442	59 (60.9)	93.40	0.1088	1.492
8443	58 (59.7)	93.40	0.1094	1.485
8447	61 (61.3)	93.40	0.1146	1.484
8448	57 (59)	93.40	0.1076	1.485
8449	59 (61.7)	93.40	0.1148	1.483
8451	59 (61.5)	93.40	0.1109	1.485
8452	59 (61.3)	93.40	0.1109	1.485
8453	60 (62.3)	93.40	0.1120	1.490
8455	61 (63.3)	93.40	0.1146	1.485
8457	58 (60.3)	94.40	0.1094	1.484
8458	60 (62.5)	93.40	0.112	1.484

(a) Masses and ^{235}U enrichments are from the nuclear material transfer document date June 3, 1969, that transferred the fissile material to Y-12. Masses in parentheses for the thin 15 in. diameter HEU metal plates were measured at ORCEF in 1969 by J. T Mihalczo and J. J. Lynn with an uncalibrated scale. The masses in the nuclear material transfer document of June 3, 1969, letter are more accurate since they were measured to 0.5 g and the ones measured at ORCEF were measured with an uncalibrated scale. Since these measurements in 1969, the central holes in some of the plates were enlarged. All mass measurements at ORNL were not in plastic bags and only the uranium metal of each plate was measured. Masses in parenthesis for Parts 8441 to 8458 were from LANL.

(b) Thicknesses are calculated from the masses and diameters assuming that the uranium metal density was 18.740 g/cm^3. Average thicknesses in brackets are recently measured by LANL after considerable oxidation of the uranium metal. The difference between values can be considered the thickness of the oxidation layer or where oxidation has separated from the plate.

(c) Numbers in braces { } are ORNL ORCEF logbook E-24 identification numbers for the uranium metal plates.

(d) These parts with an H in this column have a 1.510 in. diameter central axial hole. The masses of the plates do not include the masses of the inserts.

(e) The values in parentheses are from 1974 spectrographic analyses at LANL. The ^{234}U values are 1.002, 1.064, 1.026, and 1.033, respectively and the values for ^{236}U are 0.327, 0.079, 0.0529 and zero. Another uranium isotopic analysis for a 21 in. diameter plate cast at the same time is included below in a table.

(f) All larger diameter parts are described on drawing DWG 8M 4443.

(g) Information for inserts 8441 to 8458 from 2005 LANL inspection reports provided by Bill Myers of LANL in 2021 except for the masses not in parenthesis which are from the nuclear material transfer document dated June 3, 1969, given in Appendix A.

Table 5.1-2. Uranium dimensions and masses.

Uranium part number	Outside diameter (in.)	Inside Diameter (in.)	Thickness (in.)	Mass
8441	1.484	**0.0**	**0.1144**	60
8442	1.492	**0.0**	**0.1111**	59
8443	1.484	**0.0**	**0.1106**	58
8447	1.485	**0.0**	**0.1158**	61
8448	1.484	**0.0**	**0.1088**	57
8449	1.483	**0.0**	**0.1160**	59
8451	1.485	**0.0**	**0.1121**	59
8452	1.485	**0.0**	**0.1121**	59
8453	1.490	**0.0**	**0.1132**	60
8455	1.485	**0.0**	**0.1158**	61
8457	1.484	**0.0**	**0.1106**	58
8458	1.484	**0.0**	**0.1144**	60
8601	14.998	**0.0**	**0.11855**	**1071**
8602	14.998	**0.0**	**0.11900**	**1076**
8603	14.998	**0.0**	**0.11789**	**1066**
8654	14.998	**0.0**	**0.11977**	**1074**
8605	14.998	**0.0**	**0.11977**	**1073**
8606	14.998	**0.0**	**0.1202**	**1086**
10457	14.998	**1.510**	**0.12258**	**6587**
10458	14.998	**1.510**	**0.12054**	**6477**
10464	14.998	**1.510**	**0.11866**	**6376**
10467	14.998	**1.510**	**0.12013**	**6455**
10470	14.998	**1.510**	**0.11928**	**6409**
10475	14.998	**1.510**	**0.11838**	**6361**
10477	14.998	**1.510**	**0.12106**	**6505**
10481	14.998	**1.510**	**0.11968**	**6431**
10483	14.998	**1.510**	**0.11797**	**6339**
10485	14.998	**1.510**	**0.12000**	**6448**
10487	14.998	**1.510**	**0.11903**	**6396**
10489	14.998	**1.510**	**0.12047**	**6473**
10491	14.998	**1.510**	**0.12125**	**6515**
10493	14.998	**1.510**	**0.11961**	**6427**
10932	14.998	**0.0**	**0.12093**	**6498**
10933	14.998	**0.0**	**0.11955**	**6486**
10935	14.998	**0.0**	**0.12020**	**6471**
11017	14.998	**0.0**	**0.12014**	**6518**
11018	14.998	**0.0**	**0.11833**	**6420**
11019	14.998	**0.0**	**0.11978**	**6477**
11146	14.998	**0.0**	**0.11844** **[0.11850-1/2-8-7]**	**6426**

Table 5.1-2. Uranium dimensions and masses (continued).

Uranium part number	Outside diameter (in.)	Inside Diameter (in.)	Thickness (in.)	Mass
11147	14.998	**0.0**	**0.12049**	**6537**
11148	14.998	**0.0**	**0.11817**	**6411**
11149	14.998	**0.0**	**0.11820 [0.11811-1/16-]**	**6410**
11150	14.998	**0.0**	**0.11888**	**6445**
11151	14.998	**0.0**	**0.11760**	**6380**

The inserts for some of the thin 15 in. diameter HEU metal plates that had 1.510 in. diameter axial holes were used in order. For example, if five inserts were used for the material on the diaphragm and five for the material on the vertical lift, part 8441 would be in the thin 15 in. diameter HEU metal plate closest to the diaphragm with an axial hole, and part 8448 would be used to fill the axial hole in the top thin 15 in. diameter HEU metal plate with an axial hole. For the material on the vertical lift, part 8449 would be used on the bottom, and part 8455 would be at the top. The thickness of the uranium inserts is slightly smaller than the thin 15 in. diameter HEU metal plates. As a result, when in an assembly, there is a slight void above the inserts and below the polyethylene above the uranium plate. This can be evaluated in the uncertainty analysis by reducing the density slightly to occupy the total height available. This should be done for the assembly with the most inserts, and the result will be so small that it will not affect the k_{eff} uncertainty significantly.

Figure 5.1-1. More recent photograph of thin 15 in. diameter HEU metal plate 11150 showing deterioration since 1969. (Note irregularities at the outer surface where material is missing; writing on this plate was not present in 1969. Provided by Renee Sanchez of LANL)

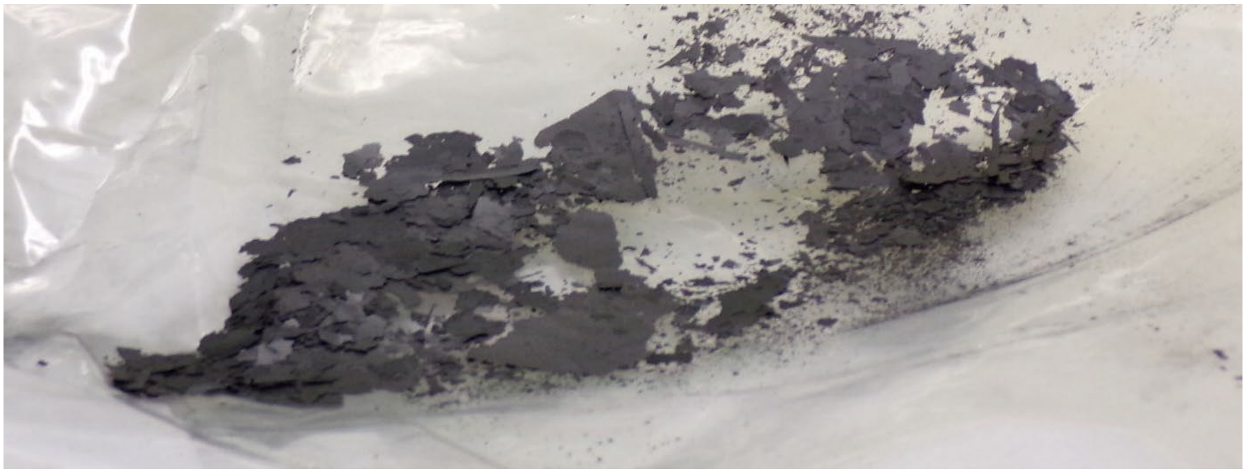

Figure 5.1-2. Photograph of extra uranium and oxide separated from the thin 15 in. diameter HEU metal plate 11150. (Provided by Rene Sanchez of LANL).

5.1.2. Uranium enrichments

The 1974 uranium isotopics from LANL are given in Table 5.1-3 for some of the thin 15 in. diameter HEU metal plates. Uranium isotopic content of ^{234}U and ^{236}U for each part should be retrieved from the Y-12 National Security Complex for the final ICSBEP benchmark if possible. This retrieval would provide the ^{234}U and ^{236}U isotopes and the ^{238}U by difference for 100. These measurements in 1974 at LANL suggest that the enrichments given in the May 20, 1960, letter from Callihan (ORNL) to Paxton (LANL) are from the Y-12 Plant; otherwise, LANL would not remeasure what they originally measured. Y-12 normally measures the enrichment of every Oralloy part made. Until uranium isotopic data are retrieved from Y-12, the 234 and 236 content could be obtained from other measurements with the same ^{235}U enrichment as described below in this section.

Table 5.1-3. Summary of LANL uranium isotopic analysis in May 1974.

Part number	Part description	^{234}U (wt %)	^{235}U (wt %)	^{236}U (wt %)	^{238}U (wt %)
10493	15 in. OD	1.069 ± 0.004	93.261 ± 0.037 (93.25) [(a)]	0.079 ± 0.004	5.591 ± 0.022
10458	15 in. OD	1.033 ± 0.020	93.507 ± 0.037 (93.40)	Reported as 0[(a)]	5.460 ± 0.109
11018	15 in. OD 1.51 in. ID	1.022 ± 0.010	93.208 ± 0.037 (93.19)	0.529 ± 0.005	5.241 ± 0.021
10932	15 in. OD disc	1.002 ± 0.006	93.143 ± 0.037 (93.15)	0.327 ± 0.003	5.528 ± 0.022
0.037B-2444-13	21 in. OD, 15in. ID	0.988 ± 0.006	93.220 ± 0.037	0.434 ± 0.004	5.583 0.021

[a]There was uranium metal at the Y-12 Plant with no ^{236}U before reactor fuel was blended in at the diffusion plant.

Typical accuracies for Y-12 plant isotopics are smaller [26] than those for uranium isotopic measurements at LANL; thus, the values for ^{235}U enrichment from the nuclear material transfer document should be used for the 1969 ORCEF benchmark. These Y-12 Plant uranium isotopic measurements for ^{234}U and ^{236}U result may be retrievable from archives of Y-12 Plant records although recent attempts have failed.

The thin 15 in. diameter HEU metal plates for these experiments were fabricated at the Y-12 Plant earlier than 1960. This is based on the Callihan (ORNL) letter to Paxton (LANL) dated May 20, 1960, transferring the material to LANL. Since there was appreciable ^{236}U in 4 of the 5 isotopic analyses given in Table 5.1-3, the material was fabricated after 1953 since at that time reprocessed uranium from reactor fuel was introduced into the diffusion process and blended with the uranium from ore. This reprocessed uranium contained ^{236}U, whereas the uranium ore did not. Before 1953, Oralloy at the Y-12 Plant contained no ^{236}U. Considerable Oralloy with no ^{236}U is still retained at the Y-12 Plant in storage.

The ^{234}U in HEU metal is a result the inefficiency in the diffusion process to separate it from the ^{235}U. HEU metal at the Y-12 Plant usually contains a little over 1 wt % ^{234}U. Over 50 isotopic enrichments of HEU metal performed in the early 1960s were evaluated. The average ratio of the ^{234}U/^{235}U enrichment was 0.01045. To obtain the ^{234}U enrichment for each part, multiply the ^{235}U enrichments of Table 5.1.1 by 0.01045. For the enrichment of ^{236}U, the values vary from 0 to 0.45 wt %. For ^{236}U enrichment assume 0.225 ± 0.225 wt %. The uncertainty in the ^{236}U enrichment should introduce a small or negligible uncertainty in the experimental neutron multiplication factor because the ^{238}U enrichment is obtained from the difference in the other three isotope from 100 wt %. The uncertainty in the ^{236}U enrichment just changes the ^{238}U enrichment and thus we are changing the enrichment of two non-fissile isotopes (236 and 238) with similar neutron cross sections and thus result in a small change. The uncertainty in the ^{235}U enrichment is discussed in reference 26.

5.1.3. Validity of the dimensions

Since the dimensional inspection reports were not available from Y-12 where the parts were fabricated or from LANL, the thicknesses were calculated from the known outside diameter (14.998 in.), the measured inside diameter of 1.510 ± 0.0005 in., the Y-12 masses measured to a small fraction of a gram (but reported within 0.5 g in Appendix A), and the average density of the uranium metal of 18.740 g/cm^3. These thicknesses are given in Table 5.1-2. For the final benchmark documentation, an attempt to retrieve the dimensional inspection reports from Y-12 should be made. However, the total measured height of some assemblies was documented in reference 2. These at the time were calculated from the individual measured thickness that were available to the author 50 years ago but not now. From differences of these measurements, the dimensions of some parts or collections of parts can be determined and compared to those calculated using the thicknesses of Table 5.1-2. The measured total thicknesses can also be compared to the calculated. For example, the difference in the dimensions of the parts for configurations of 19 and 18 thin 15 in. diameter HEU metal plates is part U-11146. The thickness obtained from the differences in the sum of the uranium height is 0.11850 in., compared to that calculated using the above assumptions: 0.11840 in., a difference of 0.0001 in., which is insignificant. Other comparisons of this type are given in Table 5.1-4. Similar difference (0.0001 in.) for part U-11149 also re-confirms the assumptions for the thickness of Table 5.1-2.

Table 5.1-4. Comparison of some measured total uranium metal thicknesses in assemblies with those obtained from sum of calculated thickness of Table 5.1-2.

Comparison	Measured total height of uranium plates	Calculated height of Uranium from Table 5.2 (in)	Difference measured minus calculated (in)
Total height of 20 plates, 1/16 polyethylene	6.083 cm or 2.39488 in.	**2.3935**	**+ 0.00138**
Total height of 19 plates, 1/16 polyethylene	5.786 cm or 2.2779 in.	**2.2744**	**+ 0.00355**

Total height of 18 plates, 1/16 polyethylene	5.486 cm or 2.1598 in.	**2.1563**	**+ 0.00354**
Total height of 14 plates, 1/16 polyethylene	4.262 cm or 1.6779 in.	**1.6762**	**+ 0.00175**
Total height of 10 plates, 1/16 polyethylene	3.041cm or 1.19724 in.	**1.19603**	**+ 0.00121**
Total height of 16 plates, 1/8 polyethylene	4.868 cm or 1.9165 in.	**1.91573**	**− 0.00080**

Table 5.1-4. Comparison of some measured total uranium metal thicknesses in assemblies with those obtained from sum of calculated thickness of Table 5.1-2 (continued).

Comparison	Measured total height of uranium plates from Table 4.2	Calculated height of Uranium from Table 5.2 (in)	Difference measured minus calculated (in)
Total height of 15 plates, 1/8 polyethylene	4.568cm or 1.7984 in.	1.79659	**+ 0.00018**
Total height of 12 plates, 1/8 polyethylene	3.658 cm or 1.4401 in.	**1.43904**	**+ 0.00112**
Total height of 10 plates, 1/8 polyethylene	3.048 cm or 1.200 in.	**1.20047**	**− 0.00047**
Total height of 12 plates, 1/4 polyethylene	3.658 cm or 1,4401 in.	**1.4337**	**− 0.00646**
Total height of 10 plates, ¼	3.043cm or 1.19803 in.	**1.19788**	**+ 0.00015**
Total height of 8 plates ¼	2.432 cm or 0.9575 in.	**0.95833**	**− 0.00085**
Total height of 6 plates ¼	1.823 cm or 0.71772 in.	**0.7177**	**−0.00003**
Total height of 8 plates ½	2.439 cm or 0.96033 in.	**0.95621**	**+ 0.00403**
Total height of 7 plates ½	2.138cm or 0.84173 in.	**0.83777**	**+ 0.00396**
Total height of 4 plates ½	1.214 cm or 0.47795 in.	**0.47914**	**− 0.00119**
8 minus 7 plates ½ defines U-11146 Thickness	**0.1185 in.**	**0.1184 in.**	**+ 0.0001**
19 minus 18 1/16 defines U-11149 thickness	**0.1181 in.**	**0.1182 in.**	**− 0.0001**

The small differences between the measured total uranium thicknesses and the total thickness obtained from the calculated thicknesses of Table 5.1-4 support the validity of the calculated thicknesses of Table 5.1-2. These thicknesses should be used for benchmark calculations unless the data from the dimensional inspection reports can be retrieved from Y-12 Plant records.

5.1.4. Impurity content

The impurities in the HEU uranium metal were obtained from reference 10 and are given in Table 5.1-5. It was assumed that the oxygen and nitrogen contents were 20 ppm, as was typical of Y-12 Plant Oralloy at that time.

Table 5.1-5. LANL impurity content of the uranium from reference 10.

(ppm)	11147	11149	11150	10932[a]	10933[a]
Li	<0.1	<0.1	<0.1	<0.1	<0.1
Be	<0.1	<0.1	<0.1	<0.1	<0.1
B	0.6	0.6	0.3	0.2	<0.1
C	1100	270	320	170	170
Na	<1	<1	<1	<1	<1
Mg	<1	<1	<1	<1	1
Al	50	40	20	150	100
Si	300	400	210	80	130
Ca	<2	<2	<2	<2	<2
V	<20	<20	<20	<20	<20
Cr	5	15	5	2	3
Mn	4	7	6	7	6
Fe	100	190	90	70	30
Co	<5	<5	<5	<5	<5
Ni	20	30	20	15	15
Cu	6	5	4	4	3
Mo	50	<25	<25	-	-
Sn	<1	<1	<1	-	-
Pb	5	<1	<1	-	-

An attempt to retrieve the chemical analysis from the Y-12 Plant at the time of fabrication before 1960 should be made and used for the final benchmark analysis.

5.2. DESCRIPTION OF THE POLYETHYLENE PARTS

The thickness of the polyethylene parts for the nominal 1/8, 1/4, and 1/2 layers were measured and those for the 1/16 in. thick were calculated from the measured masses and diameters. The actual average thicknesses were slightly different for the nominal dimensions and were 0.0606, 0.1279, 0.2464, and 0.5045 in., respectively.

5.2.1. Dimensions and masses of polyethylene parts

The dimensions and masses of the polyethylene parts are given in Table 5.2-1. The average masses, thicknesses, and densities are given in the table. Some polyethylene layers had 1.510 in. diameters; these polyethylene layers with axial holes were used in some subcritical measurements to allow the placement of the Cf source near the center of the assembly. The thicknesses of the 1/16 in. thick polyethylene layers were calculated assuming a density of 0.916 g/cm^3, a diameter of 14.990 in., and the known masses in column 2 of Table 5.2-1.

Table 5.2-1. Description of the Polyethylene parts[a].

Part #	Mass (g)	Thickness (in.)[b]	Diameter (in.)[c]		Part #	Mass (g)	Thickness (in.)	Diameter (in.)		Part #	Mass (g)	Thickness (in.)	Diameter (in.)	
ab	160	0.0604	14.990		1	345	0.1290	14.990		30	660	0.2485	14.986	
cd	159	0.0600	14.990		2	343	0.1292	14.990		31	651	0.2355	14.991	
ef	158	0.0596	14.990		3	339	0.1282	14.984		32	651	0.2455	14.988	
gh	159	0.0600	14.990		4	337	0.1280	14.980		33	659	0.2485	14.987	
ij	158	0.0596	14.990		5	343	0.1285	14.990		34	650	0.2450	14.992	
kl	165	0.0623	14.990		6	340	0.1282	14.985		35	652	0.2453	14.989	
mn	163	0.0615	14.990		7	342	0.1290	14.990		36	659	0.2470	14.990	
op	163	0.0615	14.990		8	343	0.1292	14.992		37	650	0.2450	14.990	
qr	160	0.0604	14.990		9	340	0.1282	14.994		37	660	0.2495	14.991	
st	163	0.0615	14.990		10	337	0.1292	14.990		39	661	0.2490	14.992	
uv	158	0.0596	14.990		11	340	0.1283	14.992		40	650	0.2453	14.989	
yz	166	0.0627	14.990		12	341	0.1286	14.995		41	653	0.2460	14.988	
90	163	0.0615	14.990		13	339	0.1280	14.998		42[d]	647	0.2455	14.988	
91	165	0.0623	14.990		14	342	0.1290	14.998		43[d]	644	0.2459	14.992	
92	162	0.0612	14.990		15	338	0.1288	14.994		44[d]	644	0.2453	14.989	
93	165	0.0623	14.990		16	340	0.1284	14.994		45[d]	645	0.2450	14.988	
94	162	0.0612	14.990		17	341	0.1282	14.992		46[d]	644	0.2460	14.989	
95	162	0.0612	14.990		18d	333	0.1288	14.975		47[d]	642	0.2453	14.986	
96	163	0.0615	14.990		19[d]	330	0.1260	14.980		48	650	0.2450	14.985	
97	165	0.0623	14.990		20	343	0.1266	14.995		49	648	0.2445	14.985	
98	165	0.0623	14.990		21[d]	335	0.1265	14.994		50	650	0.2455	14.986	
B1[d]	161	0.0609	14.990		22[d]	334	0.1268	14.998		51	650	0.2450	14.985	
B2[d]	161	0.0609	14.990		23[d]	330	0.1255	14.997		52	651	0.2450	14.985	
B3[d]	161	0.0609	14.990		24[d]	335	0.1275	14.996		53	658	0.2485	14.986	
B4[d]	163	0.0615	14.990		25[d]	332	0.1265	14.998		54	658	0.2490	14.985	
B5[d]	160	0.0604	14.990		26[d]	330	0.1255	14.998		55	654	0.2490	14.986	
B6[d]	164	0.0619	14.990		P6	56.5	0.1279	14.984		56	659	0.2490	14.986	
P1	27.5	0.0604	14.990		P7	56.5	0.1279	14.984		P11	109	0.2464	14.991	
P2	27.5	0.0604	14.990		P8	56.5	0.1279	14.984		P12	109	0.2464	14.991	
P3	27.5	0.0604	14.990		P9	56.5	0.1279	14.984		P13	109	0.2464	14.991	
P4	27.5	0.0604	14.990		P10	56.5	0.1279	14.984		P14	109	0.2464	14.991	
P5	27.5	0.0604	14.990		70[d]	1322	0.5005	14.992		P15	109	0.2464	14.991	
60	1337	0.5018	14.990		71[d]	1323	0.5020	14.988		80	1355	0.5105	15.001	
61	1339	0.5025	14.990		72[d]	1320	0.5022	14.985		81	1358	0.5102	14.998	
62	1336	0.5022	14.989		73	1339	0.5042	14.992		82	1361	0.5112	14.995	
63	1336	0.5022	14.987		74	1334	0.4997	14.980		83	1363	0.5112	14.997	
64	1342	0.5042	14.985		75	1343	0.5052	14.984		84	1365	0.5035	14.998	
65	1337	0.5040	14.985		76	1337	0.5038	15.002		P16	223	0.5018	14.985	
66	1341	0.5038	14.982		77	1343	0.5052	14.998		P17	223	0.5018	14.985	
67	1339	0.5038	14.983		78	1354	0.5098	14.998		P18	223	0.5018	14.985	
68	1340	0.5040	14.990		79	1354	0.5020	14.998		P19	223	0.5018	14.985	
69[d]	1330	0.5042	14.990							P20	223	0.5018	14.985	

[a] The pie section identifications initiate with the letter P, and the masses of the pie sections were assumed to be 1/6 of the average mass of the full layers.

[b] The thickness was calculated using the assumed diameter of 14.490 in. and the assumed density of 0.916 g/cm^3 and the mass given in column two.

[c] The diameter was assumed to be the average of the diameters for the 1/8 in. thick polyethylene parts.

[d] Masses of these parts with a central 1.510 in. diameter hole.

In addition to these polyethylene layers, on Aug 26, 1969, four 1/32 in. thick layers were identified as A1, A2, A3, and A4 with 1.510 in. diameter axial holes acquired. It was assumed that the weight of each one was 80.5 g and 0.0325 in. thick. These parts were used for the subcritical assemblies with 1/16 in. thick polyethylene with 18 and 19 thin 15 in. diameter HEU metal plates. The average masses, diameters, and thicknesses as well as average densities are given in Table 5.2-2.

Table 5.2-2. Average masses, diameters, and thicknesses of Polyethylene parts.

Nominal thickness (in.)	Average Thickness (in)	Average Diameter (in.)	Average Mass (g)	Density (g/cm^3)
1/16	0.0606	Assumed 14.990	162	Assumed 0.916
1/8	0.1279	14.992	339	0.916
1/4	0.2464	14.988	654	0.918
1/2-60-75/76-84[a]	0.5029/0.5075	14.987 /14.999	1339/1359	0.921

[a]For the ½ inch thick polyethylene the parameters are in two groups. For example, for parts 60 to 75, the average thickness is 0.5029 and that for parts 76 to 84 the average thickness was 0.5075.

Except where noted in the logbook, the polyethylene parts were used in numerical order from bottom to top, starting on the diaphragm. The lowest polyethylene part number was located at the bottom of the stack of material on the diaphragm. The polyethylene part after the top part on the diaphragm was the lowest part on the vertical lift, and polyethylene part numbers increased to the top of the material on the vertical lift. For a hypothetical example of this for an assembly of 15 polyethylene parts with thickness of 1/8 in. and 10 polyethylene parts on the diaphragm, Parts 1 to 10 would be in the stack on the diaphragm with Poly 1 on the bottom and Poly 10 on the top. On the vertical lift, Poly 11 would then be on the bottom and Poly 15 would be on the top. In some cases, polyethylene between uranium metal plates were not always the thickest poly parts that could be used.

5.2.2. Validity of the thicknesses of the 1/16 in. polyethylene

Since the thicknesses of the 1/16 in. thick polyethylene layers were calculated from the measured masses and outside diameters, their validity was evaluated by examining measured sums of polyethylene parts and comparing them with calculated values. These comparisons are given in Table 5.2-3 and the differences are very small, indicating their validity. They can thus be used for benchmarking the 1969 ORCEF experiments if these data cannot be retrieved from the Y-12 Plant records. Except for one of the comparisons, the differences are a thousandth of an inch or less. The largest for the sum of 18 layers was 7 thousandths of an inch. It is particularly validating for the thicknesses for the 1/16 in. thick part "ab" that the value determined from these measurement differences was within 0.001 in. of that of Table 5.2-1. Similar evaluation for POLY-63 gives a difference of 0.00015 in., a factor of ~7 lower in better agreement. Thus, the uncertainty in the thicknesses of Table 5.2-1 are less than 0.0001 in. These comparisons confirm the calculated thicknesses of Table 5.2-1.

Table 5.2-3. Comparison of some measured total polyethylene thicknesses in assemblies with those obtained from sum of calculated thickness.

Comparison	Sum of measured heights of polyethylene layers (cm)	Calculate sum of calculated height of Polyethylene layers (cm)	Difference (cm or in)
Total height of 18 1/16 polyethylene layers	2.803	2.82066	0.0176 cm or 0.0069 in. for the sum of 18 poly layers
Total height of 17 1/16 polyethylene layers	2.653	2.6532	0.0002 cm or 0.0001 in. for the sum of 17 poly layers
Total height of 13 1/16 polyethylene layers	2.027	2.0267	0.0003 cm or 0.000118 in. for the sum of 13 poly layers
Total height of 9 1/16 polyethylene layers	1.401	1.4044	0.00340 cm or 0.00134 in. for the sum of 9 poly layers
18 minus 17 1/16 defines the thickness of ab	0.150	0.1524	0.0024 cm or 0.00094 in.
7 minus 6 ½ defines the thickness of Poly 63	1.276	0.5022 in or 1.2756 cm	0.0004 cm or 0.0001575 in. good agreement with the thickness in Table 5.4

6. BENCHMARK POSSIBILITIES

There are several options as to how these data can be used to benchmark calculational methods. Except for the two configurations with k_{eff} = 1.0000 (only 2), the neutron multiplication factor of the near delayed critical configuration could be calculated from the measured reactivities. But first, to obtain the measured neutron multiplication factors from the measured reactivities in cents, where 100 cents equals the value of the effective delayed neutron fraction, the effective delayed neutron fraction needs to be calculated for each critical and subcritical configuration. In all the simulations, the stainless-steel diaphragm and other support structures must be included in the Monte Carlo model of the delayed critical configurations. Monte Carlo models of the low mass upper and lower support must be included in the models, and these may be available by direct contact with Dr. Kermit Bunde of the US DOE Idaho Operations Office. A correction for room return must also be made to obtain the experimental k_{eff} without the room, or the room must be included in the benchmark calculation. Some of these critical or very near critical configurations are sufficiently accurate such that with additional uncertainty analysis, calculations and documentation can be the basis of ICSPEP benchmarks. The most accurate measurements were those for which the gaps between layers were measured—that is, configurations of thin 15 in. diameter HEU metal plates with 1/16, 1/8, ¼, and ½ in. thick polyethylene layers. For some of the critical configurations with more than ½ in. thick polyethylene, the polyethylene parts are not clearly identified and the gaps between layers were assumed. However, they may be sufficiently accurate or have larger uncertainty in the neutron multiplications. Two types of Monte Carlo models can be used in these benchmark calculations: a detailed model, where the data for each uranium metal and polyethylene part can be described with the appropriate gaps between them, and a simplified model, where average values for various materials can be used. The best comparisons will be obtained with the detailed models.

Some of reactivities from the IKRD measurements are sufficiently accurate for neutron multiplication factors greater than 0.90 such that the subcritical reactivities can be converted to neutron multiplication factor using calculated values of the effective delayed neutron fraction. With relevant uncertainty analysis, the neutron multiplication factor can be used for subcritical ICSBEP benchmarks.

The prompt neutron decay measurements may be the basis for an IRPhE benchmark. The configurations are cylindrically symmetric and can be calculated by both Sn and Monte Carlo transport theory methods. The prompt neutron time decay constant measurements at delayed criticality can also be calculated directly by Monte Carlo methods such as MCNP-PoliMi [27] and can thus be used for benchmarking calculational methods for the IRPhE. Both the randomly pulsed neutron and the Rossi-α measurement data can be calculated by Monte Carlo methods if the detectors are included in the calculation. The detection efficiency used in MCNP-PoliMi should be adjusted to match the measured detection efficiency as a function of time, given in Figure 4.2-2, for the liquid scintillator with gamma discrimination. The calculations should include the simulation of the means of data acquisition with the type of time analysis equipment described in reference 22. The prompt neutron decay data are available from the Records Management Services Records Department of ORNL, from OSTI, and from ICSBEP at INL. A suggestion for future work to complete the documentation of the critical and subcritical experiments is given in Appendix F.

7. CONCLUSIONS

The highly enriched uranium metal 15 in. diameter uranium metal plates were assembled to delayed criticality at the Oak Ridge Critical Experiments Facility (ORCEF) in 1969 with various thicknesses of polyethylene (varying from 1/16 to 2 ⅜ inches) between plates. The average enrichment was 93.27 wt % ^{235}U. The critical configuration contained from 4 ⅔ to 20 ⅚ thin 15 in. diameter HEU metal plates (on loan from LANL) depending on the thickness of polyethylene with enriched uranium masses varying from 28,053 to 135,148 g. In addition to the measurement at delayed criticality some subcritical measurements were performed by the inverse kinetic rod drop method. Prompt neutron decay constant measurements were also performed by the Rossi-alpha and randomly pulsed neutron method using a time-tagged, centrally located, spontaneous fission Cf neutron source, but only a few details of the data are reported here. These accurate descriptions of the 10 critical configurations (with some variations) and materials allow these experiments to be used to prepare a benchmark for incorporation into to the ICSBEP. Uncertainty analysis must be performed to determine the accuracy of the experimental neutron multiplication factors, k_{eff}. This analysis should mimic that performed for other ICSBEP nuclear criticality safety benchmarks already documented with these materials in the ICSBEP and Nuclear Energy Agency programs such as HEU-MET-FAST-051 and others. Because of the accurate descriptions of the configuration and materials [28], the uncertainties in the k_{eff} values should be very low for many of the configurations. Because of incomplete descriptions in the logbook, some assumptions were made regarding the material configuration based on the author's memory. The future uncertainty analysis will ascertain which configurations are not properly described and should not be used for benchmark applications. With the proper uncertainty analyses and documentation, the data from the prompt neutron decay constant measurements may be used for IRPhE benchmarks.

This report documents the experimental information for the measurements performed so that later researchers can perform the required uncertainty and calculational analyses and documentation to use these data for an International Nuclear Criticality Safety Benchmark Evaluation Program (ICSBEP) or a Nuclear Energy Agency (NEA) benchmark. The data from the experiments described should be acceptable for use as criticality safety benchmark experiments for the ICSBEP and the NEA nuclear criticality safety benchmark program once the uncertainty analysis is completed. Based on previous ICSBEP benchmarks with this enriched uranium metal at ORCEF, the uncertainties in k_{eff} could be as low as ± 0.0002 for some configurations. Other experiments with these thin 15 in. diameter HEU metal plates have been benchmarked in reference 26.

Preparation of the present report is part of a larger effort at ORNL to document more than 15 undocumented critical and subcritical experiments enumerated in ORNL/TM-2019/18 and performed by

ORNL at ORCEF and other US DOE critical experiments facilities using more than 500 operational days of critical facility time. The publication of this report was supported by the Nuclear Criticality Radiation Transport and Safety NCSP program at ORNL.

8. REFERENCES

1. John T Mihalczo, "Heterogeneous Critical Assemblies of Enriched Uranium Metal Plates and Polyethylene" American Nuclear Society 1995 Winter Meeting, San Francisco, California, *Trans. Amer. Nucl. Soc*., 73, 219–220 (1995). [OSTI #411655]
2. J. T. Mihalczo, "Use of ^{252}Cf as a Randomly Pulsed Neutron Source for Prompt Neutron Decay Measurements" Union Carbide Corp Nuclear Division, Oak Ridge Y-12 Plant, Y-DR-41 (Jan 1971).
3. John T. Mihalczo, "Time Domain Measurements for Fast Metal Assemblies with ^{252}CF" Annals of Nuclear Energy, Vol. 2. pp 161 to 175, *Pergamon Press* (1975).
4. C. M. Hopper, W. C. Jordan, "Calculated Neutron Spectra for Heterogeneous U93) and CG2 Critical Assemblies," American Nuclear Society 1995 Winter Meeting, San Francisco, California, *Trans. Amer. Nucl. Soc*., 73, 220–221 (1995).
5. J. B. Bullock, J. T. Mihalczo, and M. V. Mathis, "IKRD Measurements with a Mockup of the CRBR Shield," *Trans. Am. Nucl. Soc.* 18, 347 (1974).
6. John D. Orndoff, "Prompt Neutron Periods of Metal Critical Assemblies," *Nucl. Sci. Eng.*, **2**, no. 4, 450–460 (1957).
7. J. T. Mihalczo, "The Use of Californium-252 as a Randomly Pulsed Neutron Source for Prompt Neutron Decay Measurements," *Nucl. Sci. Eng*., 53, 393–414 (1974).
8. J. D. Norris, R. Araj, D. P. Heinrichs, C. G. Percher, M. L. Zerkle, "TEX-HEU Baseline Assemblies: Highly Enriched Uranium Plates with Polyethylene Moderator and Polyethylene Reflector" LLNL-TR-829327-DRAFT (2021).
9. Burton J. Krohn, "Criticality safety analysis of the early (unreflected) "JEMIMA " and the (reflected) "BIG TEN" Experiments: calculated effects of fuel homogenization" Los Alamos National Laboratory, LA-UR 95-2244, Fifth International Conference on Nuclear Criticality Safety Albuquerque, NM (1995).
10. Burton J Krohn, "The Early JEMIMA Experiments: Bare Cylindrical Configurations of Enriched and Natural Uranium" IEU-MET_FAST-001, NEA/NSC/DOC(95))03/111 (1995).
11. John T. Mihalczo, "Critical and Subcritical NEA Benchmark Possibilities for Measurements at ORCEF and Other US DOE Facilities", ORNL/TM-2019/1188 (June 2019).
12. J. T. Mihalczo, Brief Summary of Unreflected and Unmoderated Cylindrical Critical Experiments with Oralloy at Oak Ridge, ORNL/TM-1999/302, Oak Ridge National Laboratory, Oak Ridge, TN (November 1999).
13. J. T. Mihalczo, "Prompt-Neutron Decay in a Two-Component Enriched Uranium Metal Critical Assembly," *Trans. Am. Nucl. Soc.* **6**, 60 (1963).
14. J. T. Mihalczo, "Prompt Neutron Decay in a Two-Component Enriched Uranium Metal Critical Assembly," ORNL/TM-470, Oak Ridge National Laboratory, Oak Ridge, TN (1963).
15. J. T. Mihalczo, "Graphite and Polyethylene Reflected Uranium-Metal Cylinders and Annuli," Y-DR-81, Oak Ridge Y-12 Plant, Oak Ridge, TN (1972).

16. J. T. Mihalczo, “Prompt Neutron Lifetime in Critical Enriched-Uranium Metal Cylinders and Annuli,” *Nucl. Sci. Eng*. **20**, 60–65 (1964).

17. J. T. Mihalczo, “Monte Carlo Calculations of Two Core Delayed Critical Assemblies,” *Trans. Am. Nucl. Soc.* **11**, 603 (1968).

18. J. T. Mihalczo, “Prompt Neutron Time Behavior in Delayed Critical Coupled Uranium Metal Cylinders,” *Proceedings of the International Conference on Fast Critical Experiments and Their Analysis*, ANL-7320, 237–41 (October 1966).

19. J. T. Mihalczo, J. J. Lynn, and J. R. Taylor, Delayed Critical ORNL Unreflected Uranium (93.20) Metal Sphere and the Pure Unreflected Uranium (93.80) Sphere Critical Mass, Ann. of Nucl. Energy **29**, 525 (2002).

20. Robert H. Elwood and John T. Mihalczo, “Uranium (93.2) Metal Cylinders (7-inch, 9-Inch, 11-inch, 13-inch, and 15-inch Diameter) and Two 11-inch-Diameter Interacting Uranium (93.2) Metal Cylinders” HEU-MET-FAST-051, NSC/DOC/(95)03/II Volume II (2021).

21. “Oak Ridge Critical Experiments Facility Operating Procedures”, Oak Ridge Y-12 Plant Y-DR-54 (Sept 1971).

22. Cesar A. Sastre, “The Measurement of Reactivity” Nucl. Sci. Eng. **B**, 443 (1960).

23. John T. Mihalczo, “Data from Rossi-α and Pulsed Neutron Prompt neutron Time Decay Measurements at ORCEF” Oak Ridge national Laboratory, ORNL/TM-2019/1455 (April 2019). [OSTI number 1543205]

24. J. T. Mihalczo, “Prompt Neutron Lifetime in Critical Enriched-Uranium Metal Cylinders and Annuli *Nucl. Sci. Eng*., 20, 60 (1964). [OSTI #403157]

25. William Myers, Los Alamos National Laboratory, Personal communication (2021).

26. John T. Mihalczo, Uncertainties in Masses, Dimensions, Impurities, and Isotopics of HEU Metal Used in Critical Experiments at ORCEF, ORNL/TM-2012/32, Oak Ridge National Laboratory, Oak Ridge, TN (September 2012). [OSTI #1052246]

27. Sara A. Pozzi, Enrico Padovani & Marzio Marseguerra, “MCNP-PoLiMi: a Monte Carlo Code for Correlation Measurements” Nuclear Instruments and Methods in Physics Research Section A; Accelerators, Spectrometers, Detectors and Associated Equipment, Volume 513, Issue 3, 11 November 2003, Pages 550-558.

28. “International Handbook of Evaluated Criticality Safety Benchmark Experiments” NEA No 7360 (Dec 2021).

APPENDIX A. FISSILE MATERIAL TRANSFER FORM AEC-101 AND MAY 20, 1960, LETTER FROM A. D. CALLIHAN OF ORNL TO H. D. PAXTON OF LANL

This appendix presents the nuclear material transfer document (AEC-101) dated July 3, 1969 (Table A.1.) documents the total mass of uranium and total ^{235}U mass sent to ORNL. Also included in Table A-1 is the SS transfer form that documents the masses and enrichment of the uranium metal plates sent from LANL on June 2, 1969. Portions of the transfer form have not been copied here to make the masses and enrichments more readable.

A copy of the 1960 letter (Table A.2) documenting the masses and ^{235}U enrichments of the various thin 15 in. diameter HEU metal plates produced for LANL by the Y-12 Plant is also given in this appendix. The masses of each part presented in this letter were measured to a small fraction of a gram but listed in this letter to one gram and thus are accurate to ± 0.5 grams. The measured ^{235}U enrichments are also presented, but not the ^{234}U and ^{236}U enrichments. The enrichments given for each part were measured at the Y-12 plant at the time of fabrication as per usual procedures for Oralloy parts. This assumption is confirmed by the LANL enrichments of 1974 for some of the parts. Why would LANL measure the enrichment of some few parts in 1974 if LANL measured them initially right after shipment to LANL? The accuracy of the Y-12 ^{235}U enrichments is discussed in a reference [26]. These along with the dimensional inspection results may be retrievable from the Y-12 archives and these would be desirable for any future ICSBEP or IRPhE benchmarking analysis. This letter given in Table A.2 contains a typographical error: part number 14085 should be part number 10485.

Table A.1. Material transfer form AEC-101 documenting the total uranium mass and ^{235}U mass and average enrichment of ~15 in. diameter thi15 in. diameter HEU metal enriched uranium metal plates.[a]

Form AEC-101 (Rev. 8-64)
U.S. Atomic Energy Commission
AECM-7401

NUCLEAR MATERIAL TRANSFER DOCUMENT   JEMIMA

1. TRANSFER NO. AUA-FZB-283

2. SHIPPER'S FACILITY CODE AUA
Name Los Alamos Scientific Laboratory
Address P. O. Box 1663
Los Alamos, New Mexico 87544
G. R. Champion

3. RECEIVER'S FACILITY CODE FZB
Name Union Carbide Corporation
Address Nuclear Division, Y-12 Plant
Oak Ridge, Tennessee 37830
Attention: Edward Owings/Dixon Callihan

4. No.	DISTRIBUTION of COPIES
1	FZB - AUA
2	FZB
3	FZB - AAA
4	AAA
5	FZB - FAA
6	FAA
7	AUA
8	AUA
9	None
10	None
11	None

5. SHIPPED FOR ACCOUNT OF (Facility Code)
Name
Address

6. SHIPPED TO ACCOUNT OF (Facility Code)
Name
Address

7. MATERIAL TRANSFERRED IS: (Check if applicable) Shipper Receiver
a. Under Supply Agreement with AEC ( ) ( )

8. THIS TRANSFER:
a. Initiates or Alters Financial Liability to the AEC ( )
b. Does Not Initiate or Alter Financial Liability to the AEC ( )

9. DOCUMENTATION (If document is classified)
a. Page ___ of ___ Pages
b. Copy 5 of ___ Copies
c. Series ___

10. TRANSFER AUTHORITY: K 291, K 292, K 293, K 204, K 295

11. MATERIAL TYPE AND DESCRIPTION
Enriched Uranium

12. TRANSFER DATA
a. The Quantities Listed Below Were Shipped On June 3 1969
(Signature of Shipper's Authorized Representative)
b. Weight Units grams
c. From-AEC Project No. A-42000-00-1

13. a.*
(Signature of Receiver's Authorized Representative)
*FOR OTHER THAN AEC COST-TYPE CONTRACTORS, COMPLETION OF BLOCK 13. a. CONSTITUTES ACCEPTANCE OF THE DATA IN BLOCK 12: IF THE RECEIVER INTENDS TO CONTEST THE DATA, BLOCK 13. a. SHOULD NOT BE COMPLETED AND THE SHIPPER SO NOTIFIED.
AEC COST-TYPE CONTRACTORS MUST SHOW THEIR RECEIVER'S DATA IN BLOCK 13.
b. To-AEC Project No.
c. Date Material Received

d. Lot & container no.	e. Gross weight	f. Net weight	g. Element weight	h. Weight % Isotope	i. Isotope weight	d. Gross weight	e. Net weight	f. Element weight	g. Weight % Isotope	h. Isotope weight
6 55 gal. barrels AL-L16										
Enriched Uranium Wt in grams			174,865		163,091					
					93.267					
LASL SH 4443										
REF: Letter dated May 20, 1969										
Dixon Callihan to H. C. Paxton										

[a]Average enrichment can be determined from the total ^{235}U mass divided by the total uranium mass.

SS TRANSACTIONS

TRANS-ACTION NUMBER		DATE M	DATE D	DATE Y	LOT IDENTIFICATION NUMBER TO LETTERS	TO NUMBERS	FROM LETTERS	FROM NUMBERS	ACCOUNT NUMBER TO	ACCOUNT NUMBER FROM	BULK VOLUME OR WEIGHT QUANTITY	UNIT	SS IDENT	SS (OR T) VALUE	% ENRICH	ISOTOPE WEIGHT
K292	1	6	29					10932	410452			1	25	6498	7215	66063
	2							10491						6515	37	6083
	3							11160						6445	17	6005
	4							11149						6410	24	5977
	5							11017						6518	31	6022
	6							10477						6505	35	6072
	7							11146						6426	30	5993
	8							11019						6477	18	6035
	9							10493						6427	25	5993
	0							10459						6473	7277	6045

REMARKS: (GIVE ALL DETAILS NEEDED TO COMPLETELY DESCRIBE ITEM, SUCH AS TYPE AND CONCENTRATION OF ACID OR ACIDS, TYPE & CONCENTRATION OF ORGANICS, FORM OF MATERIAL (SOLUTION, METAL, OXIDE, PLASTIC, ETC.) CONCENTRATION OF CONSTITUENTS, ETC.)

64,694

SS TRANSACTIONS

TRANS-ACTION NUMBER		DATE M	DATE D	DATE Y	LOT IDENTIFICATION NUMBER TO LETTERS	TO NUMBERS	FROM LETTERS	FROM NUMBERS	ACCOUNT NUMBER TO	ACCOUNT NUMBER FROM	BULK VOLUME OR WEIGHT QUANTITY	UNIT	SS IDENT	SS (OR T) VALUE	% ENRICH	ISOTOPE WEIGHT
K291	1	6	29					11148	410452			1	25	6441	7218	6002
	2							10457						6587	44	6155
	3							10935						6471	18	6030
	4							10469						6376	38	5954
	5							10495						6448	24	6012
	6							10470						6408	41	5986
	7							10933						6486	16	6042
	8							11019						6420	19	5973
	9							10475						6361	7240	5941
	0															

REMARKS: (GIVE ALL DETAILS NEEDED TO COMPLETELY DESCRIBE ITEM, SUCH AS TYPE AND CONCENTRATION OF ACID OR ACIDS, TYPE & CONCENTRATION OF ORGANICS, FORM OF MATERIAL (SOLUTION, METAL, OXIDE, PLASTIC, ETC.) CONCENTRATION OF CONSTITUENTS, ETC.)

Item 1 to 5 packed in BARREL #3 57,958 Include 3 inserts

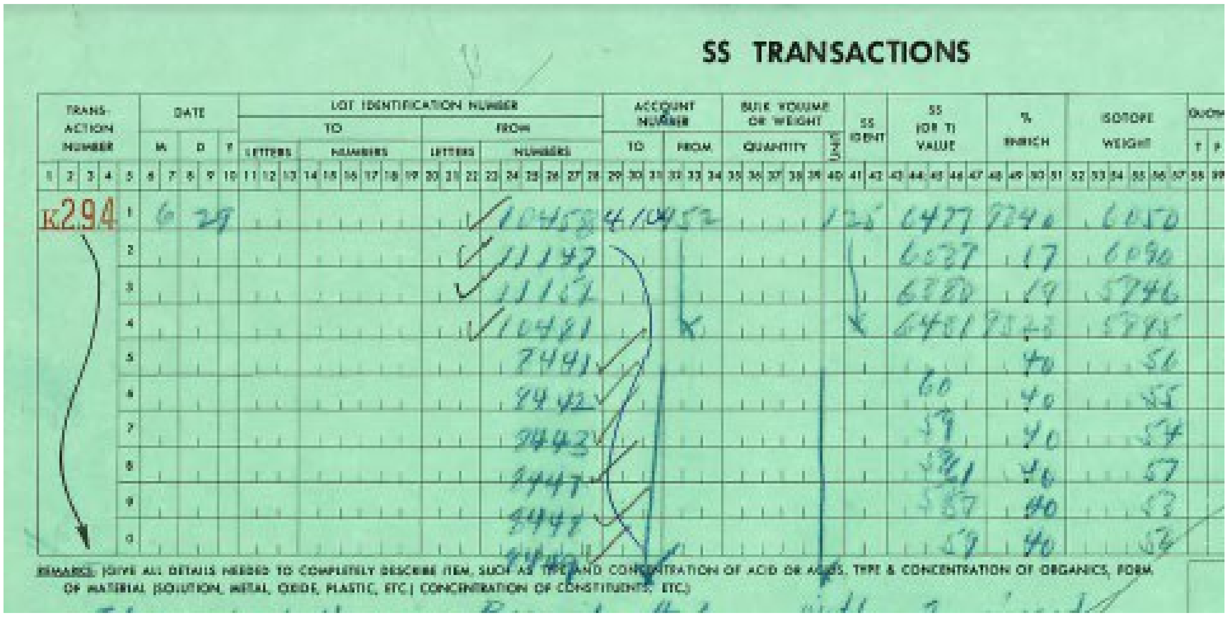

SS TRANSACTIONS

Trans-action Number	Line	Date M	Date D	Date Y	Lot Identification Number To Letters	To Numbers	From Letters	From Numbers	Account Number To	Account Number From	Bulk Volume or Weight Quantity	Unit	SS Ident	SS (or T) Value	% Enrich	Isotope Weight
K294	1	6	29					10458	4	10452			125	6477	9340	6050
	2							11147						6037	17	6090
	3							11162						6380	19	5946
	4							10481						6481	9343	5995
	5							9441							40	56
	6							9442						60	40	55
	7							9443						59	40	54
	8							9447						58	40	57
	9							9447						58	40	53
	0							9449						57	40	53

REMARKS: (GIVE ALL DETAILS NEEDED TO COMPLETELY DESCRIBE ITEM, SUCH AS TYPE AND CONCENTRATION OF ACID OR ACIDS, TYPE & CONCENTRATION OF ORGANICS, FORM OF MATERIAL (SOLUTION, METAL, OXIDE, PLASTIC, ETC.) CONCENTRATION OF CONSTITUENTS, ETC.)

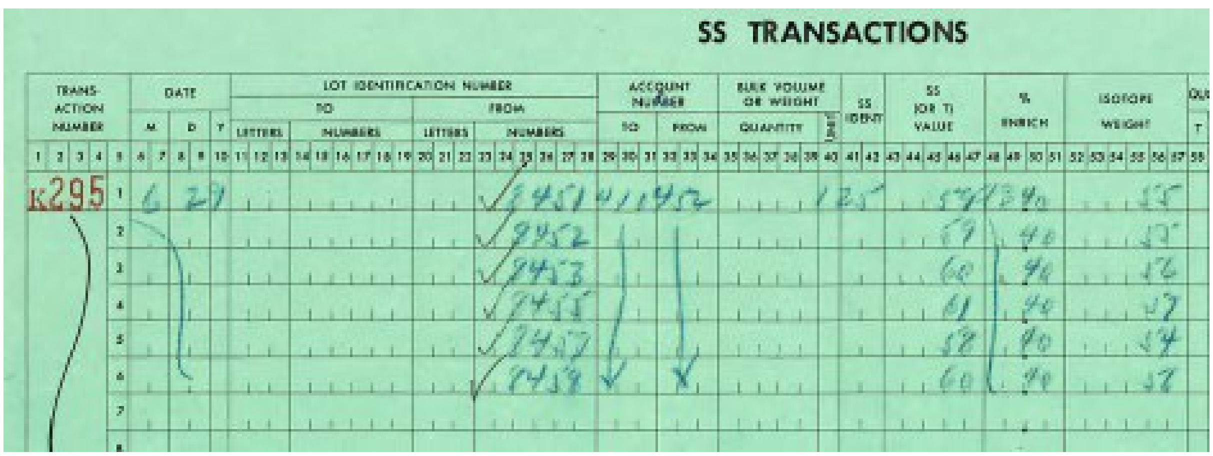

SS TRANSACTIONS

Trans-action Number	Line	Date M	Date D	Date Y	Lot Identification Number To Letters	To Numbers	From Letters	From Numbers	Account Number To	Account Number From	Bulk Volume or Weight Quantity	Unit	SS Ident	SS (or T) Value	% Enrich	Isotope Weight
K295	1	6	29					9451	4	11452			125	59	9340	55
	2							9452						59	40	55
	3							9453						60	40	56
	4							9455						61	40	57
	5							9457						58	40	54
	6							9459						60	40	58
	7															
	8															

Table A.2. Copy of the letter from A. D. Callihan (ORNL-Y-12) to H. C. Paxton (LANL) documents the mass and ^{235}U enrichment of each full 15 in. diameter thin HEU metal plate, the pie sections and the uranium metal inserts. (The typical method of measuring the uranium isotopics at Y-12 was to divide a metal chip into three pieces and perform three separate spectrographic measurements. Usually (90 % of the time) all three measurements gave the same enrichment to four digits.

REF: Letter dated May 20, 1960, Dixon Callihan to H. C. Paxton
LASL SM 4443

Enriched Uranium Wt in grams	BBL No.	SS Net Wt	% enrichment	U-235
10932	1	6498	93.15	6053
10491	With 1	6515	93.37	6083
11150	insert	6445	93.17	6005
11149		6410	93.24	5977
11017		6518	93.31	6082
10477	2	6505	93.35	6072
11146	With 2	6426	93.20	5989
11019	inserts	6477	93.18	6035
10493		6427	93.25	5993
10489		6473	93.39	6045
11148	3	6441	93.18	6002
10457	With 3	6587	93.44	6155
10935	inserts	6471	93.18	6030
10464		6376	93.38	5954
14085		6448	93.24	6012
10470	4	6408	93.41	5986
10933	With 2	6486	93.16	6042
11018	inserts	6420	93.19	5983
10475		6361	93.40	5941
10483	5	6339	93.24	5910
10467	With 2	6455	93.41	6030
8601	inserts	1072	93.13	998
8062		1076	93.13	1002
8063		1066	93.13	992
8064		1074	93.13	1000
8065		1073	93.13	999
8066		1086	93.13	1011
10487		6396	93.26	5965
10458	6	6477	93.40	6050
11147	With 2	6537	93.17	6090
11151	inserts	6380	93.19	5946
10481		6431	93.23	5995

INSERTS

Enriched Uranium Wts in grams	SS Net Wt	%	U-235
8441	60	93.40	56
8442	59	93.40	55
8443	58	93.40	54
8447	61	93.40	57
8448	57	93.40	53
8449	59	93.40	56
8451	59	93.40	55
8452	59	93.40	55
8453	60	93.40	56
8455	61	93.40	57
8457	58	93.40	54
8458	60	93.40	56

APPENDIX B. EXISTING REPORTS IN THE DOCUMENTATION OF PREVIOUSLY UNDOCUMENTED CRITICAL AND SUBCRITICAL EXPERIMENTS

This documentation effort was initiated by the author of this report in 2018 to document previously undocumented critical and subcritical experiments. The purpose of this work is to summarize information from past experiments from logbooks, experimenter's notes, inspection reports and the experimenter's memory so that future researchers could use this information to provide benchmarks for the International Criticality Safety Benchmark Evaluation Program and the International Reactor Physics Benchmark Evaluation Program. The report published so far are as follows.

1. John T. Mihalczo, "Delayed Critical and Subcritical Experiments with Polyethylene Moderated Unreflected Thin 15 in. diameter HEU Metal Plates" ORNL/TM-2024 (Feb 2023)

2. John T. Mihalczo, "Delayed Critical Enriched Uranium Metal, 7-in.-Diam Cylinder with Thin Stainless-Steel Reflector on Top and Bottom" ORNL/TM-2022/2481 (2022) [OSTI 1887691]

3. John T. Mihalczo, ´Uranium-Molybdenum Alloy Critical Experiment for the Health Physics Research Reactor" ORNL/TM2021/2234 (June 2022) [OSTI #1887715]

4. John T. Mihalczo, "Critical and Californium Source-Driven Noise Analysis Subcritical Measurements with an Unreflected Cylindrical Tank of Mixed Uranium-Plutonium Nitrate Solution" ORNL/TM-2021/1606 (Dec 2021)

5. John T. Mihalczo, "Subcritical Measurements for a Changing Concentration Uranyl Nitrate Solution Tank by the Californium Source Driven Noise Analysis" (2022) [OSTI #1887710]

6. John T. Mihalczo, "Critical and Subcritical Californium Source Driven Noise Analysis Experiments with Fresh PWR Fuel Pins" ORNL/TM-2020/1606 (Dec 2021)

7. John T. Mihalczo, "Subcritical Californium Source-Driven Noise Analysis Measurements with Unreflected Uranium (93.15) Hydride" ORNL/TM-2021/1963 (June 2021)

8. John T. Mihalczo, "Data from Rossi-α and Pulsed Neutron Prompt neutron Time Decay Measurements at ORCEF" Oak Ridge national Laboratory, ORNL/TM-2019/1455 (April 2019) [OSTI number 1543205]

9. John T. Mihalczo, "Three Delayed Critical 15-inch-Diameter Interacting Enriched (93.14) Uranium Metal Cylinders without Moderator and Reflector" ORNL/TM-2019/1456 (2019)

10. John T. Mihalczo, "Two Delayed Critical 15-inch-Diameter Interaction Enriched (93.14) Uranium Metal Cylinders without Moderator and Reflector" ORNL/TM-2019/1409 [OSTI #1661251]

11. John T. Mihalczo, "Two Delayed Critical 7-inch-Diameter Interaction Enriched (93.14) Uranium Metal Cylinders without Moderator and Reflector" ORNL/TM-2019/1396 (Nov 2019) [OSTI 1606828]

12. John T. Mihalczo, "Reactor Physics Experiment Possibilities from Measurement at ORCEF and Other USDOE Facilities", ORNL/TM-2019/384 (Dec 2019) [OSTI #1615820]

13. John T. Mihalczo, "Critical and Subcritical NEA Benchmark Possibilities for Measurements at ORCEF and Other US DOE Facilities", ORNL/TM-2019/1188 (June 2019)

APENDIX C: SUPPORT STRUCTURE DESCRIPTION

The support structure is described in this appendix. Figure C.1 represents the diaphragm and rings with its support structure. Figure C.2 represents the low-mass lower support structure. Both structures can be seen in Figure 2.3-2. These support structures were used in many other critical experiments with enriched uranium metal at ORCEF [20]. Stainless steel diaphragms of varying thicknesses were available, but for these experiments, the thickness of the diaphragm was 0.010 in.

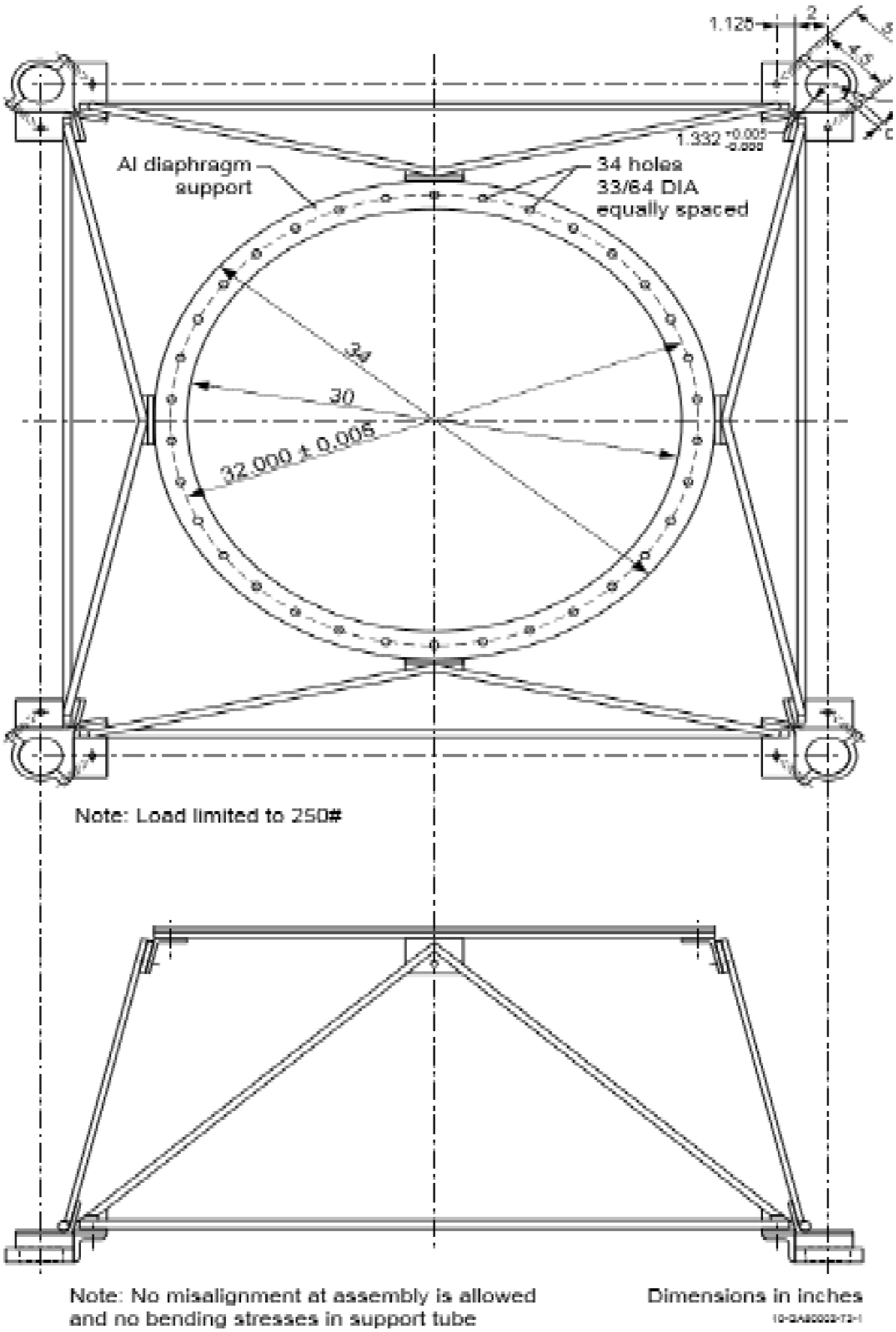

Figure C.1. Diaphragm support structure for upper section. (Diaphragm used in these experiments was 0.010 in. thick.)

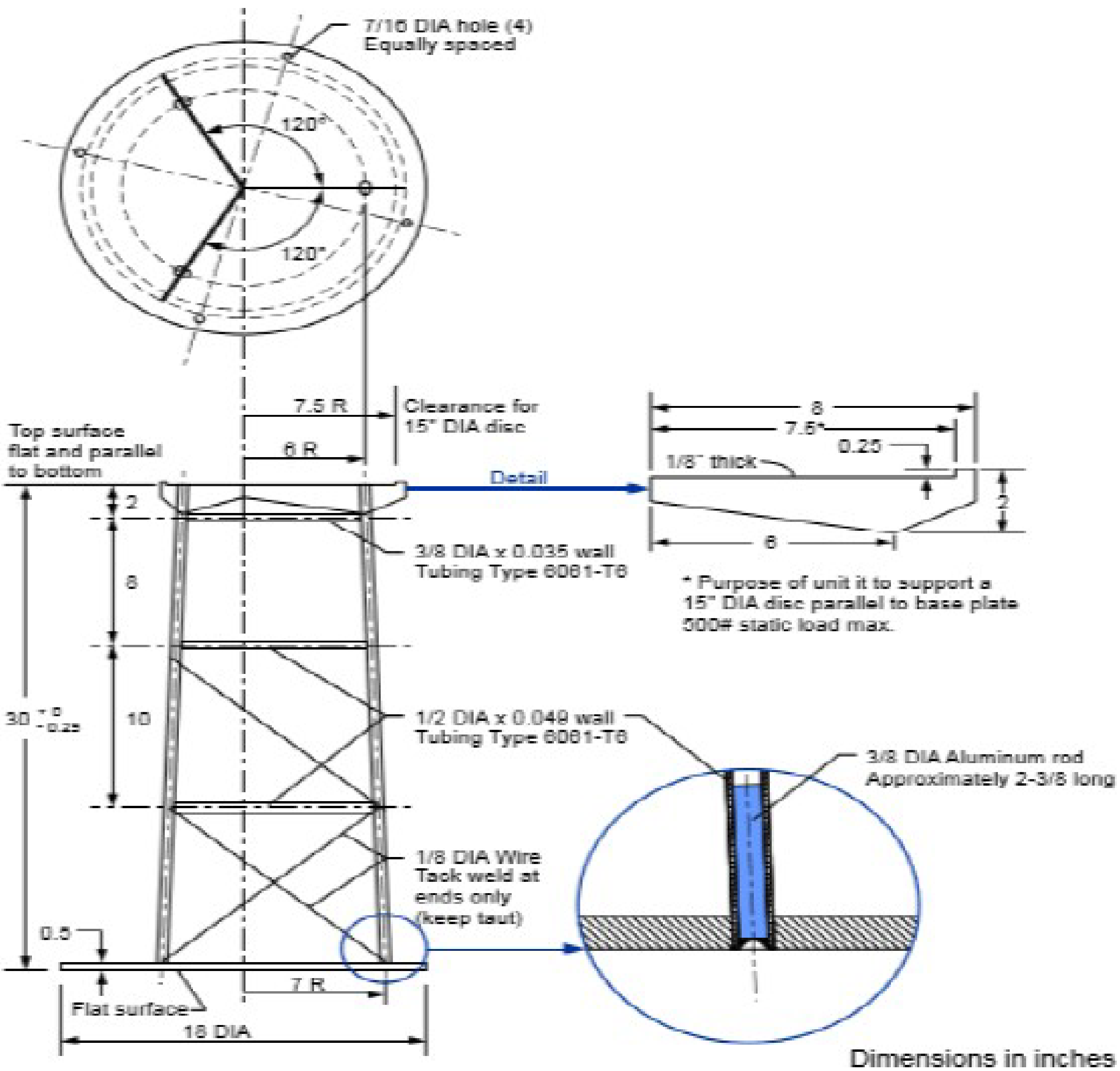

Figure C.2. Lower Support structure.

APPENDIX D: CONFIGURATION OF THE CALIFORNIUM IONIZATION CHAMBERS

There were four singly contained aluminum Cf ionization chambers available for the randomly pulsed neutron measurements. These sources were also used for Rossi-α measurements for subcritical configurations. A sketch of the Cf ionization chamber is given in Figure D.1.

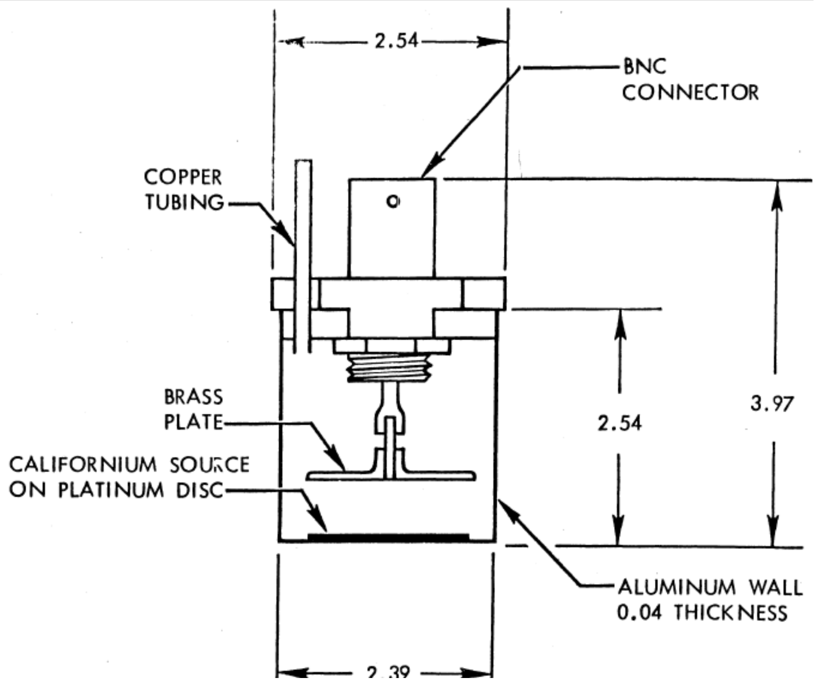

Figure D.1. Configuration of the aluminum Cf ion chambers. (Single containment)

A photograph of the electronic pulses from the Cf ionization chamber amplifier is shown in Figure D.2. The larger pulses are from fission, and those of lower amplitude are from alpha decay. The difference between the highest alpha pulses and the smallest fission pulses allows good discrimination of the alpha pulses so that only fission pulses are used. The four chambers varied in fission rate from 700 to 125,000 fissions per second. The sources were designated A, B, C, and D and had fission rates of 8170, 125,000, 33,000 and 700 fissions per second, respectively on July 1, 1969.

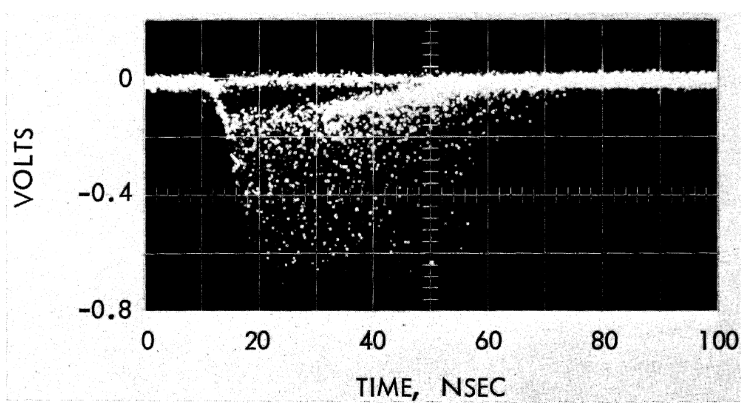

Figure D.2. Photograph of the Cf ion chamber pulses after amplification.

APPENDIX E: GAMMA ACTIVITY OF THIN 15 IN. DIAMETER HEU METAL PLATES IN 1969

When the thin 15 in. diameter HEU metal plates were received in ORCEF in 1969, it was noticed in dosimetry surveys that the gamma dose was considerably higher than Oralloy in use at ORCEF. The activity was measured by placing the 0.5 in. thick plastic scintillator with the flat face of the scintillator adjacent to the flat surface of the uranium plate at a radius 5 in. with the detector axis perpendicular to the flat surface of the plate. There were 0.025 inches of iron between the detector and the plate so as not to contaminate the detector with oxide. The detector threshold was set to not count gamma rays with energy less than 220 Kev. The results are given in Table E.1.

Table E.1. Relative gamma ray activity of the thin 15 in. diameter HEU metal plates.

Part number	Counts per second	Gamma emission relative to ORCEF Oralloy
10933	2,729	2.3
11151	7,084	5.9
11149	3,498	2.9
11150	55,243	46.4
11146	4,117	3.5
11148	2,488	2.1
11147	2,807	2.4
10493	7,002	5.9
10470	7212	6.1
10485	7,752	6.5
10477	6,448	4.6
10491	4,744	4.0
10487	7,007	5.9
10475	4,450	3.7
10458	6,517	5.5
10481	8,453	7.1
11018	3,241	2.7
10935	3,987	3.3
11017	5,501	4.6
10932	2,386	2.0
11019	44,420	37.3
10483	9,854	8.3
10457	6,594	5.5
10467	6,785	5.7
10489	8,461	7.1
10464	6,195	5.2
ORCEF Oralloy plate	1,191	1.0

These plates were obviously used in high fission rate experiments, especially 11150 and 11019, and these two plates were not used in all but one of the configurations in the measurements reported here to minimize radiation dose to the experimenters. The relative activity compared to an ORCEF 15 in. diameter, 0.25 in. thick plate is given in column 3 of the table and except for two plates varied from a factor of 2 to 8 higher than Y-12 Oralloy. This higher activity resulted in the necessity of pulse shape discrimination to reject gamma rays for the subcritical prompt neutron decay constant measurements.

APPENDIX F: CONFIGURATION OF THE SUBCRITICAL ASSEMBLIES

The parts lists for the subcritical assemblies are given in Table F.1 to F.4. These are the configurations for prompt neutron time decay measurements with the Cf source near the center. The description of the individual parts is given in the description of the materials in Section 5. The location of the diaphragm for most assemblies is also listed in the tables. For most subcritical systems, all the material was on the diaphragm. For all but the highest number of plates the source was centrally located and for the highest number of plates for polyethylene thicknesses of 1⁄16, 1⁄8, 1⁄4 and 1⁄2 inches, the source was centered on the top plate. The table also contains the sum of the measured thicknesses of each uranium plate (known in 1969 but not now) and the sum of the thicknesses of each plate given in this report (Table 5.1-2) and the difference between the two. The table also contains the date of the measurements and page in the ORCEF logbook.

Table F.1. Parts list for subcritical configurations with 1/16 in. thick polyethylene layers from top to bottom.

Parts list for 20 plates with 1/16 in. thick polyethylene	Parts list for 19 plates with 1/16 in. thick polyethylene	Parts list for 18 plates with 1/16 in. thick polyethylene	Parts list for 14 plates with 1/16 in. thick polyethylene	Parts list for 12 plates with 1/16 in. thick polyethylene	Parts list for 10 plates with 1/16 in. thick polyethylene
11147 on poly ef	10483 with hole on Poly A3&A4	10483 with hole on Poly A3&A4	10481 with hole on Poly B6	10470 with hole on Poly B5	10485 with hole on Poly B4
11149 on poly cd	10489 with hole on Poly A1&A2	10489 with hole on Poly A1&A2	10470 with hole on Poly B5	10485 with hole on Poly B4	10487 with hole on Poly B3
11146 on poly ab	10481 with hole on poly B6	10481 with hole on poly B6	10485 with hole on Poly B4	10487 with hole on Poly B3	10493 with hole on Poly B2
10491 on poly 98	10470 with hole on poly B5	10470 with hole on poly B5	10487 with hole on Poly B3	10467 with hole on Poly B2	10467 on Poly B1
10477 on poly 97	10485with hole on poly B4	10485 with hole on poly B4	10493 with hole on Poly B2	10467 with hole on Poly B1	10491 on Poly 94
10458 on poly 96	10487 with hole on poly B3	10487 with hole on poly B3	10467 with hole on Poly B1	10491 with hole on Poly 95	11017 on Poly 93
10457 on poly 95	10493 with hole on poly B2	10493 with hole on poly B2	10491 with insert 8447 on Poly 95	10464 with hole on Poly 94	10475 with insert 8441 on Poly 92
10464 on poly 94	10467with hole on poly B1	10467 with hole on poly B1	10457 with insert 8443 on Poly 94	11017 on Poly 93	10935 on Poly 91
11017 on poly 93	10491with insert 8449 on poly 98	10491 on poly 98	10464 with insert 8442 on Poly 93	10475 with insert 8441 on Poly 92	11018 on Poly 90
10475 on poly 92	10477 with insert 8448 on Poly 97	10477 with insert 8445 on Poly 97	11017 on Poly 92	10935 on Poly 91	10933 on diaphragm
10935 on poly 91	10458 with insert 8447 on Poly 96	10458 with insert 8447 on Poly 96	10475 with insert 8441 on Poly 92	10481 on Poly 90	
11018 on poly 90	10457 with insert 8443 on Poly 95	10457 with insert 8443 on Poly 95	10935 on Poly 91	10933 on diaphragm	

10933 on diaphragm	10464 with insert 8442 on Poly 94	10464 with insert 8442 on Poly 94	11018 on Poly 90		

Table F.1. Parts list for subcritical configurations with 1/16 in. thick polyethylene layers from top to bottom (continued).

Parts list for 20 plates with 1/16 in. thick polyethylene	Parts list for 19 plates with 1/16 in. thick polyethylene	Parts list for 18 plates with 1/16 in. thick polyethylene	Parts list for 14 plates with 1/16 in. thick polyethylene	Parts list for 12 plates with 1/16 in. thick polyethylene	Parts list for 10 plates with 1/16 in. thick polyethylene
Poly st	11017 on Poly 93	10935 on Poly 94	10933 on diaphragm		
10467 on poly qr	10475 with insert 8441 on Poly 92	10475 with insert 8441 on Poly 92			
10493 on poly op	10935 on Poly 91	10935 on Poly 91			
10487 on poly mn	11018 on Poly 90	11018 on Poly 90			
11151 on poly kl	10933 on Diaphragm	10933 on Diaphragm			
10470 on poly ij	11149 with Poly ab above it				
10485 on poly gh					
10489					
Source adjacent to top of U-11147	Source adjacent to top of U-10491	Source adjacent to top of Poly B1	Source adjacent to top of Poly 96	Source adjacent to top of poly 95	Source adjacent to top of Poly B1
Page 39 of ORCEF logbook E-24	Page 58 of ORCEF logbook E-24	Page 58 of ORCEF logbook E-24	Page 59 of ORCEF logbook E-24	Page 59 of ORCEF logbook E-24	Page 63 of ORCEF logbook E-24
July 29,1969	August 27,1969	August 26,1969	Sept 5,1969	Sept 9. 1969	Sept 16, 1969
Total Uranium thickness[(a)] is 2.3949 in	Total Uranium thickness is 2.2779 in	Total Uranium thickness is 2.1598 in	Total Uranium thickness is 1.6779 in	Not measured	Total Uranium thickness is 1.1972 in
Total Uranium thickness[(b)] from Table 5.2 is 2.39394 in.	Total Uranium thickness[(b)] from Table 5.2 is 2.27506 in.	Total Uranium thickness[(b)] from Table 5.2 is 2.15692 in.	Total Uranium thickness[(b)] from Table 5.2 is 1.687682	Total Uranium thickness[(b)] from Table 5.2 is	Total Uranium thickness[(b)] from Table 5.2 is 1.19662 in.
Uranium thickness difference is 0.0014 in.	Uranium thickness difference is 0.0028 in.	Uranium thickness difference is 0.0029 in.	Uranium thickness difference is 0.00978 in		Uranium thickness difference is 0.0011 in

(a) Sum of the known thicknesses of thin 15 in. diameter HEU metal plates in 1969. Data not presently available
(b) Sum of assumed thicknesses from Table 5.1-2

The small differences between the thickness stated in Reference 2 and those calculated from Table 5.1-2 (0.0011 to 0.00978 in.) enhance the validity of the thicknesses of Table 5.1-2. The total thicknesses in reference 2 were obtained from the individual measured (by Y-12-dimensional inspection) thickness of each plate that are not now available.

The subcritical configuration for 20 thin 15 in. diameter HEU metal plates with 1/16 in. thick polyethylene is the same as Experiment 1 but without the pie sections on top and consisted of full layers. Based on height measurements for subcritical configurations, the gap between polyethylene and uranium layers for this assembly is 0.0032 in. The Cf source was centered on the top of the top uranium metal plate. The sketches of the other subcritical configuration and those for other polyethylene layers are given in Figures F.1 to F15.

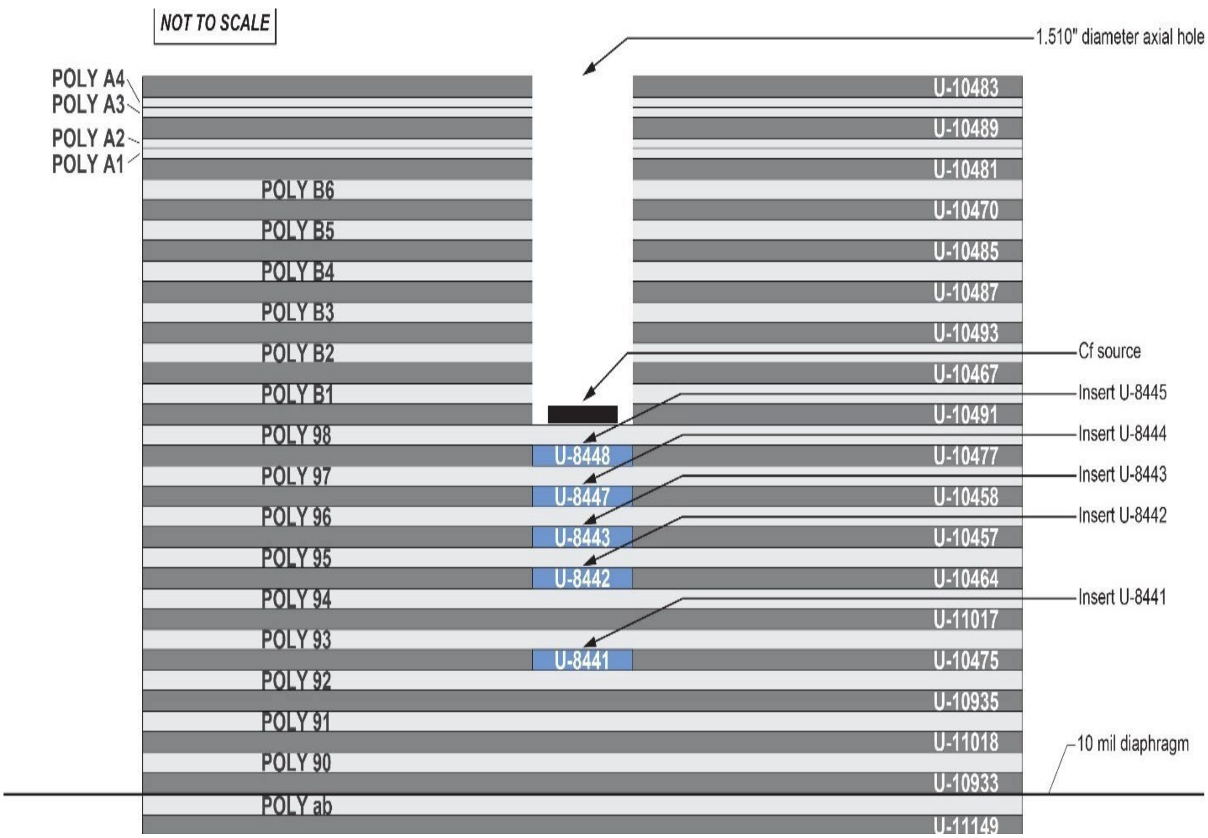

Figure F.1. Subcritical configuration for 19 thin 15 in. diameter HEU metal plates with 1/16 in. thick polyethylene. (Based on height measurements for this subcritical configuration, the gap between polyethylene and uranium layers for this assembly is 0.0032 inches).

The configuration of subcritical configuration for 18 thin 15 in. diameter HEU metal plates with 1/16 in. thick polyethylene was the same as Figure E.1 but with the uranium plate and polyethylene layer below the diaphragm removed. Based on height measurements for this subcritical configuration, the gap between polyethylene and uranium layers for this assembly is 0.0032 in.

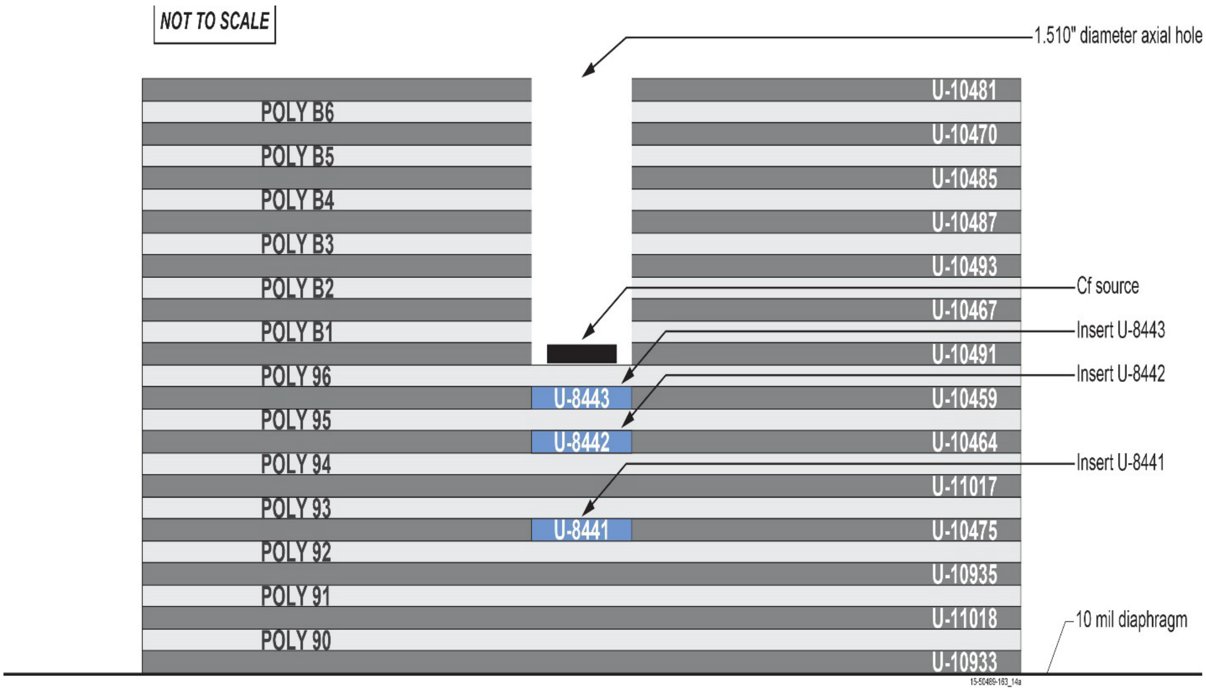

Table F.2. Subcritical configuration for 14 thin 15- n. diameter HEU metal plates with 1/16 in. thick polyethylene. (Based on height measurements for subcritical configurations, the gap between polyethylene and uranium layers for this assembly is 0.0038 inches)

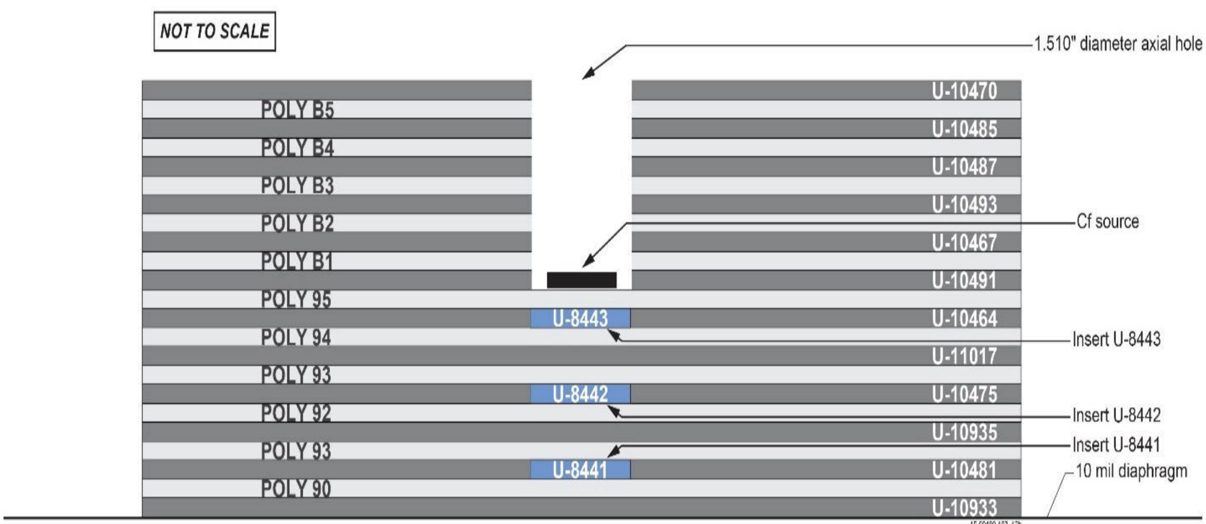

Figure F.3. Subcritical configuration for 12 thin 15 in. diameter HEU metal plates with 1/16 in. thick polyethylene. (Based on height measurements for subcritical configurations, the gap between polyethylene and uranium layers for this assembly is 0.0038 in.)

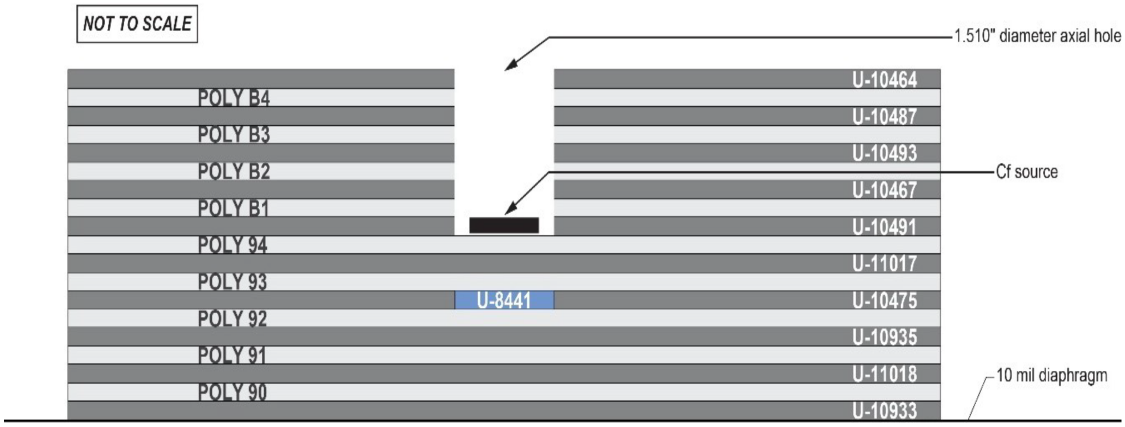

Figure F.4. Subcritical configuration for 10 thin 15 in. diameter HEU metal plates with 1/16 in. thick polyethylene. (Based on height measurements for subcritical configurations, the gap between polyethylene and uranium layers for this assembly is 0.0037 in.)

Table F.2. Parts list for subcritical configurations with 1/8 in. thick polyethylene layers from top to bottom.

Parts list for 16 plates with 1/8 in. thick polyethylene	Parts list for 15 plates with 1/8 in. thick polyethylene	Parts list for 12 plates with 1/8 in. thick polyethylene	Parts list for 10 plates with 1/8 in. thick polyethylene
11148 on Poly 13	10470 with hole on Poly 26	10467 with hole on Poly25	10491 with hole on Poly 22
11147 on Poly 12	10493 with hole on Poly 25	10491 with hole on Poly 24	10477 with hole on Poly 21
11149 on Poly 11	10467 with hole on Poly 24	10477 with hole on Poly 23	10458 with hole on Poly 19
11146 on Poly 10	10491 with hole on Poly 23	10458 with hole on Poly 22	104ﬁ75 with hole on Poly 18
10491 with insert 8449 on Poly 9	10477 with hole on Poly 22	10475 with hole on Poly 21	10457 with hole on Poly 5
10477 with insert 8448on Poly 8	10458 with hole on Poly 21	10457 with insert 8442with on Poly 6	11146 on Poly 4
10458 with insert 8447 on Poly 7	10475 with hole on Poly 20	11149 with insert 8441 with hole on Poly 5	11017 on Poly 3
10457 with insert 8443on Poly 6	10457 with hole on Poly 19	11146 on Poly 4	10935 on Poly 2
10464 with insert 8442 on Poly 5	10464 with insert 8442 with hole on Poly 18	11017 on Poly 3	11018 on Poly 1
11017 on Poly 4	10487 with insert 8441 on Poly 6	10935 on Poly 3	10933 on diaphragm
10475 with insert 8441 on Poly 3	11146 on Poly 5	11018 on Poly 1	
10935 on Poly 2	11017 on Poly 4	10933 on diaphragm	
11018 on Poly 1	10935 on Poly 3		
10933 on diaphragm	11018 on Poly 2		

Table F.2. Parts list for subcritical configurations with 1/8 in. thick polyethylene layers from top to bottom (continued).

Parts list for 16 plates with 1/8 in. thick polyethylene	Parts list for 15 plates with 1/8 in. thick polyethylene	Parts list for 12 plates with 1/8 in. thick polyethylene	Parts list for 10 plates with 1/8 in. thick polyethylene
Poly 15	10933 on Poly 1		
10467 with insert 8452 on Poly 14			
10493 with insert 8451 on ram			
Source adjacent to top of 11148	Source adjacent to top of 10457	Source adjacent to top of Poly 6	Source adjacent to top of Poly 5
Page 40 of ORCEF E-24	Page 58 of ORCEF logbook E-24	Page 59 of ORCEF logbook E-24	Page 60 of ORCEF logbook E-24
July 31, 1969	Aug 29, 1969	Sept 10, 1969	Sept 11, 1969
Total Uranium Thickness is 1.9165 in	Total Uranium Thickness is 1.7984 in	Total Uranium Thickness is 1.4402	Total Uranium Thickness is 1.2000
Uranium thickness from Table 5.2 is 1.91573 in.	Uranium thickness from Table 5.2 is 1.79718 in.	Uranium thickness from Table 5.2 is 1.4388 in.	Uranium thickness from Table 5.2 is 1.20047 in.
Uranium thickness difference is 0.00077 in.	Uranium thickness difference is 0.00122 in.	Uranium thickness difference is 0.0014 in.	Uranium thickness difference is 0.00047 in.

The small differences between the thickness stated in Reference 2 and those calculated from Table 5.1-2 0.00047 to 0.0014) enhance the validity of the thicknesses of Table 5.1-2. The total thicknesses in reference 2 were obtained from the individual measured (by Y-12-dimensional inspection) thickness of each plate that are not now available.

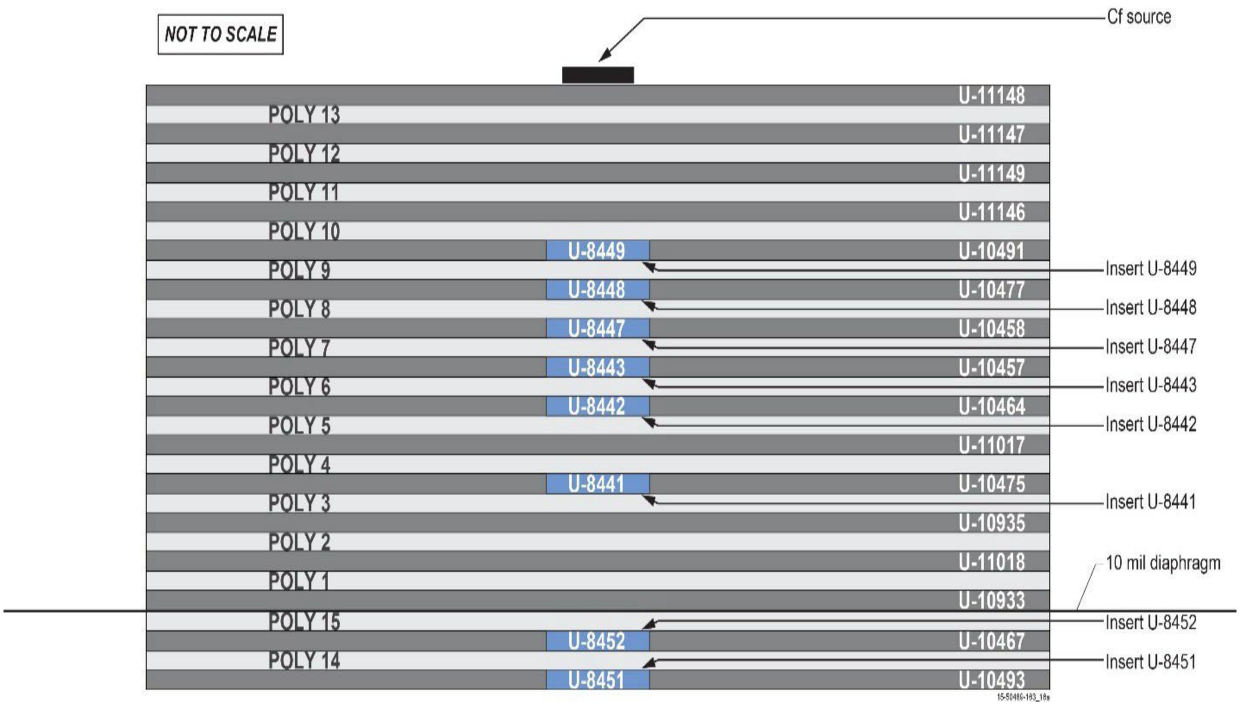

Figure F.5. Subcritical configuration for 16 thin 15 in. diameter HEU metal plates with 1/8 in. thick polyethylene. (Based on height measurements for subcritical configurations, the gap between polyethylene and uranium layers for this assembly is 0.0032 in.)

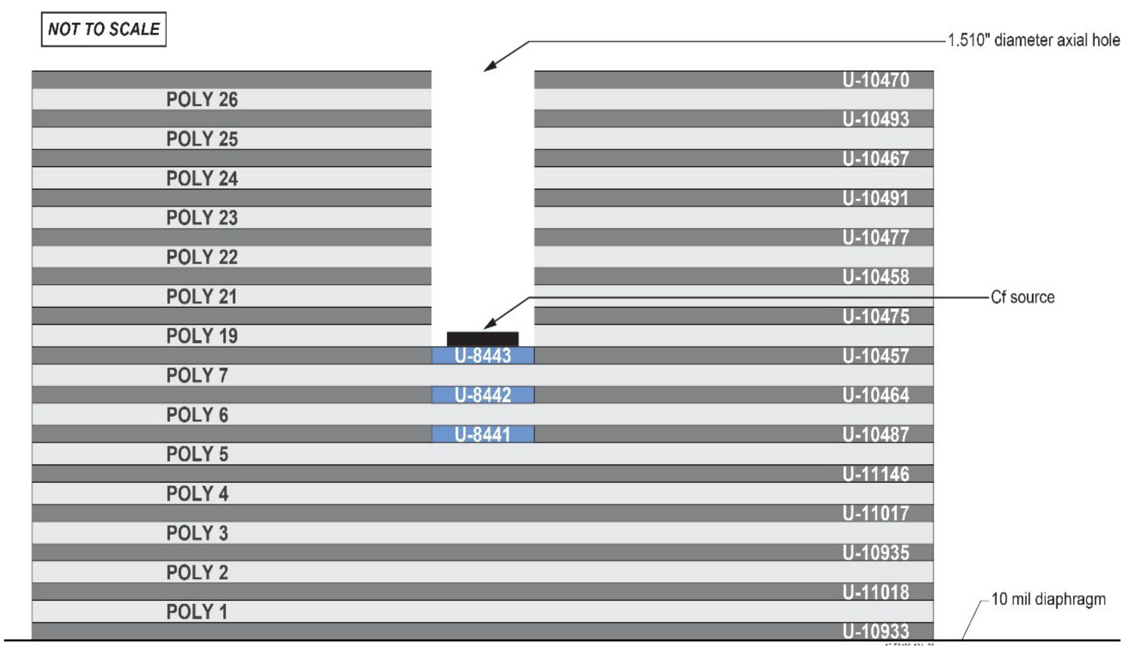

Figure F.6. Subcritical configuration for 15 thin 15 in. diameter HEU metal plates with 1/8 in. thick polyethylene. (Based on height measurements for subcritical configurations, the gap between polyethylene and uranium layers for this assembly is 0.0037 in.)

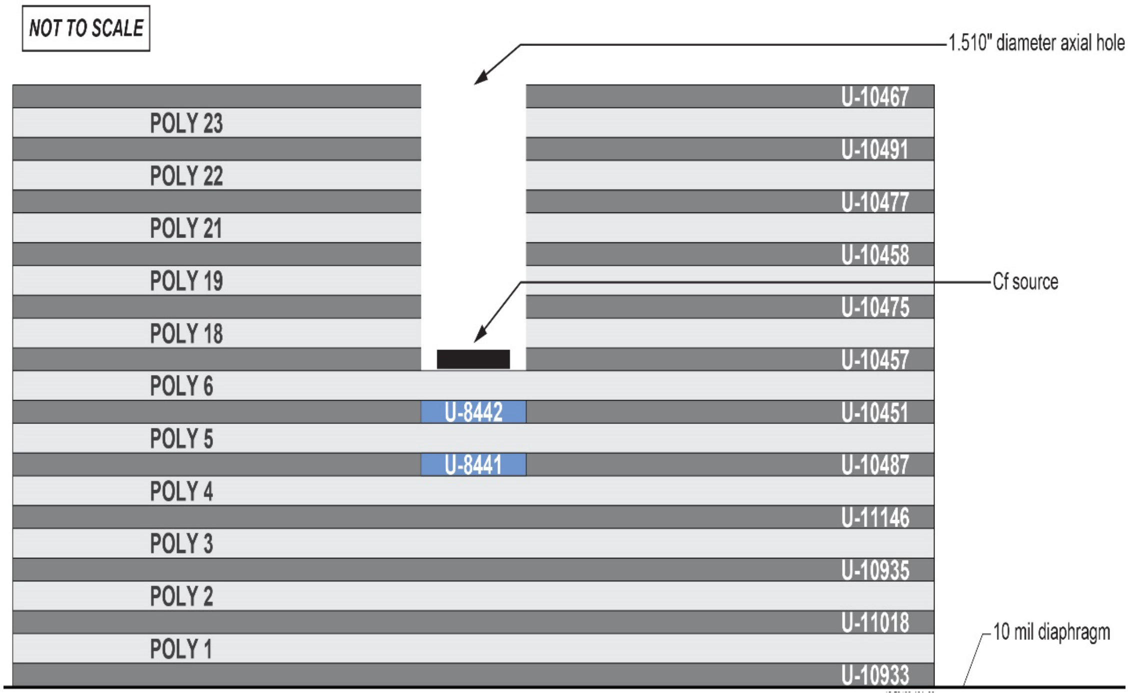

Figure F.7. Subcritical configuration for 12 thin 15 in. diameter HEU metal plates with 1/8 in. thick polyethylene. (Based on height measurements for subcritical configurations, the gap between polyethylene and uranium layers for this assembly is 0.0035 in.)

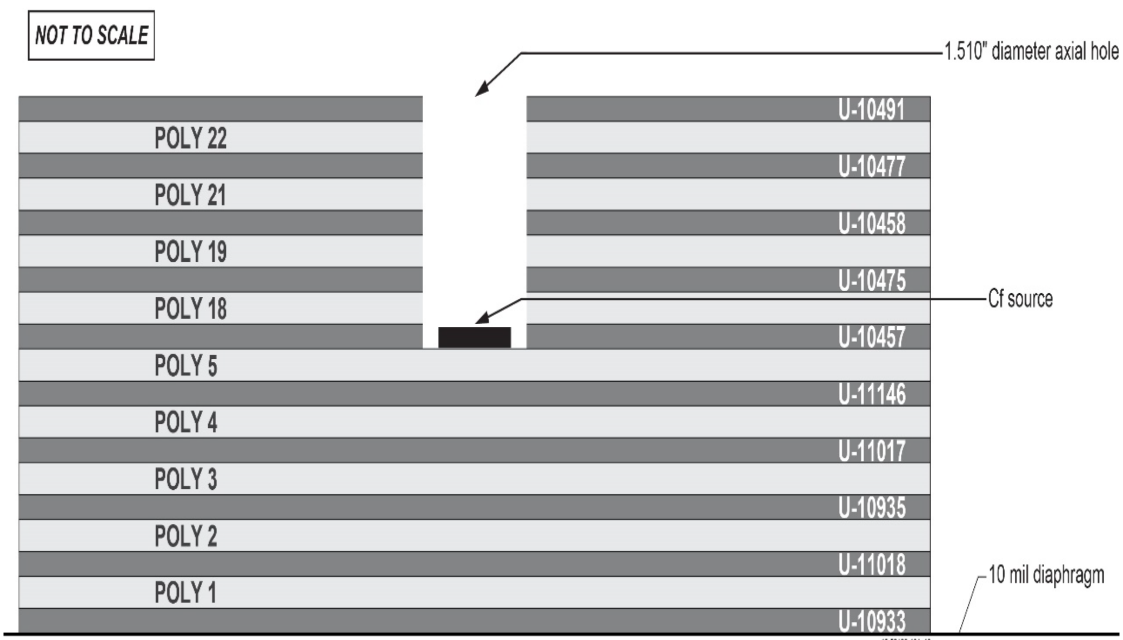

Figure F.8. Subcritical configuration for 10 thin 15 in. diameter HEU metal plates with 1/8 in. thick polyethylene. (Based on height measurements for subcritical configurations, the gap between polyethylene and uranium layers for this assembly is 0.0034 in.)

Table F.3. Parts list for subcritical configurations with ¼ in. thick polyethylene layers from top to bottom.

Parts list for 12 plates with ¼ in. thick polyethylene	Parts list for 10 plates with ¼ in. thick polyethylene	Parts list for 8 plates with ¼ in. thick polyethylene	Parts list for 6 plates with ¼ in. thick polyethylen4
11148 on Poly 38	10477 with hole on Poly 45	10458 with hole on Poly 44	10475 with hole on Poly 43
11147 on Poly 37	10458 with hole on Poly 44	10475 with hole on Poly 43	10457 with hole on Poly 42
11149 on Poly 36	10475 with hole on Poly 43	10457 with hole on Poly 42	10464 with hole on Poly 32
11146 on Poly 35	10457 with hole on Poly 42	10464 with hole on Poly 33	10935 on Poly 31
10491 on Poly 34	10464 with hole on Poly 34	11017 on Poly 32	11018 on Poly 30
11017 on Poly 33	11146 on Poly 33	10935 on Poly 31	10933 on Diaphragm
10475 on Poly 32	11017 on Poly 32	11018 on Poly 30	
10935 on Poly 31	10935 on Poly 31	10933 on Diaphragm	
11018 on poly 30	11018 on Poly 30		
10933 on diaphragm	10933 on Diaphragm		
Poly 40			
10464 on poly 39			
10477			
Source adjacent to the top of U-11148	Source adjacent to the top of Poly 34	Source adjacent to the top of Poly 33	Source adjacent to the top of Poly 32
Page 49 of ORCEF logbook E-24	Page 59 of ORCEF logbook E-24	Page 60 of ORCEF logbook E-24	Page 60 of logbook ORCEF E2-4
Aug 8, 1969	Sept 1, 1969	Sept 15, 1969	Sept 14, 1969
Uranium Thickness from Ref 2 is 1.4402 in	Uranium Thickness is 1.1980 in	Uranium Thickness is 0.95748	Uranium Thickness is 0.71890.
Total uranium thickness from Table 5.2 is 1.43287 in.	Total uranium thickness from Table 5.2 is 1.19788 in.	Total uranium thickness from Table 5.2 is 0.95838 in.	Total uranium thickness from Table 5.2 is 0.71770 in.
Uranium thickness difference is 0.0073 in.	Uranium thickness difference is 0.001012 in.	Uranium thickness difference is 0.00109in.	Uranium thickness difference is 0.00121 in.

The small differences between the thickness stated in Reference 2 and those calculated from Table 5.1-2 (0.00101 to 0.0073 in.) enhance the validity of the thicknesses of Table 5.1-2. The total thicknesses in reference 2 were obtained from the individual measured (by Y-12-dimensional inspection) thickness of each plate that are now not available.

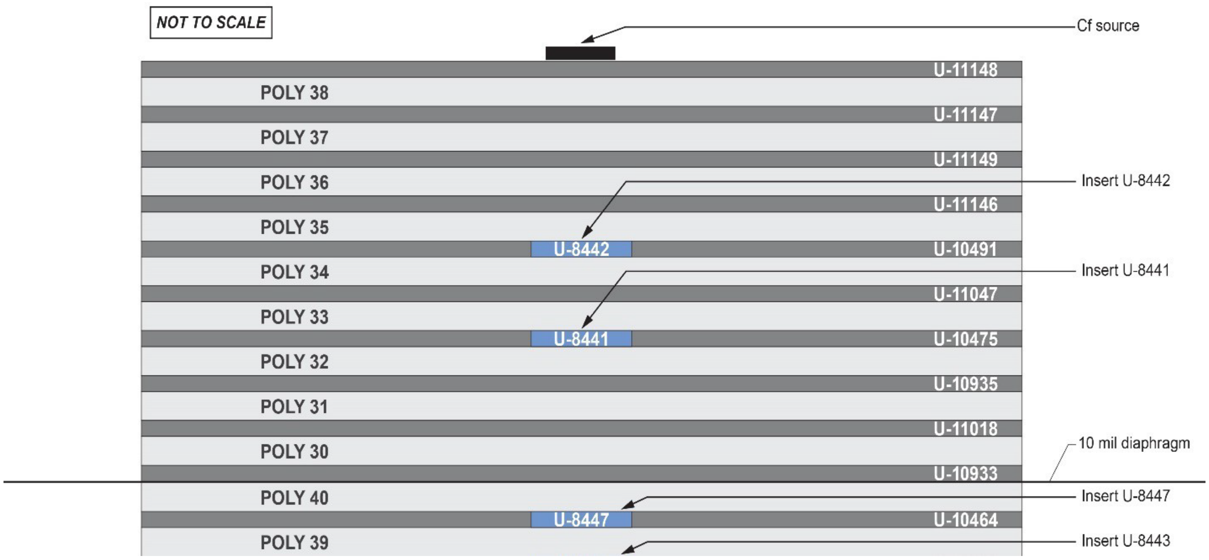

Figure F.9. Subcritical configuration for 12 thin 15 in. diameter HEU metal plates with ¼ in. thick polyethylene. (Based on height measurements for subcritical configurations, the gap between polyethylene and uranium layers for this assembly is 0.0032 in.)

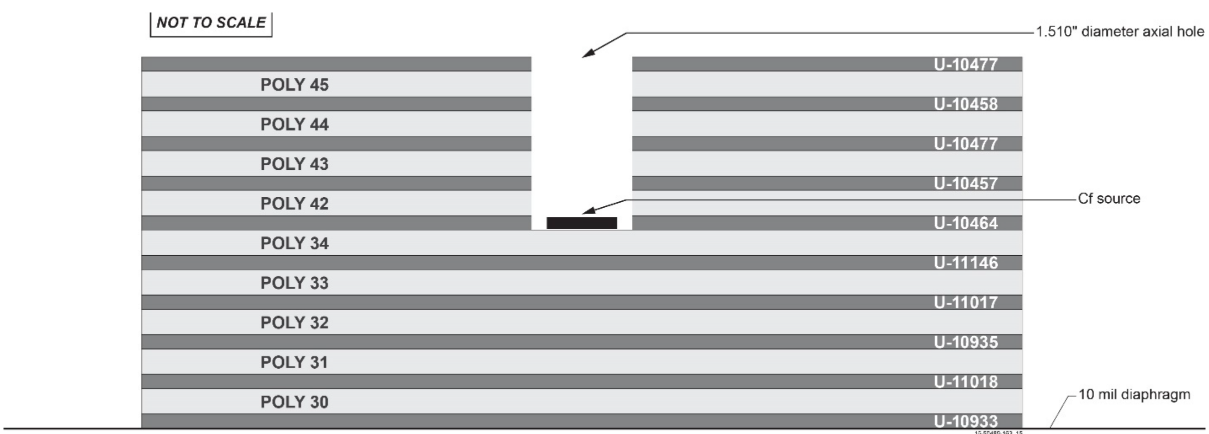

Figure F.10. Subcritical configuration for 10 thin 15 in. diameter HEU metal plates with ¼ in. thick polyethylene. (Based on height measurements for subcritical configurations, the gap between polyethylene and uranium layers for this assembly is 0.0033 in.)

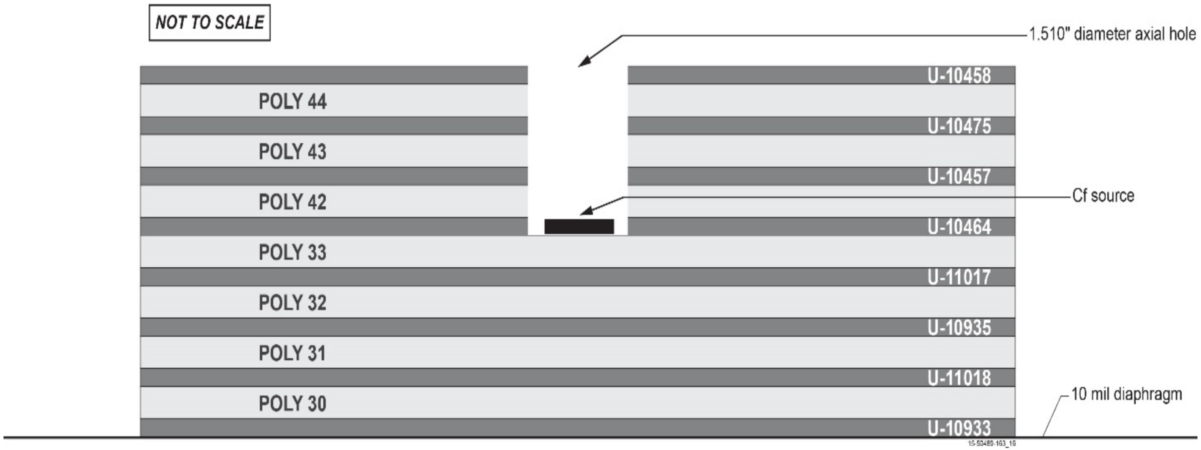

Figure F11. Subcritical configuration for 8 thin 15 in. diameter HEU metal plates with ¼ in. thick polyethylene. (Based on height measurements for subcritical configurations, the gap between polyethylene and uranium layers for this assembly is 0.0040 in.)

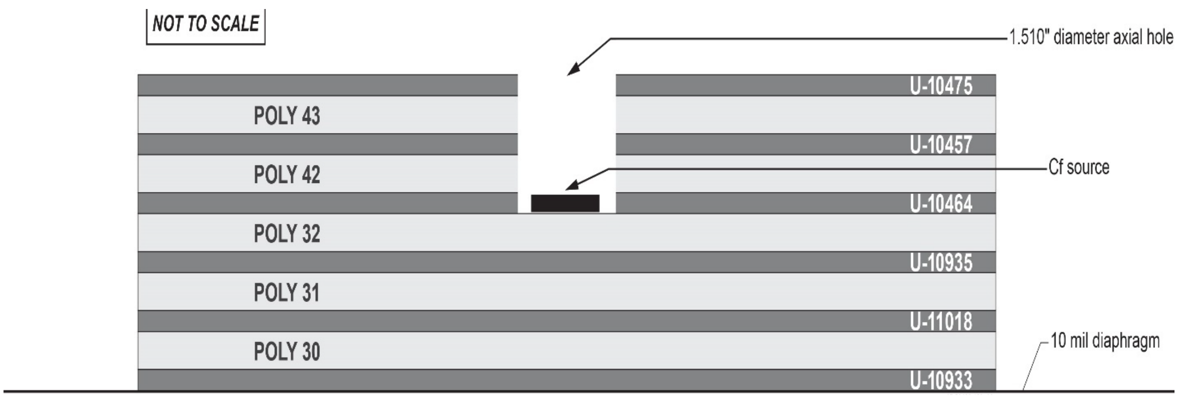

Figure F.12. Subcritical configuration for 6 thin 15 in. diameter HEU metal plates with ¼ in. thick polyethylene. (Based on height measurements for subcritical configurations, the gap between polyethylene and uranium layers for this assembly is 0.0049 in.)

The small differences between the thickness stated in Reference 2 and those calculated from Table 5.1-2 (0.000350 to 0.00403) enhance the validity of the thicknesses of Table 5.1-2. The total thicknesses in reference 2 were obtained from the individual measured (by the Y-12 Plant dimensional inspection) thickness of each plate that are now not available.

Table F.4.. Parts list for subcritical configurations with ½ in. thick polyethylene layers from top to bottom.

Parts list for 8 plates with ½ in. thick polyethylene	Parts list for 7 plates with ½ in. thick polyethylene	Parts list for 4 plates with ½ in. thick polyethylen4
10458 with hole on Poly 71	10458 with hole on Poly 71	10477 with hole on Poly 69
10477 on top of Poly 70	10477 with hole on Poly 70	10464 with hole on Poly 61
10464 on top of Poly 69	10464 with hole on top of Poly 69	11018 0n Poly 60
10491 on top of Poly 62	10491 with insert 8442 with hole on top of Poly 62	10933 on Diaphragm
10475 on top of Poly 61	10475 with insert 8441 on top of Poly 61	
11018 on top of Poly 60	11018 on top of Poly 60	
10933 on diaphragm	10933 on Diaphragm	
11146 on ram with poly 63 on top		
Source adjacent to the top of Poly 62	Source adjacent to the top of U-10491	Source adjacent to the top of Poly 61
Page 64 of ORCEF logbook E-24	Page 67 of ORCEF logbook E-24	Page 64 of logbook ORCEF E-24
Sept 20, 1969	Sept 26, 1969	Sept 17, 1969
Total uranium thickness from Ref 2 is 0.96024 in.	Total uranium thickness from Ref 2 is 0.84173 in.	Total uranium thickness from Ref 2 is 0.47795 in.
Total uranium thickness from Table 2 is 0.95621 in.	Total uranium thickness from Table 2 is 0.83777 in.	Total uranium thickness from Table 2 is 0.4776 in
Uranium thickness difference is 0.00403 in.	Uranium thickness difference is 0.004 in.	Uranium thickness difference is 0.00035 in.

Figure F.13. Subcritical configuration for 8 thin 15 in. diameter HEU metal plates with ½ in. thick polyethylene. (Based on height measurements for subcritical configurations, the gap between polyethylene and uranium layers for this assembly is 0.0043 in.)

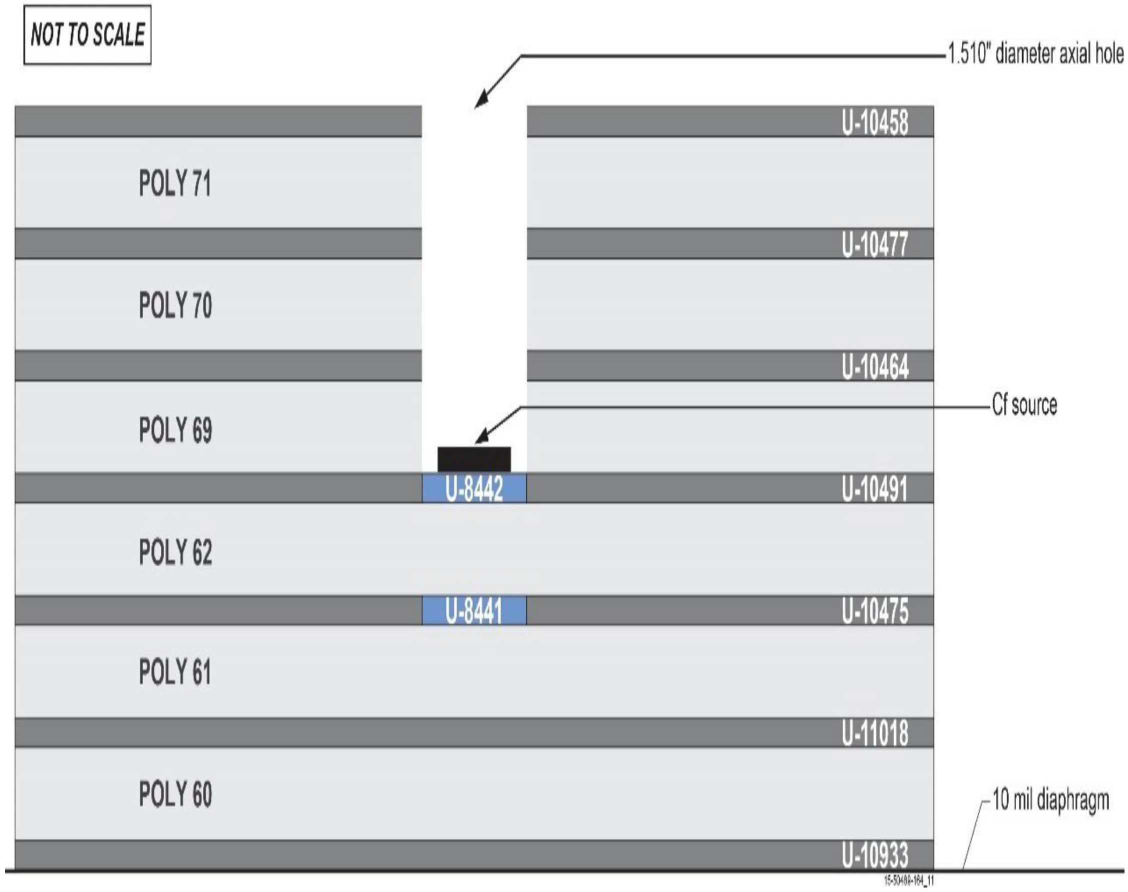

Figure F.14. Subcritical configuration for 7 thin 15 in. diameter HEU metal plates with ½ in. thick polyethylene. (Based on height measurements for subcritical configurations, the gap between polyethylene and uranium layers for this assembly is 0.0059 in.)

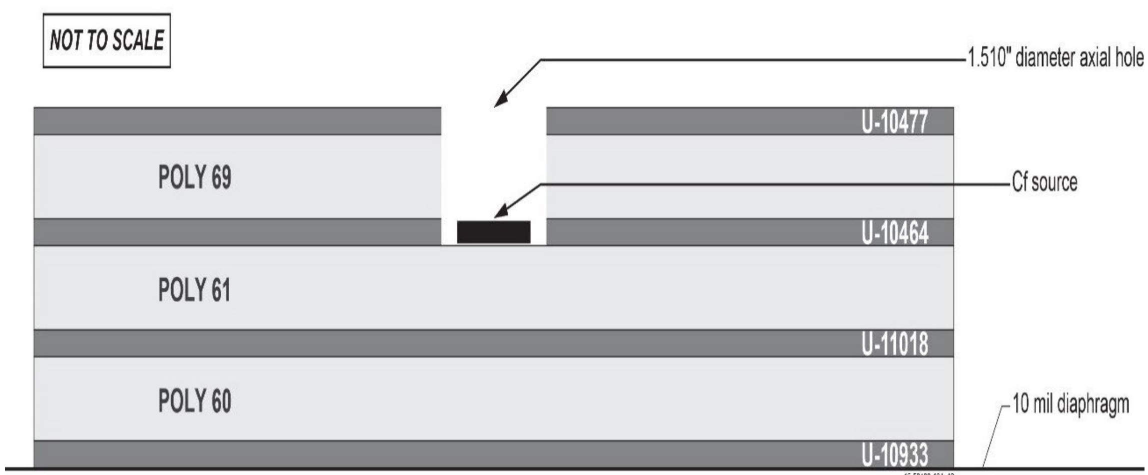

Figure F.15. Subcritical configuration for 4 thin 15 in. diameter HEU metal plates with ½ in. thick polyethylene. (Based on height measurements for subcritical configurations, the gap between polyethylene and uranium layers for this assembly is 0.0081 in.

APPENDIX G: SUGGESTED FUTURE WORK

1) Search the records at the Y-12 Plant and Los Alamos National Laboratory archives for the dimensional analysis reports and the isotopic enrichment analysis documentation. B W. Myers of LANL in the past sent me the dimensional analysis reports for 21-in.outside diameter, 15 in. inside diameter HEU metal annuli that fit around these 15 in. diameter HEU metal plates. This suggests that LANL was also sent the dimensional analysis data for the 15 in, diameter HEU metal plates. It is not conceivable that the Y-12 Plant would not send the dimensional inspection reports for the 15 in. diameter HEU metal plates to LANL

2) Calculate the effects of room return or include the room in your calculational comparisons. Include the air and the 0.5 in. thick Al base of the lower support and the 1.0 in. thick steel table to which it is attached. The steel could absorb thermal neurons from returning from the floor or scatter fast neutrons back to the assembly. This effect was calculated for an unmoderated and unreflected 15 in. diameter Oralloy assembly in the same location on the same vertical assembly machine [20]. This small change in the neutron multiplication factor will require longer than usual Monte Carlo calculations. Previous calculations used 1,050 generation of 1,000,000 histories neglecting the first 50 generations.

3) Create detailed and simple models of all configurations. In the detailed model, each part is described. In the simple model, average values are used.

4) Calculate the effective delayed neutron fraction (β_{eff}) for all critical and subcritical configurations. This can be done by performing two calculations: the normal one and one with the delayed neutrons from the various isotopes inducing fission removed from the emission spectrum of the neutron produced in fission. The number of fissions from each uranium isotope causing fission can be obtained from the normal calculation. The neutron multiplication factor from the two calculations is subtracted to obtain the effective delayed neutron fraction. Since the delayed neutron fraction is about 0.0070 the precision of the calculations should be ± 0.00001, which is quite small and will require a large number of neutron histories in a Monte Carlo calculation.

5) Convert the reactivity in cents and dollars to k_{eff} units, where one dollar or 100 cents equals the effective delayed neutron fraction. This will be done for all variations of the near critical configurations, the IKRD measurements and any subcritical reactivities obtained from the prompt neutron decay measurements, the latter using corrections for changes in the neutron lifetime and effective delayed neutron fraction.

6) Calculate the prompt neutron lifetime for all configurations. For the critical configurations, this can be compared to the prompt neutron lifetime (**l**) from the prompt neutron decay constant (α) at delayed critical using the effective delayed neutron fraction (β_{eff}) since at delayed critical $\boldsymbol{\alpha = (\beta_{eff})/l}$.

7) Use the fundamental mode decay constant from the prompt neutron time decay measurements to obtain the subcriticality in dollars. This requires the changes in effective delayed neutron fraction and the prompt neutron lifetime with subcriticality for each polyethylene thickness 1/16, 1/8, ¼, and ½ poly thicknesses. Use near delayed critical as a reference reactivity. The changes in the effective delayed neutron fraction and the prompt neutron lifetime are obtained from calculations.

8) Convert the reactivity in cents and dollars to k_{eff} units where one dollar or 100 cents equals the effective delayed neutron fraction. Note that the reactivity from the prompt neutron decay measurement and the IKRD may differ slightly for the same number of thin 15 in. diameter HEU metals plates and polyethylene thicknesses because there were no empty axial holes in the IKRD

measurements. They may differ from each other and the actual values below $k_{eff} = 0.85$ because of the point kinetics assumptions in the analysis.

9) Perform the uncertainty analysis for the measured k_{eff} values.

10) Compare the experimental neutron multiplication with calculations.